

Evaluation of a Particle Beam Interface for LC/MS

by

Laura F. Cerruti

Thesis submitted to the Graduate faculty of the
Virginia Polytechnic Institute and State University
in partial fulfillment of the requirements for the degree

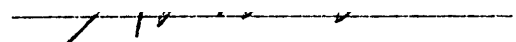
of

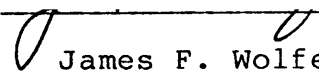
Masters

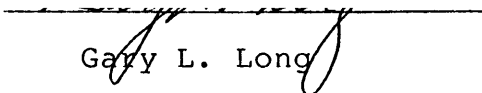
in

Chemistry

Approved:


Harold M. McNair, Chairman


James F. Wolfe


Gary L. Long

March, 1989
Blacksburg, Virginia

ACKNOWLEDGEMENTS

I would like to thank the following people for their help:

Dr. Harold McNair, who offered invaluable support and guidance during my research and more importantly, who set an example of professionalism which I will benefit from in my future endeavors. I would also like to extend my deep appreciation for his understanding during the difficult time of my father's illness and death.

of Hewlett Packard, who gave me the opportunity to work on the Particle Beam project under his instruction, without which this thesis would not be possible. I will always be grateful for the special friendship which has developed between us.

of Hewlett Packard, whose undying commitment in helping this thesis reach fruition made this time of testing more bearable. Without his love and understanding, I would have surely self destructed.

Finally, the members of Dr. McNair's research group. A special thanks to the strange and wonderful

who shared three years of my life both in and out of the lab.

CONTENTS

ACKNOWLEDGEMENTS.....	iii
LIST OF TABLES.....	v
LIST OF FIGURES.....	vi
<u>Chapter</u>	
I. INTRODUCTION.....	1
Importance of LC/MS.....	1
Review of LC/MS.....	3
Development of MAGIC LC/MS Interface.....	11
Development of Particle Beam LC/MS Interface.....	13
Scope and Goals.....	15
II. EXPERIMENTAL.....	19
Materials.....	19
Equipment.....	19
Methods.....	20
III. RESULTS AND DISCUSSION.....	22
Introduction.....	22
Minimum Detectable Quantity.....	23
Linearity.....	40
Band Broadening.....	66
IV. CONCLUSIONS.....	82
REFERENCES.....	84
APPENDIX A.....	86
APPENDIX B.....	97
VITA.....	105

LIST OF TABLES

<u>Table</u>	<u>page</u>
1. Minimum Detectable Quantities for EI MS.....	26
2. Minimum Detectable Quantities for PCI MS.....	30
3. Minimum Detectable Quantities for NCI MS.....	34
4. Combination of EI, PCI, and NCI MDQ's.....	37
5. Linearity Compound Names and Mol. Weights.....	41
6. Extrapolated and Experimental MDQ's.....	64
7. Combinations of Independent Variables.....	69
8. Experimental and Fitted Sigma and Residuals...	71

LIST OF FIGURES

<u>Figure</u>	<u>page</u>
1. Schematic of a Moving Belt Interface.....	5
2. Schematic of a Direct Liquid Introduction Interface.....	8
3. Schematic of a Thermospray Interface.....	10
4. Schematic of a MAGIC Interface.....	14
5. Schematic of a Particle Beam Nebulizer.....	16
6. Schematic of a Particle Beam Interface.....	17
7. Electron Impact MDQ's of 106 compounds.....	25
8. Positive CI MDQ's for 90 compounds.....	29
9. Negative CI MDQ's for 56 compounds.....	33
10. Comparison of EI,PCI, and NCI sensitivities.....	36
11. Ion chromatogram at m/z 72 of Diuron.....	43
12. Ion chromatogram at m/z 184 of Benzidine.....	44
13. Ion chromatogram at m/z 182 of Phosalone.....	45
14. Ion chromatogram at m/z 58 of Dipropetryn.....	46
15. Ion chromatogram at m/z 198 of Metribuzin.....	47
16. Ion chromatogram at m/z 144 of Carbaryl.....	48
17. Ion chromatogram at m/z 125 of Fenvalerate.....	49
18. Ion chromatogram at m/z 84 of Amitrole.....	50
19. Ion chromatogram at m/z 68 of Aldicarb.....	51
20. Ion chromatogram at m/z 171 of Paraquat.....	52
21. Area and RF vs Amount Injected of Diuron.....	53
22. Area and RF vs Amount Injected of Benzidine.....	54
23. Area and RF vs Amount Injected of Phosalone.....	55

24.	Area and RF vs Amount Injected of Dipropetryn.....	56
25.	Area and RF vs Amount Injected of Metribuzin.....	57
26.	Area and RF vs Amount Injected of Carbaryl.....	58
27.	Area and RF vs Amount Injected of Fenvalerate.....	59
28.	Area and RF vs Amount Injected of Amitrole.....	60
29.	Area and RF vs Amount Injected of Aldicarb.....	61
30.	Area and RF vs Amount Injected of Paraquat.....	62
31.	Geometrical Representation of 3-Dimensional Box- Behnken Design.....	68
32.	Normal Probability Plot of Residuals.....	72
33.	Effect of Source Temperature and %Methanol on Sigma 1.....	74
34.	Effect of %Methanol and Helium Flow on Sigma 1...	75
35.	Effect of Source Temperature and Helium Flow on Sigma 1.....	76
36.	Effect of %Methanol and Desolvation Chamber Temperature on Sigma 1.....	77
37.	Effect of Desolvation Chamber Temperature and and Helium Flow on Sigma 1.....	78
38.	Effect of Desolvation Chamber Temperature and Source Temperature on Sigma 1.....	79
A1.	Electron Impact Spectrum of Diuron.....	87
A2.	Electron Impact Spectrum of Benzidine.....	88
A3.	Electron Impact Spectrum of Phosalone.....	89
A4.	Electron Impact Spectrum of Dipropetryn.....	90
A5.	Electron Impact Spectrum of Metribuzin.....	91
A6.	Electron Impact Spectrum of Carbaryl.....	92
A7.	Electron Impact Spectrum of Fenvalerate.....	93

A8.	Electron Impact Spectrum of Amitrole.....	94
A9.	Electron Impact Spectrum of Aldicarb.....	95
A10.	Electron Impact Spectrum of Paraquat.....	96
B1.	Normal Probability Plot of Residuals.....	98
B2.	Effect of Desolvation Chamber Temperature and Helium Flow on Sigma 2.....	99
B3.	Effect of Desolvation Chamber Temperature and Source Temperature on Sigma 2.....	100
B4.	Effect of %Methanol and Helium Flow on Sigma 2..	101
B5.	Effect of %Methanol and Source Temperature on Sigma 2.....	102
B6.	Effect of %Methanol and Desolvation Chamber Temperature on Sigma 2.....	103
B7.	Effect of Source Temperature and Helium Flow on Sigma 2.....	104

CHAPTER I

INTRODUCTION

1.1 IMPORTANCE OF LIQUID CHROMATOGRAPHY/MASS SPECTROMETRY

Hyphenated mass spectrometry techniques are now the preferred methods for the determination of a wide range of natural products (1-3), environmental pollutants (4-8), metabolites (1,2,9), and synthetic organic reaction mixtures (2). These techniques include gas chromatography/mass spectrometry (GC/MS), supercritical fluid/mass spectrometry (SFC/MS) and liquid chromatography/mass spectrometry (LC/MS). In recent years, liquid chromatography (LC) has matured into the most versatile of the chromatographic techniques. LC has fewer sample restrictions when compared to SFC or GC, basically, the only requirement being that the sample have slight solubility in the mobile phase. Nonvolatile and very polar samples are routinely analyzed by LC. The technique has further matured due to advances in column and detector technology. New column packing materials and improved column packing procedures have expanded the

range of compounds amenable to separation by HPLC(10,11). Because of this, LC/MS is regarded as the most powerful of the chromatography/MS techniques.

LC/MS offers several benefits to the chromatographer. First, the MS is a universal detector. Unlike detection by UV or visible absorption, no derivatization is necessary to assure an absorbing functional group is present. Detection levels in MS are not effected by extinction coefficients as is detection by these photometric methods. The MS is also not limited to isocratic separations as is the refractive index detector. Gradients normally do not affect the sensitivity of the MS. Second, the MS is a tool used both to detect and identify molecules. LC/MS yields three dimensional data. Both a chromatographic response of detector signal versus retention time and a mass spectrum are available for each eluting component. The mass spectrum often includes the most important information necessary for the identification of the analyte; the molecular ion and fragment ions defining various substructures present in the molecule. Third, MS detection levels are routinely on the order of picograms. Such sensitivity can be achieved by one of 3 ionization modes: electron impact (EI), positive ion chemical ionization (PCI), or negative ion chemical ionization (NCI). Molecules which are electro-positive are amenable

to detection by PCI or if electro-negative they are amenable to NCI.

Just as liquid chromatography has matured, so has mass spectrometry. A variety of ionization techniques coupled with high mass ranges are now available to analyze compounds that were previously not possible because of low volatility or high polarity. These advances have forced chemists to explore new methods of separation and on-line introduction into the mass spectrometer. Some of these new methods of sample introduction are discussed in the following section.

1.2 REVIEW OF LC/MS TECHNIQUES

While the coupling of liquid chromatography with mass spectrometry has afforded chemists the ability to separate and identify molecules that were previously impossible to resolve and identify by other techniques, the problems involved in interfacing the LC to the MS are not trivial. A few of the problems are described below. The LC is operated at near ambient temperature, while the MS is typically operated at elevated temperatures such as 250°C. This requires rapid heating of the LC effluent to a suitable temperature before entering the MS. Because of the elevated temperatures and high vacuum in the MS, molecules must be in the vapor phase in order to be

analyzed. This is clearly a problem for LC which operates at ambient temperature. The LC also operates with liquid flow rates between 0.1 and 2 ml/min., while mass spectrometers are designed to operate at high vacuum and to accommodate gas flows of up to 10 ml/min. A simple conversion of LC flow rates to gas volume dramatically demonstrates the incompatibility between LC and MS. One milliliter of water generates approximately 1200 ml of gas at STP, assuming an ideal gas.

Early efforts to combine LC and MS made use of a moving belt interface(1). This interface may best be described as a flexible ribbon of polyimide continuously moving around a set of rollers. One roller is located outside the MS, but still inside a chamber evacuated by a rotary pump. A small portion of the LC effluent (5-20 μ l/min.) is deposited on the ribbon. The ribbon then transports the effluent through a series of heaters and vacuum locks in order to evaporate the solvent off the analyte. The other roller is located inside the MS in a position similar to that of the terminus of a direct insertion probe. At this point the ribbon is heated rapidly in order to evaporate the analyte into the ion source of the MS (see fig. 1).

The major advantage of the moving belt interface is its ability to use several modes of ionization. The solvent is removed from the analyte during the transport

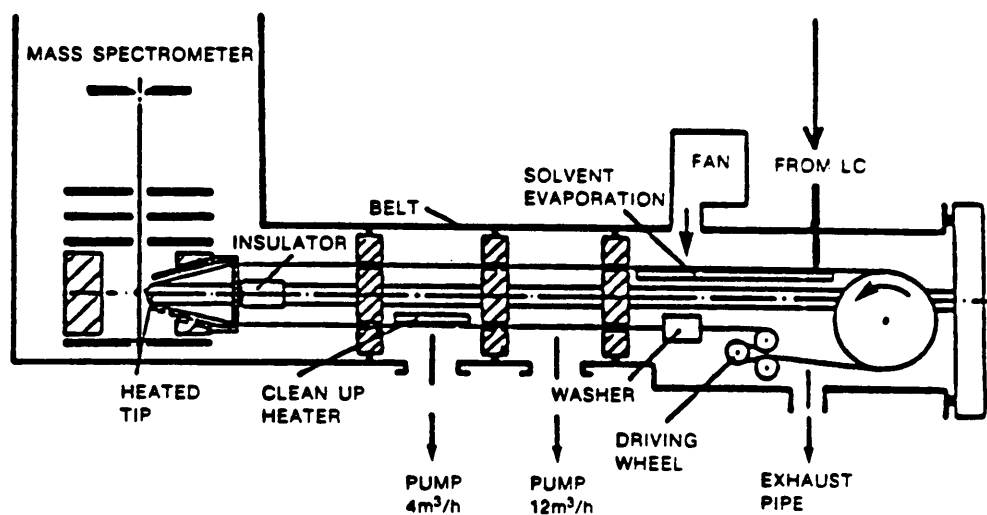


Figure 1 :Schematic of a Moving Belt LC/MS Interface

process. This allows for classical electron impact (EI) spectra without interference from solvent gas chemical ionization or self chemical ionization both of which can occur when the pressure inside the ion source rises. In addition, chemical ionization (CI) spectra are possible, using the reagent gas of choice. Unfortunately, despite this advantage, the moving belt interface has fallen from favor. Several problems associated with this interface include: 1) the uneven deposition of LC effluent compromises the chromatography by increasing the band width of each peak; 2) the difficulty in evaporating highly aqueous mobile phases from the analyte during transport, which leads to vacuum problems in the MS; 3) the loss of volatile analytes during mobile phase evaporation; and 4) the difficulty in evaporating thermally labile and non-volatile analytes from the moving belt once it is inside the ion source. All these factors have made other LC/MS interface methods more attractive.

Direct-liquid introduction was another early LC/MS interface method (1). This method was, and is still, the simplest and least expensive interface for LC/MS. The method involves the introduction of a fine jet of LC effluent directly into the ion source of the MS. The effluent is limited to 10-20 $\mu\text{l}/\text{min}$. because of MS vacuum limitations. No attempt is made to remove the solvent

and therefore, only CI is possible. Unfortunately, the solvent from the LC must act as the reagent gas (see fig. 2). There is, however, no heating of the effluent prior to MS analysis and for this reason, DLI-LC/MS is often associated with the analysis of difficult thermally labile or fragile analytes such as carbohydrates(3), peptides(12), and sterol glycosides(13).

Despite the simplicity and advantages DLI-LC/MS offers for thermally labile analytes, it suffers from several problems: 1) DLI-LC/MS requires that the MS have cryopumping capabilities, which in turn requires the lab to maintain a supply of liquid nitrogen; 2) In order to restrict the flow of effluent into the MS ion source and generate the fine jet of liquid necessary for introduction into the ion source, the DLI interface uses a frit with a 5 um pinhole. This pinhole can, and often does, become clogged during operation of the interface; 3) Frequently the effluent from the LC separation is not acceptable as a reagent gas for the chemical ionization of the analyte. This is often the case when water must serve as the reagent gas and its proton affinity is too low for a soft ionization of labile analytes. Or in the case of very stable analytes the proton affinity may be too high for the amount of fragmentation necessary for the determination of substructure, therefore making identification difficult.

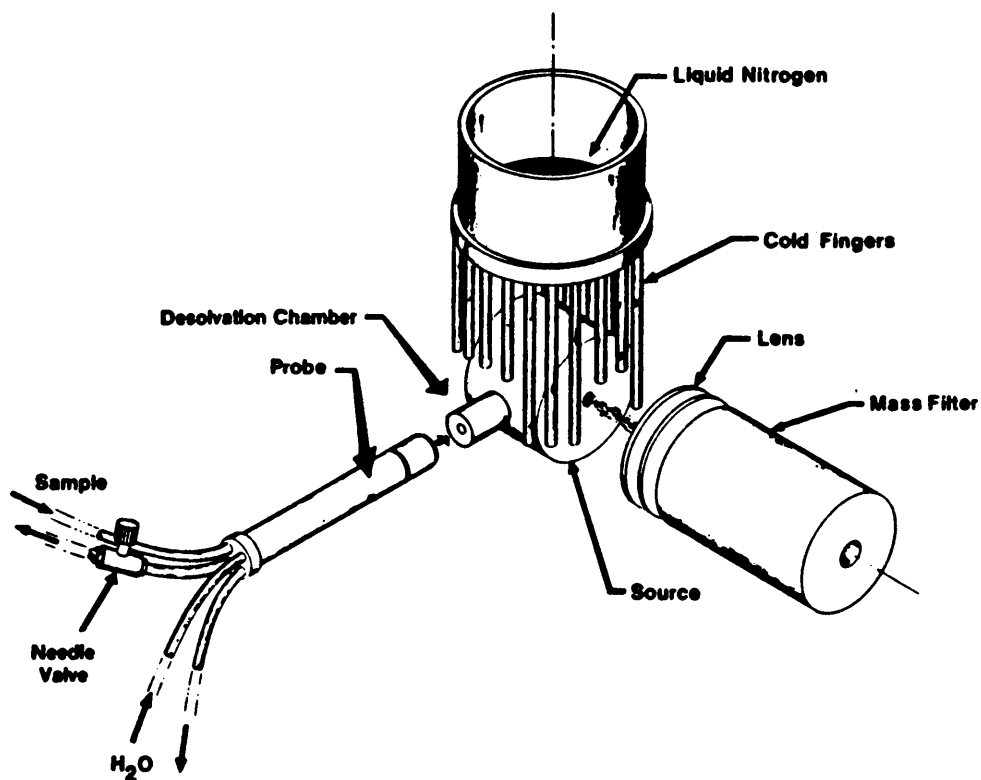


Figure 2 :Schematic of a Direct Liquid Introduction LC/MS Interface

Thermospray is currently the most popular method for LC/MS and can be credited with bringing routine LC/MS into the laboratory(14). Its development was a result of research designed to improve the operation of DLI-LC/MS. This research consisted of efforts to rapidly heat the LC effluent prior to introduction into the MS and thereby improving its vaporization. This resulted in the formation of ions when the LC effluent, which contained an electrolyte, was subjected to rapid heating in a vaporizer tip and then introduced into a heated ion source in the form of an aerosol. This is thought to occur through the a process called "ion evaporation"(14) (see fig. 3). Ion evaporation is a result of a portion of the droplets from an aerosol containing an electrolyte being charged. These charged droplets will eject an ion as the solvating layer around the charge is evaporated. The ejected ions are then sampled through a cone in much the same way ions are sampled from a CI ion source. Later development allowed the production of ions through conventional CI processes in which a filament is used with the solvent and electrolyte acting as reagent gas. In either case the ionization is very mild and the analyte is ionized directly from the effluent. Samples need not be in the vapor phase before entering the ion source making thermospray useful for the analysis of non-volatile compounds such as carbohydrates(15);

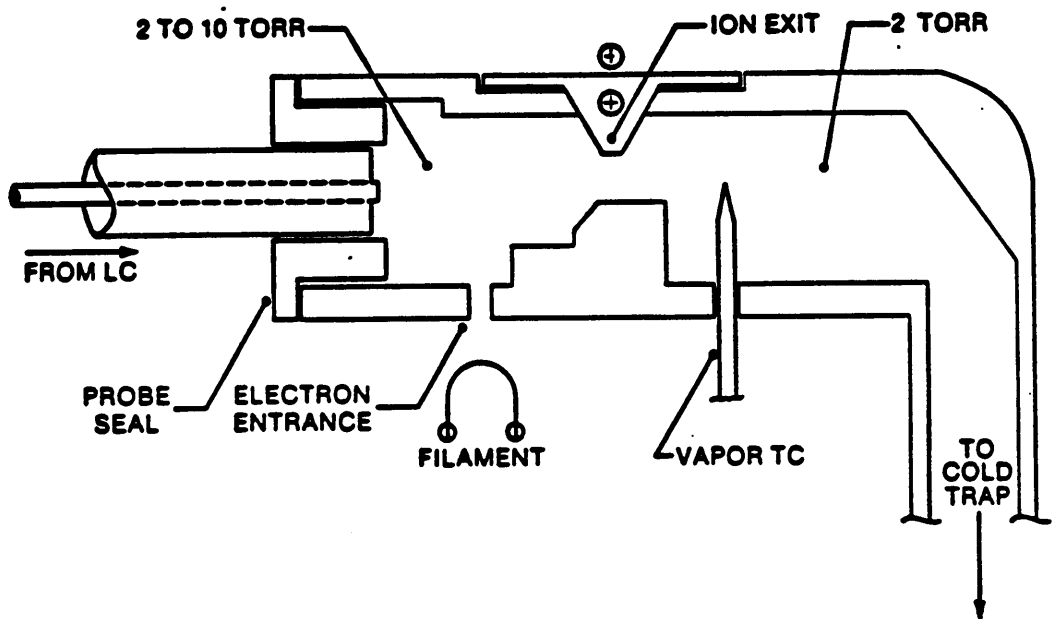


Figure 3 :Schematic of a Thermospray LC/MS Interface

peptides(16); and antibiotics(14). Another advantage of thermospray is that the ion source allows a design that accomodates typical LC flow rates of 0.4 - 2 ml/min. This is accomplished by removal of excess vapor to a methanol-dry ice temperature cryopump.

Thermospray's current use is widespread. It is however, not a simple technique to operate. The temperature of the vaporizer probe is critical as is the temperature of the ion source. In addition, although the orifice of the vaporizer tip is large (150 um) in comparison to DLI's 5 um frit, the vaporizer tip still has a tendency to clog. This is especially true when the vaporizer is operated at a temperature high enough to produce a dry aerosol. Finally, this technique is unable to produce EI spectruea due to the high concentration of solvent molecules. For unknown analytes this means only molecular weight information may be obtained.

These disadvantages for the current LC/MS interfaces and the desire for a more routine, simple to operate, and dependable interface led to the development of the particle beam LC/MS interface. Its development is described below.

1.3 DEVELOPMENT OF THE MAGIC LC/MS INTERFACE

Monodispersed Aerosol Generation Interface Combining LC and MS (MAGIC LC/MS)(17) was the first interface to

incorporate many of the advantages of the early LC/MS interfaces without many of the disadvantages. MAGIC LC/MS provides for solvent removal in order to generate classical EI spectra and for selection of CI reagent gas. The sample transport into the ion source is gentle as in the DLI interface and will accommodate typical LC flow rates as in thermospray. The MAGIC LC/MS interface consists of two parts, the nebulizer and the momentum separator. It operates as follows: a gas nebulizer (typically helium at 1-2 liters/min.) generates an aerosol using the LC effluent as it exits a 100 μm capillary. This creates droplets of approximately 10 μm diameter (18). The aerosol is then passed through the temperature controlled desolvation chamber where the solvent is evaporated from the analyte. After solvent removal, the analyte forms a moist sub-micron particle. The solvent vapor and submicron particles pass through a nozzle which serves to funnel them into a two stage momentum separator. Upon entering the first stage separator the vapor and particles undergo a supersonic expansion due to the high vacuum. The lighter solvent vapors diffuse more rapidly and are pumped away, while the analytes which possess a greater momentum travel along the axis into the second stage separator. The process is repeated in the second stage of the momentum separator. The supersonic particles exiting the momentum

separator are transported directly to the ion source via a transport tube. The particles reaching the ion source are devoid of solvent and can be volatilized and analyzed by standard MS techniques including EI and CI (see fig. 4).

The original design for the MAGIC LC/MS interface used a right angle nebulizer adjusted by screws with three degrees of freedom. Adjustments were made in the z-axis to bring the nebulizing gas nearer to the jet of LC effluent, and in the x- and y-axes to bring the nebulizing gas in line with the effluent jet. The momentum separator needed to be adjusted in order to allow maximum sample transport and solute enrichment (23).

The principle of the MAGIC LC/MS interface interested the Hewlett-Packard company and a commercial version of the MAGIC LC/MS interface known as the particle beam LC/MS (PBLC/MS) interface was developed as follows.

1.4 DEVELOPMENT OF THE PARTICLE BEAM LC/MS INTERFACE

The original design of the MAGIC LC/MS interface had three basic flaws that were corrected in the commercial version, PB-LC/MS(18). The three degrees of adjustment needed to optimize the nebulizer made the operation of the MAGIC system cumbersome. This was replaced with a

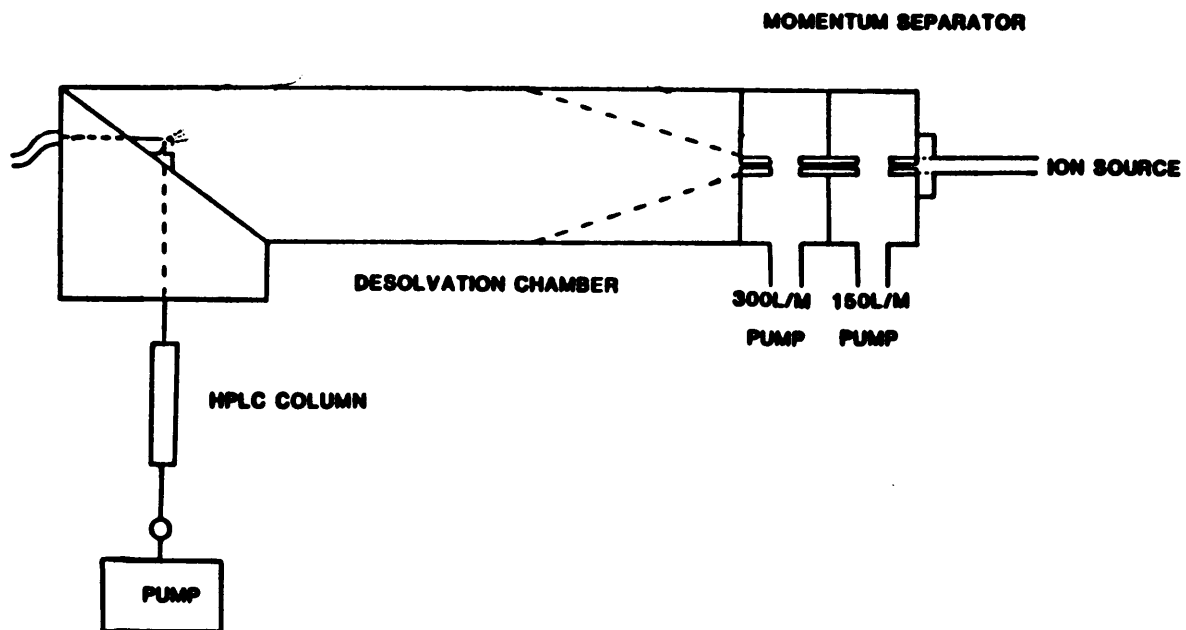


Figure 4 :Schematic of a MAGIC LC/MS Interface

co-axial helium nebulizer requiring only one degree of adjustment, the position of the effluent capillary relative to the nebulizer gas (see fig. 5). The helium flow was maintained at 1-2 liters/min. which generated a pressure of approximately 200 torr in the desolvation chamber. The other two enhancements are in the momentum separator. The shape and angle of the momentum separator was changed by using CAD (computer aided design) modeling and empirical testing to optimize the pumping of solvent vapors and transmission of the particle beam to the ion source. After the modelling was completed, a cast with pre-aligned separators was made. This eliminates the difficult alignment steps which were necessary to optimize the response of the original design. The final version of the PB-LC/MS was able to maintain a pressure of approximately 200 torr in the desolvation chamber, 5-20 torr in the first stage of the momentum separator, and approximately 0.2 torr in the second stage of the momentum separator (see fig. 6).

1.5 SCOPE AND GOALS

The scope of this thesis was to examine the performance characteristics of the PB-LC/MS for the chromatographic and mass spectral analysis of model compounds that have a high priority as candidates for LC/MS. The EPA appendix VIII and IX compounds were chosen due to their difficulty and lack of alternate

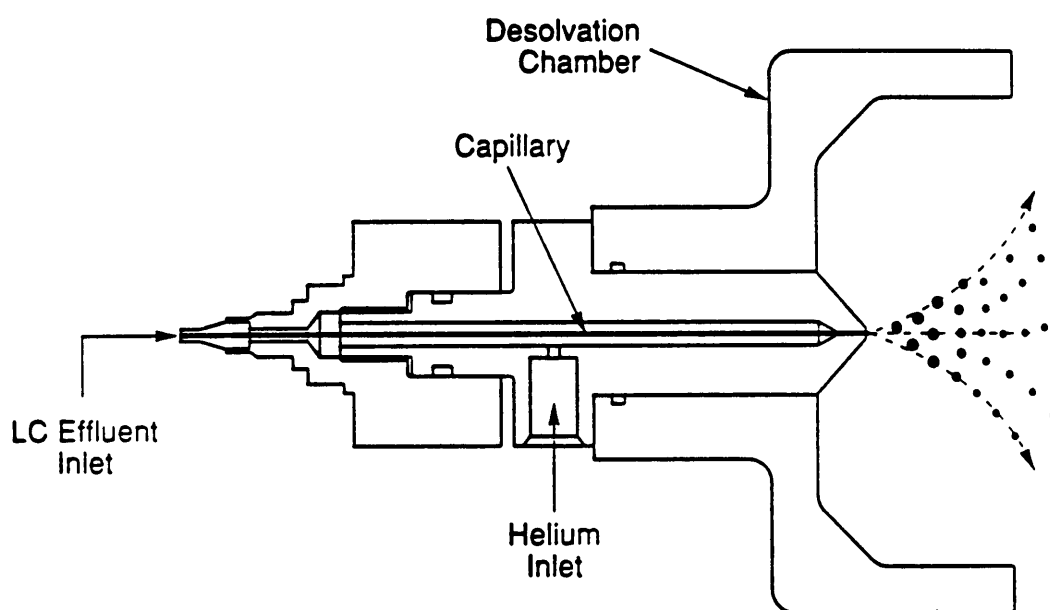


Figure 5 :Schematic of a Particle Beam Nebulizer

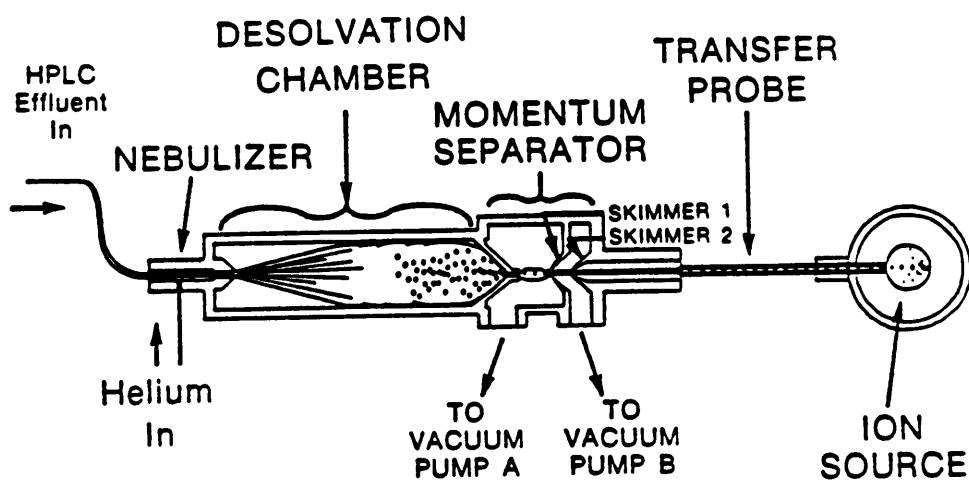


Figure 6 :Schematic of a Particle Beam LC/MS Interface

methods of detection and quantitation. The goals of this thesis were to determine if in fact the EPA appendix VIII and IX compounds could be analyzed by PB-LC/MS and if so, what were the optimum PB interface and MS conditions for the analyses.

CHAPTER II

EXPERIMENTAL

2.1 MATERIALS

Diazepam, methyl stearate, and caffeine were obtained from Sigma Chemical Company, (St.Louis, MO). HPLC grade methanol and HPLC grade water were obtained from Fisher Scientific Company, (Fair Lawn, NJ). Samples listed in the appendix VIII and appendix IX compounds (see table 1) were obtained from the U.S. Environmental Protection Agency, (Research Triangle, NC) . Methane reagent gas was U.H.P. grade (Matheson Gas Products, INC., East Rutheford, NJ). Helium carrier and nebulizer gas was U.H.P. grade (Matheson Gas Products, INC., East Rutheford, NJ).

2.2 EQUIPMENT

All analysis were performed on a Hewlett-Packard (HP) 5988A Mass Spectrometer equipped with negative ion detection and mass range 2000. In addition the 5988A was equipped with an HP 5890 GC and HP 7673 automatic sampler. The 5988A was controlled by an HP 9000 series 300 Chemstation. Data files were uploaded to an HP 1000 A-series computer for additional data processing. Liquid

sample introduction was through an HP model 1090L Liquid Chromatograph with DR-5 ternary solvent delivery system fitted with a 25 ul automatic injector and automatic sampler. The interface between the LC and the MS was an HP 59980A Particle Beam interface.

2.3 Methods

Sample introduction for all PB-LC/MS analysis was by flow injection analysis (FIA) unless stated otherwise. All LC/MS samples were made to a concentration of 100 ng/ul unless stated otherwise. LC mobile phase was 100% methanol at a flow rate of 0.4 ml/min.

PB nebulizer helium flow was approximately 1.5 - 2 liters/min. unless stated otherwise. PB desolvation chamber temperature was 45°C unless stated otherwise. PB nebulizer settings were optimized using caffeine. This was accomplished by adjusting the positions to achieve the maximum signal.

The HP 5988A MS was operated at a source temperature of 250°C unless stated otherwise. The MS was tuned manually for EI analyses by optimizing for mass 219 of perfluorotributyl amine. All positive CI and negative CI analyses were performed with methane as reagent gas at a source temperature of 250°C and a source pressure of 1 torr.

The HP 5890 GC was operated in the splitless mode using a 12 m x 0.20 mm i.d. HP-1 fused silica capillary

column and a linear gas velocity of 35 cm/sec. at 240°C. The oven temperature program was 1 min. at an initial temperature of 100°C. Then increased at 30°C/min. to 280°C where it was maintained for 5 min.

CHAPTER III

RESULTS AND DISCUSSION

3.1 INTRODUCTION

The results and discussion are divided into three sections: minimum detectable quantity (MDQ), linearity, and band broadening. Each section contains an explanation of the experimental design and theory. The MDQ study was a comprehensive examination of 158 EPA appendix VIII and IX compounds detected in the EI, positive CI, and negative CI modes. An explanation as to the performance of particular compounds is offered. The linearity study illustrated the response of 10 compounds analyzed at five different concentrations. Response factors (RF) are generated and graphed versus amount of analyte injected. The particle beam's contribution to peak broadening was explored using a Box-Behnken experimental design. The individual and combined effects of source temperature, desolvation chamber temperature, helium flow, and percent methanol are demonstrated using response surfaces.

3.2 MINIMUM DETECTABLE QUANTITY

This was a comprehensive study of the detection limits of a wide variety of compounds known to be environmental pollutants. Sample preparation and instrumentation is described in chapter II section 2.2, 2.3. Each sample was injected at a concentration of 100 ng/ul or increments thereof depending on the sample response. A procedure file was written to baseline subtract out the random noise which changes from day to day. This is considered normal data treatment. The signal to noise ratio (S/N) was then calculated from the total ion chromatogram and defined as:

$$S/N = (\text{MAXIMUM SIGNAL} - \text{DC NOISE}) / \text{RMS NOISE}$$

where

$$\text{DC NOISE} = \text{AVERAGE NOISE RELATIVE TO 0}$$

and

$$\text{RMS NOISE} = (\text{MAXIMUM NOISE} - \text{MINIMUM NOISE}) / 5.$$

The calculated S/N's for the three injections per compound were then averaged. The MDQ was defined in this study as the amount of analyte required which yields a S/N of 2. Therefore, the equation used to calculate the MDQ is defined as:

$$\text{MDQ} = 2 (\text{AMOUNT INJECTED}) / (\text{AVERAGE S/N}).$$

The MDQ's of 106 appendix VIII and IX compounds analyzed by EI are shown in bar graph form in figure 7. The compounds are sorted by increasing MDQ. Table 1 contains the list of compounds corresponding to the compounds in the bar graph.

Chemical selectivity and technical considerations allowed 90 of the compounds to be analyzed by methane positive CI and 56 of the compounds to be analyzed by methane negative CI. Not all compounds are amenable to methane CI due to proton affinity and electronegativity characteristics. The MDQ results for the positive CI analyses are graphed and listed in figure 8 and table 2, respectively. The MDQ results for the negative CI analyses are shown in figure 9 and table 3. As with the EI MDQ's, the positive CI and negative CI MDQ's are sorted by increasing MDQ. A comparison of the relative MDQ's for 56 of the compounds analyzed in all three ionization modes is presented in figure 10 and table 4. Figure 10 clearly shows that for compounds amenable to all three modes of ionization (EI, positive CI, and negative CI), negative CI analyses are the most sensitive. This is probably not a function of the particle beam interface, but may be due to the mass spectrometer design. The 5988A MS utilizes a 2400V

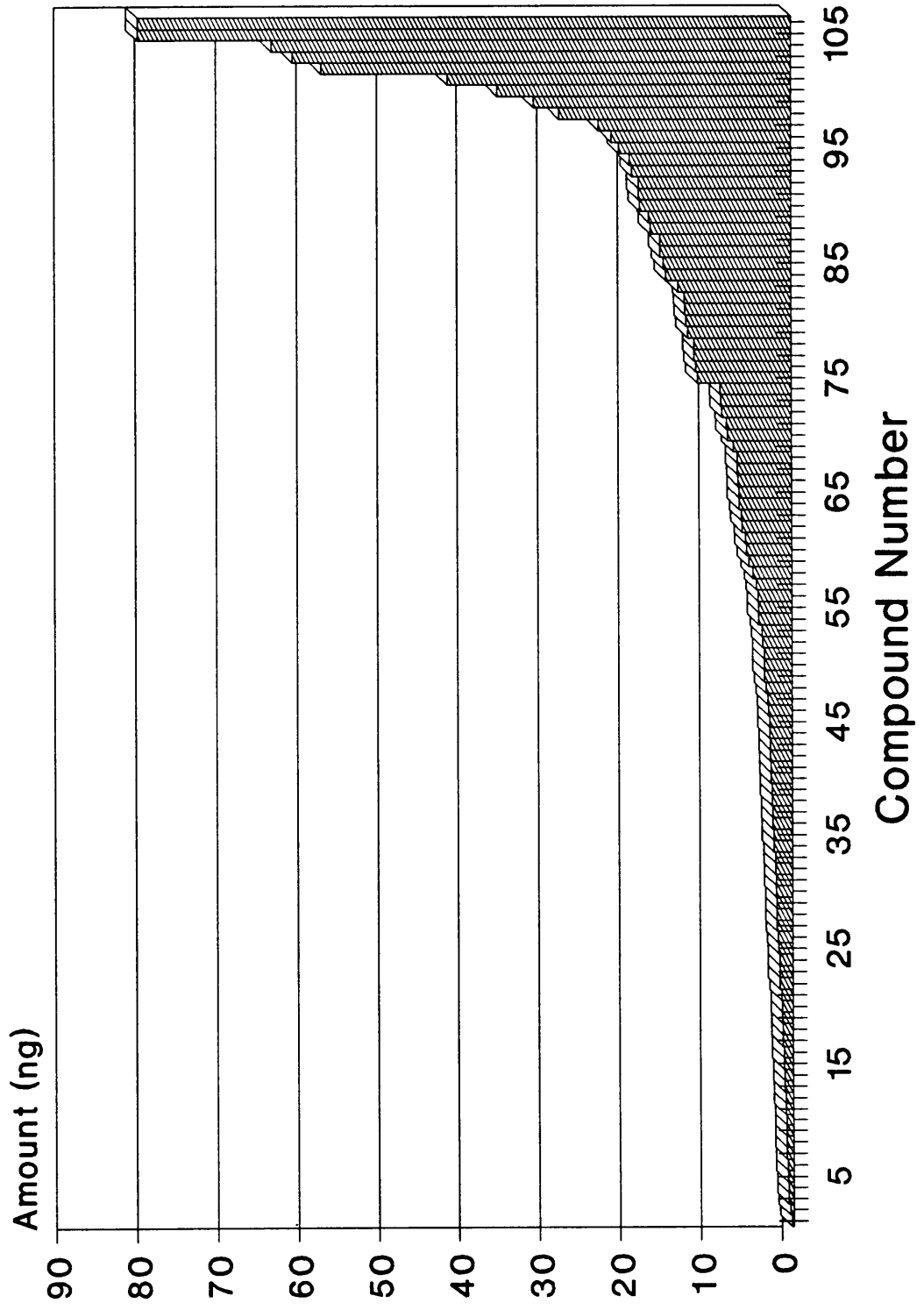


Figure 7 :Electron Impact MDQ's of 106 compounds

TABLE 1

Minimum Detectable Quantities* for EI MS

<u>Compound Name</u>	<u>EI MDQ (ng)</u>
Piperonyl butoxide	0.2
Phenothiazine	0.4
Benzidine	0.6
Diuron	0.6
3,3-Dichlorobenzidine	0.7
Phosalone	0.7
3,3'-Dimethoxybenzidine	0.8
Hexazinone	0.8
Isofenphos	0.8
Tebuthiuron	0.8
Cyprazine	0.9
Methoxuron	0.9
Atrazine	1.0
Siduron	1.0
Cyanazine	1.1
Proparagite	1.1
4,4-Methylenebis(o-chloroaniline)	1.2
Sulprofos	1.2
Fenvalerate	1.3
Oxyfluorfen	1.3
Fluometuron	1.4
Benzenesulfonamide	1.6
Methiocarb	1.6
Prometryn	1.6
Methidathion	1.7
Pyrethrins	1.8
2,4-D	1.9
Allethrin	1.9
Terbutryn	1.9
Neburon	2.0
Terbuthylazine	2.0
Aldicarb sulfone	2.1
Dipropetryn	2.1
Chlorobromuron	2.3
Procyazine	2.3
Bifenox	2.4
Paraquat	2.4
1-(2-Chlorophenyl-2-thiourea)	2.5
Linuron	2.5
Phenylthiourea	2.6
Thiourea	2.6
Desmedipham	2.7

*MDQ's have been extrapolated assuming a linear response.

TABLE 1 (cont.)

<u>Compound Name</u>	<u>EI MDQ (ng)</u>
Metribuzin	2.7
Ametryn	2.8
Chlortoluron	2.8
Phenylendiamine	2.9
Ethylenethiourea	3.0
Cycloheximide	3.2
Atraton	3.4
Prometon	3.4
Temephos	3.4
Metolachlor	3.6
Amitrole	3.7
Karbutilate	4.1
Monuron	4.1
Diquat	4.2
Carbaryl	4.4
1,2-Dimethyl hydrazine	4.8
Aminocarb	5.3
Anilazine	5.6
Propoxur	5.7
N-methyl-N-nitrosoourea	6.1
N-methyl-N-nitroso-N'-nitroquandine	6.2
Metobromuron	6.5
Trietazine	6.5
Vinylidene chloride	6.6
Chlorpyrifos methyl	6.7
Propazine	6.7
Pendimethalin	7.2
Isoproturon	7.9
Thiofanox	8.0
Monolinuron	8.6
Methomyl	8.7
Acephate	8.8
Chlorophacinone	11.6
Phenylarsonic acid	11.8
Dodine	12.0
Bromoxynil	12.7
Promcarb	12.8
Perfluidone	13.0
2,3-epoxy-1-propanol	13.1
Coumafuryl	13.2
Thiram	14.0
Mefluidide	15.5
Benzyl benzoate	15.8
Aldicarb	16.2

*MDQ's have been extrapolated assuming a linear response.

TABLE 1 (cont.)

<u>Compound Name</u>	<u>EI MDQ (ng)</u>
Naptalam sodium	16.2
2,4-toluene diamine	17.4
Warfarin	17.6
2,4,5-T	18.7
1,3-Propane sulfone	18.9
Bromoacetone	18.9
Chloramben	19.7
Endothal	20.0
Saccharin	21.3
Maleic hydrazide	22.2
Silvex	23.8
4-Aminopyridine	28.7
Crotonaldehyde	31.9
Propham	36.4
Ethylene diamine	42.6
Creosote	58.3
2-Butanone peroxide	61.9
Choroacetaldehyde	64.5
2-Chloroethylvinyl ether	81.1
Glyphosine	81.1

*MDQ's have been extrapolated assuming a linear response.

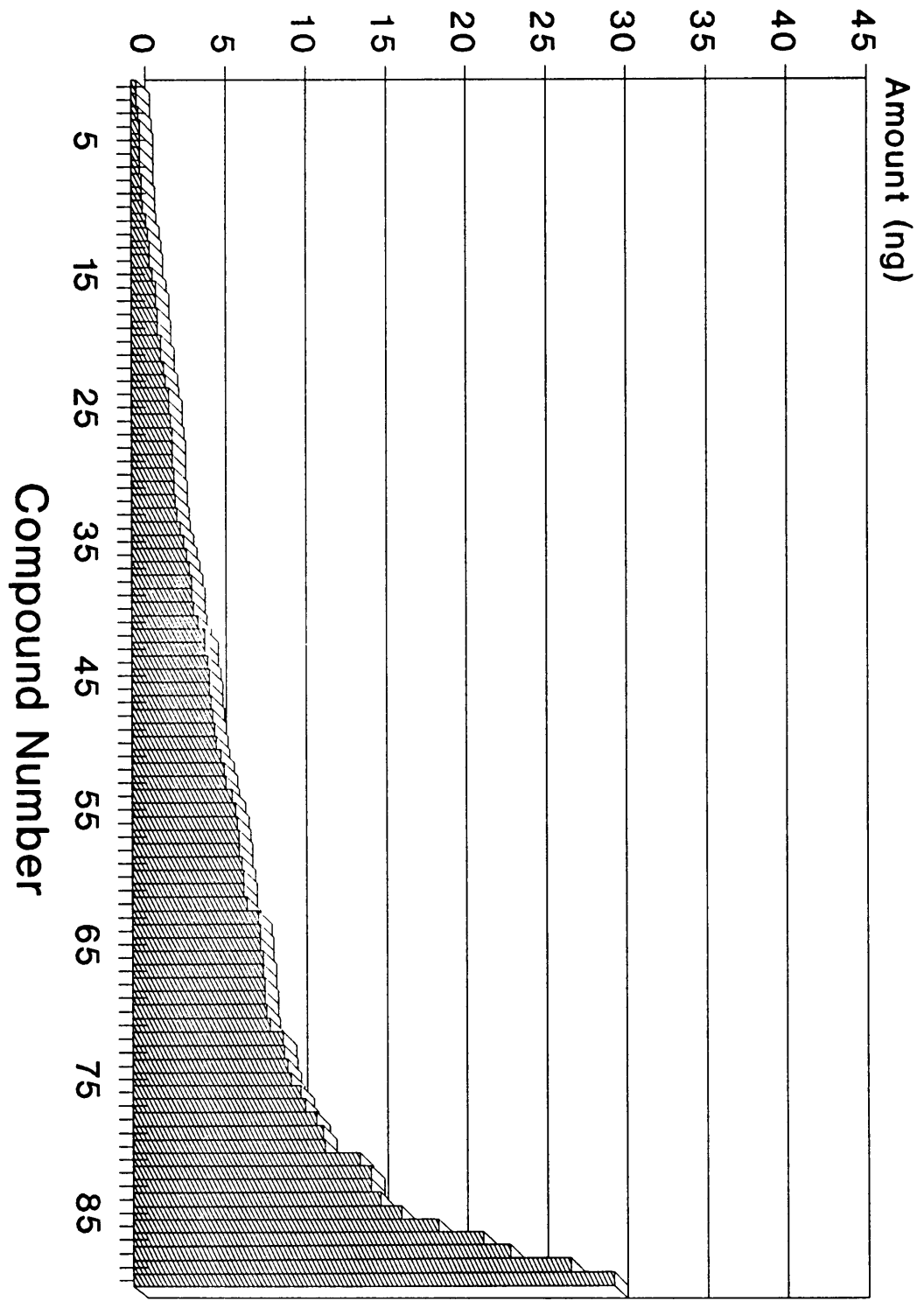


Figure 8: Positive CI MDQ's of 90 compounds

TABLE 2

Minimum Detectable Quantities* for PCI MS

<u>Compound Name</u>	<u>PCI MDQ (ng)</u>
Cyanazine	0.3
Phenothiazine	0.3
Aldicarb sulfone	0.5
4,4-Methylenebis(o-chloroaniline)	0.5
Atrazine	0.5
Cyprazine	0.5
Piperonyl butoxide	0.5
Allethrin	0.6
Methidathion	0.6
Diuron	0.7
Metribuzin	0.9
Sulprofos	1.0
Cycloheximide	1.1
Oxyfluorfen	1.1
Phosalone	1.3
Fenvalerate	1.5
Siduron	1.5
Benzidine	1.6
Methoxuron	1.6
Fluometuron	1.8
Neburon	1.8
Chlorbromuron	2.0
Hexazinone	2.1
3,3-Dimethoxybenzidine	2.3
Chlortoluron	2.3
Linuron	2.4
Karbutilate	2.5
Phenylthiourea	2.5
Tebuthiuron	2.5
Benzyl benzoate	2.6
Phenylenediamine	2.6
Terbuthylazine	2.7
Aldicarb	2.8
Desmedipham	3.0
Endothal	3.2
Monolinuron	3.4
Anilazine	3.5
Dipropetryn	3.7
Proparagite	3.7
Thiram	3.8
Ethylene thiourea	4.1
2,4-D	4.5

*MDQ's have been extrapolated assuming a linear response.

TABLE 2 (cont.)

<u>Compound Name</u>	<u>PCI MDQ (ng)</u>
Procyazine	4.5
3,3-Dichlorobenzidine	4.8
Prometryn	4.8
Thiourea	4.9
Methomyl	5.0
4-Aminopyridine	5.1
Benzenesulfonamide	5.2
Monuron	5.5
Atraton	5.7
Silvex	5.8
Glyphosine	6.2
Terbutryn	6.4
Pyrethrins	6.5
Acephate	6.6
Chloramben	6.6
Amitrole	6.8
Pendimethalin	6.9
Propazine	6.9
Trietazine	7.1
Chlorophacinone	7.8
Metolachlor	7.9
Paraquat	7.9
Aminocarb	8.1
Isofenphos	8.1
Coumafuryl	8.2
Metobromuron	8.2
Warfarin	8.3
Promecarb	8.5
Carbaryl	9.3
Methiocarb	9.4
Naptalam sodium	9.6
Mefluidide	9.8
Prometon	10.4
Isoproturon	10.7
2,4,5-T	11.4
Bromoxynil	11.8
1,2-Dimethyl hydrazine	11.9
Thiofanox	14.1
Chlorpyrifos methyl	14.8
Diquat	14.8
Maleic hydrazide	15.4
Bifenox	16.7
Perfluidone	19.0
Temephos	21.8

*MDQ's have been extrapolated assuming a linear response.

TABLE 2 (cont.)

<u>Compound Name</u>	<u>PCI MDO (ng)</u>
Dodine	23.5
Propoxur	27.3
Saccharin	30.0

*MDQ's have been extrapolated assuming a linear response.

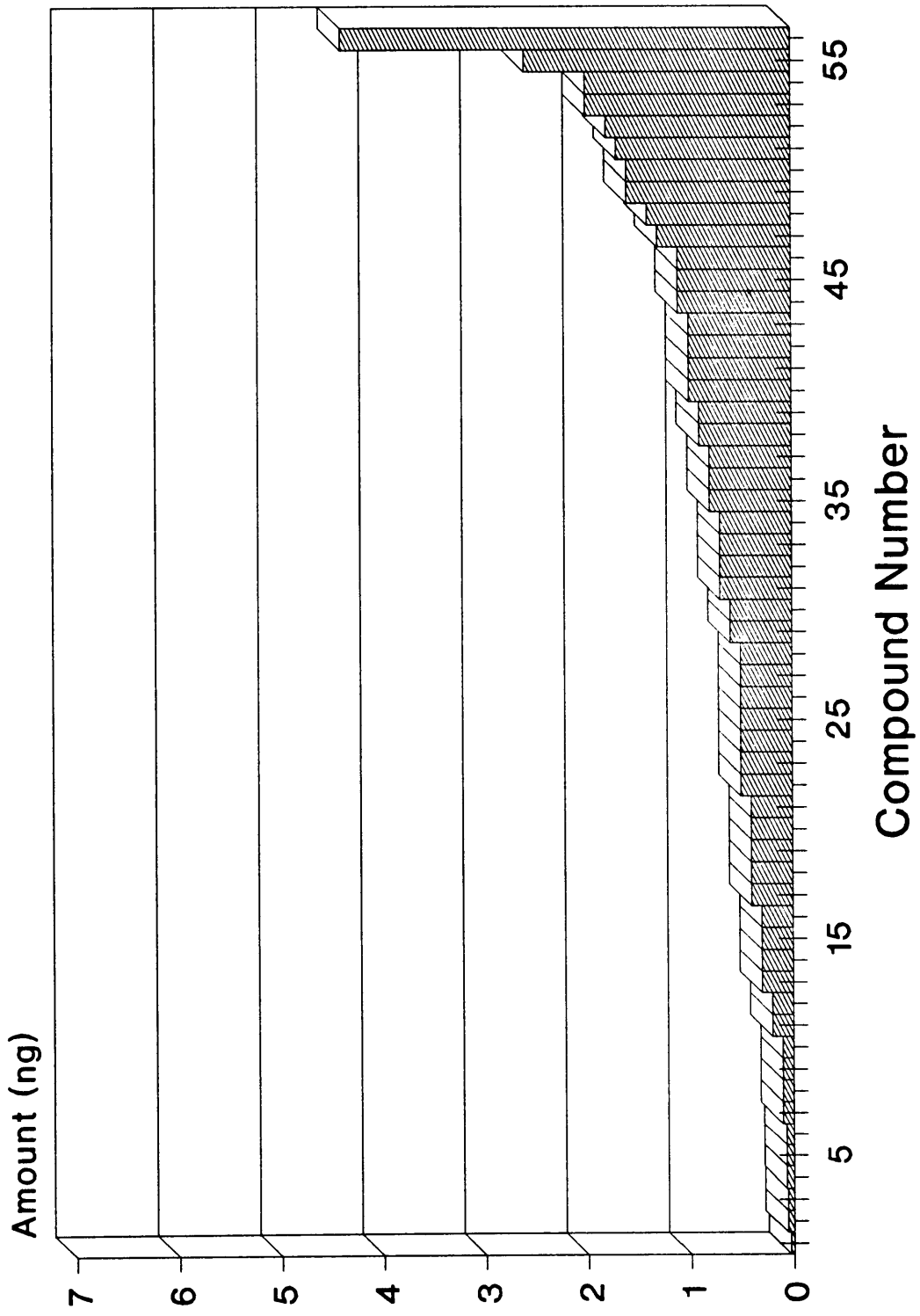


Figure 9 :Negative CI MDQ's of 56 compounds

TABLE 3

Minimum Detectable Quantities* for NCI MS

<u>Compound Name</u>	<u>NCI MDQ (ng)</u>
Diuron	0.1
Allethrin	0.1
Metribuzin	0.1
Cyanazine	0.1
Linuron	0.1
Methidathion	0.1
Aldicarb sulfone	0.1
Anilazine	0.1
Chlorbromuron	0.1
Pendimethalin	0.1
Cyprazine	0.2
Neburon	0.2
Atrazine	0.3
Dipropetryn	0.3
Methoxuron	0.3
Propazine	0.3
Atraton	0.4
Prometryn	0.4
Siduron	0.4
Silvex	0.4
Terbuthylazine	0.4
2,4,5-T	0.5
Ametryn	0.5
Fluometuron	0.5
Hexazinone	0.5
Methiocarb	0.5
Metobromuron	0.5
Terbutryn	0.5
Chloramben	0.6
Chlortoluron	0.6
Coumafuryl	0.7
Endothal	0.7
Phenothiazine	0.7
Warfarin	0.7
Bromoxynil	0.8
Isoproturon	0.8
Prometon	0.8
Aldicarb	0.9
Carbaryl	0.9
Aminocarb	1.0
Methomyl	1.0
Metolachlor	1.0

*MDQ's have been extrapolated assuming a linear response.

TABLE 3 (cont.)

<u>Compound Name</u>	<u>NCI MDQ (ng)</u>
Monuron	1.0
Acephate	1.1
Desmedipham	1.1
Monolinuron	1.1
Benzyl benzoate	1.3
Trietazine	1.4
Amitrole	1.6
Promecarb	1.6
Karbutilate	1.7
Propoxur	1.8
Glyphosine	2.0
Propham	2.0
Cycloheximide	2.6
Dodine	4.4

*MDQ's have been extrapolated assuming a linear response.

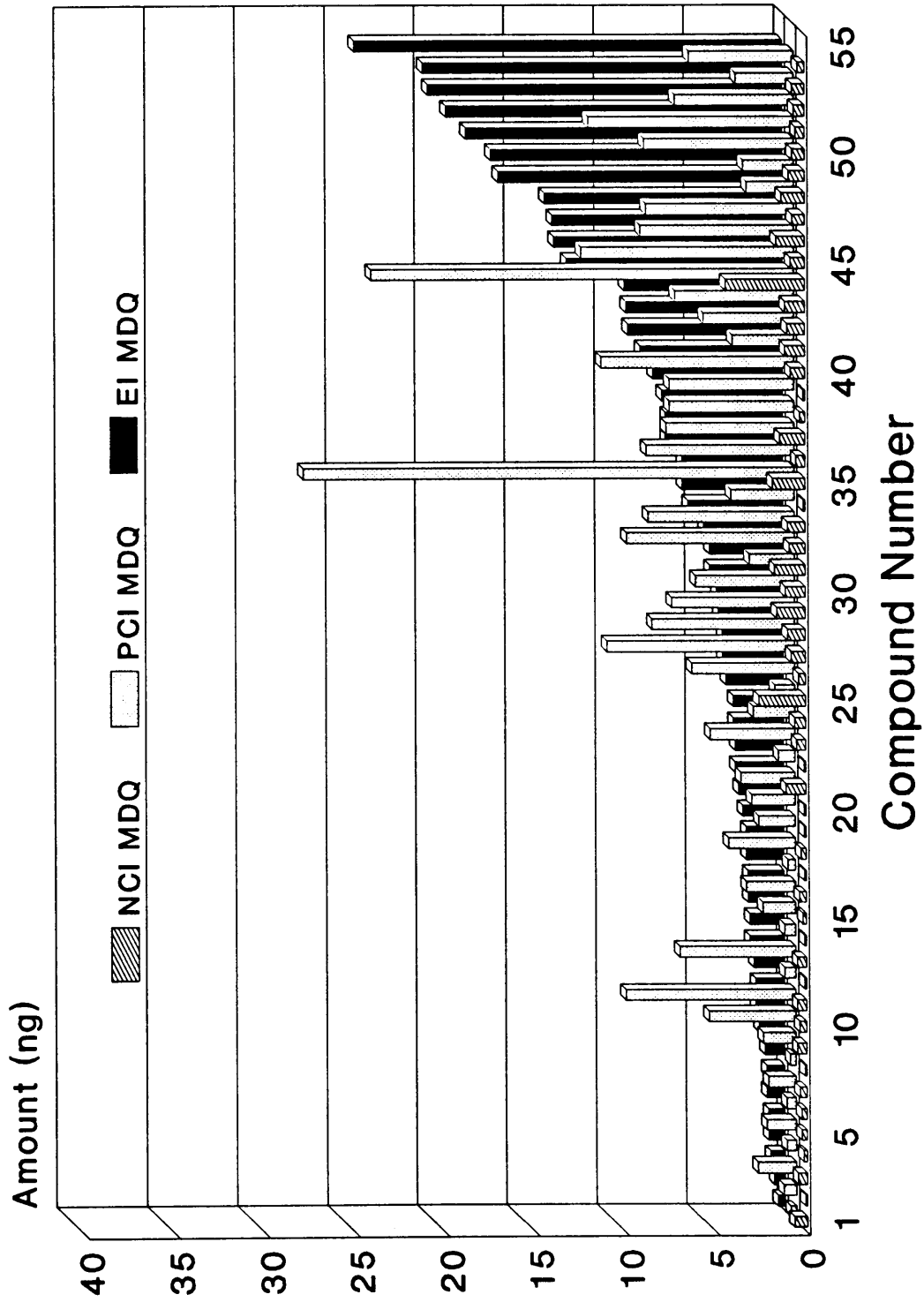


Figure 10 :A comparison of NCI, PCI, and EI sensitivities

TABLE 4

Minimum Detectable Quantities* for EI, PCI, NCI MS

Compound Name	EI MDQ (ng)	PCI MDQ (ng)	NCI MDQ (ng)
Phenothiazine	0.4	0.3	0.7
Diuron	0.6	0.7	0.1
Hexazinone	0.8	2.1	0.5
Methoxuron	0.9	1.6	0.3
Cyprazine	1.0	0.5	0.2
Atrazine	1.0	0.5	0.3
Siduron	1.0	1.5	0.4
Cyanazine	1.1	0.3	0.1
Fluometuron	1.4	1.8	0.5
Methiocarb	1.6	9.4	0.5
Prometryn	1.6	4.8	0.4
Methidathion	1.7	0.6	0.1
Allethrin	1.9	0.6	0.1
Terbutryn	1.9	6.4	0.5
Neburon	2.0	1.8	0.2
Terbuthylazine	2.0	2.7	0.4
Aldicarb sulfone	2.1	0.4	0.1
Dipropetryn	2.1	3.7	0.3
Chlorobromuron	2.3	2.0	0.1
Linuron	2.5	2.4	0.1
Desmedipham	2.7	3.0	1.1
Metribuzin	2.7	0.9	0.1
Ametryn	2.8	4.7	0.5
Chlortoluron	2.8	2.3	0.6
Cycloheximide	3.2	1.1	2.6
Atraton	3.4	5.7	0.4
Prometon	3.4	10.4	0.8
Metolachlor	3.6	7.9	1.0
Amitrole	3.7	6.8	1.6
Karbutilate	4.1	2.5	1.7
Monuron	4.1	5.5	1.0
Carbaryl	4.4	9.3	1.0
Aminocarb	5.3	8.1	1.0
Anilazine	5.6	3.5	0.1
Propoxur	5.7	27.3	1.8
Metobromuron	6.5	8.2	0.5
Trietazine	6.5	7.1	1.4
Propazine	6.7	6.9	0.3
Pendimethalin	7.2	6.9	0.1
Isoproturon	7.9	10.7	0.8

*MDQ's have been extrapolated assuming a linear response.

TABLE 4 (cont.)

Compound Name	EI MDQ (ng)	PCI MDQ (ng)	NCI MDQ (ng)
Monolinuron	8.6	3.4	1.1
Methomyl	8.7	5.0	1.0
Acephate	8.8	6.6	1.1
Dodine	12.0	23.5	4.4
Bromoxynil	12.7	11.8	0.8
Promcarb	12.8	8.5	1.6
Coumafuryl	13.2	8.2	0.7
Benzyl benzoate	15.8	2.6	1.2
Aldicarb	16.2	2.8	0.9
Warfarin	17.6	8.3	0.7
2,4,5-T	18.7	11.4	0.4
Chloramben	19.7	6.6	0.6
Endothal	20.0	3.2	0.7
Silvex	23.8	5.8	0.4

*MDQ's have been extrapolated assuming a linear response.

dynode conversion electrode to accelerate negative ions prior to entrance into the electron multiplier. In the positive ion modes (EI and positive CI) this voltage is limited to 255V. Certainly, the electronegativity of some of the compounds, which allows them to easily capture electrons in the ion source, also makes them more sensitive in negative CI. This is not surprising since the compounds were chosen from the appendix VIII and IX lists, which consists of many triazines and halogenated hydrocarbons. Several explanations may be offered to describe the trends in response one sees in tables 1 and 2. A large portion of the compounds showing poor sensitivity in EI and PCI have molecular weights at or below 100 amu. (i.e. crotonaldehyde: MW = 70.1) This loss in signal could suggest that the majority of particles formed by the lighter analytes have insufficient momentum to travel into the ion source. For those compounds of higher MW which gave poor signal response, the problem might be associated with the ion source temperature. Some analyte response increases with increasing source temperature. Furthermore carbamates, such as aldicarb and protham, are notoriously thermally labile and produce spectra containing no predominant m/z ion with a significant signal to noise ratio. This would result in less sensitivity.

It is important to realize that the determination of MDQ's by extrapolation, as was done in this study, assumes a linear response over all tested concentrations. In order to examine the "validity" of these approximations a linearity study was performed.

3.3 LINEARITY

The linearity of response of an analytical instrument is routinely determined so that experiments in quantitation are performed in the instrument's linear response range. The PB-LC/MS has several locations in which analyte could potentially be lost, thus introducing a deviation from linear response. The analyte must pass through five orifices in order to enter the ion source (see fig. 6). The analyte must traverse the nebulizer, the nozzle, the first and second separators, and the ion source entrance. The interface must operate efficiently at each stage to prevent unacceptable losses of analyte.

For the linearity study, ten compounds with varying structures and molecular weights were chosen from the EPA appendix VIII and IX lists (see table 5). The compounds chosen spanned a molecular weight range from 84 to 420 and the diversity of structures ranged from a carbamate (OCONH) to an organochlorine (RCl). This assured results that were not biased toward one functional group or mass range. Five replicate injections of 1000 ng, 500

TABLE 5

Linearity Study:Compound Names and Molecular Weights

<u>Compound Name</u>	<u>Molecular Weight</u>
Diuron	233.10
Benzidine	184.23
Phosalone	367.80
Dipropetryn	255.40
Metribuzin	214.28
Carbaryl	201.22
Fenvalerate	419.92
Amitrole	84.08
Aldicarb	190.30
Paraquat	186.25

ng, 250 ng, 125 ng, and 62.5 ng were made of each analyte. Amitrole, aldicarb, and paraquat required that the amount injected be doubled due to a low response.

The MS was operated with a scan range of 50 - 450 amu. This scan range produced mass spectra that were capable of characterizing each analyte. Standard MS quantitation procedures for integration and calibration make use of ion chromatograms which are extracted from the total ion information by the data system. This procedure affords the best possible S/N for each component, while using a scanning technique that could potentially identify an unknown if it were present. Figures 11 to 20 are ion chromatograms; each a unique mass to charge ratio (m/z) from one of the analytes. The ion used for each analyte is listed in the figure.

The integration results from the extracted ion chromatograms were then used to generate area and response factor (RF) versus amount injected curves. These are labeled figures 21 to 30. The RF was defined as:

$$RF = (AREA) / (AMOUNT INJECTED)$$

All points shown in figures 21 to 30 were subjected to the Q-tested at the 90% confidence level. For the five replicate injections at each concentration level,

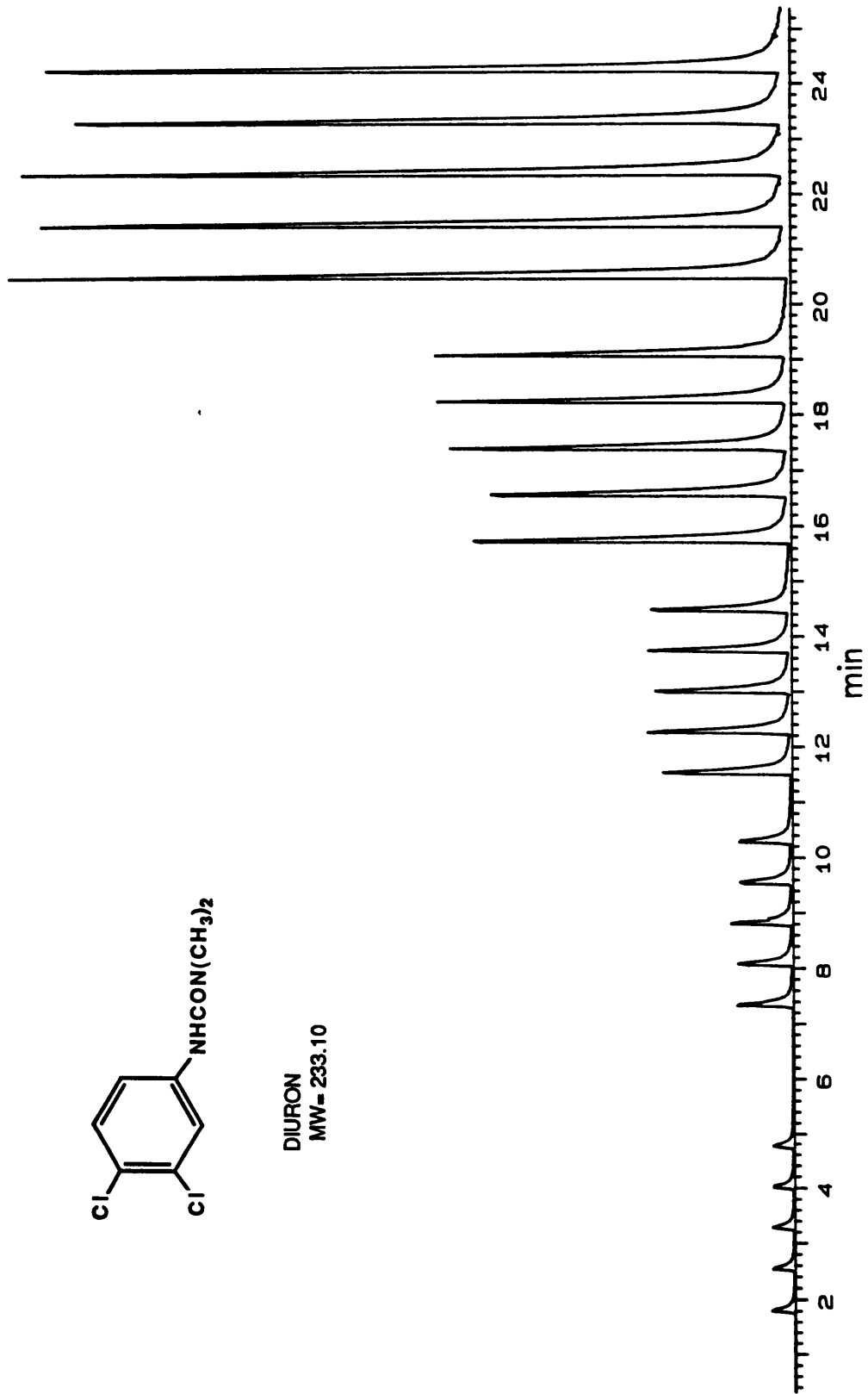


Figure 11: Ion chromatogram at m/z 72 of Diuron

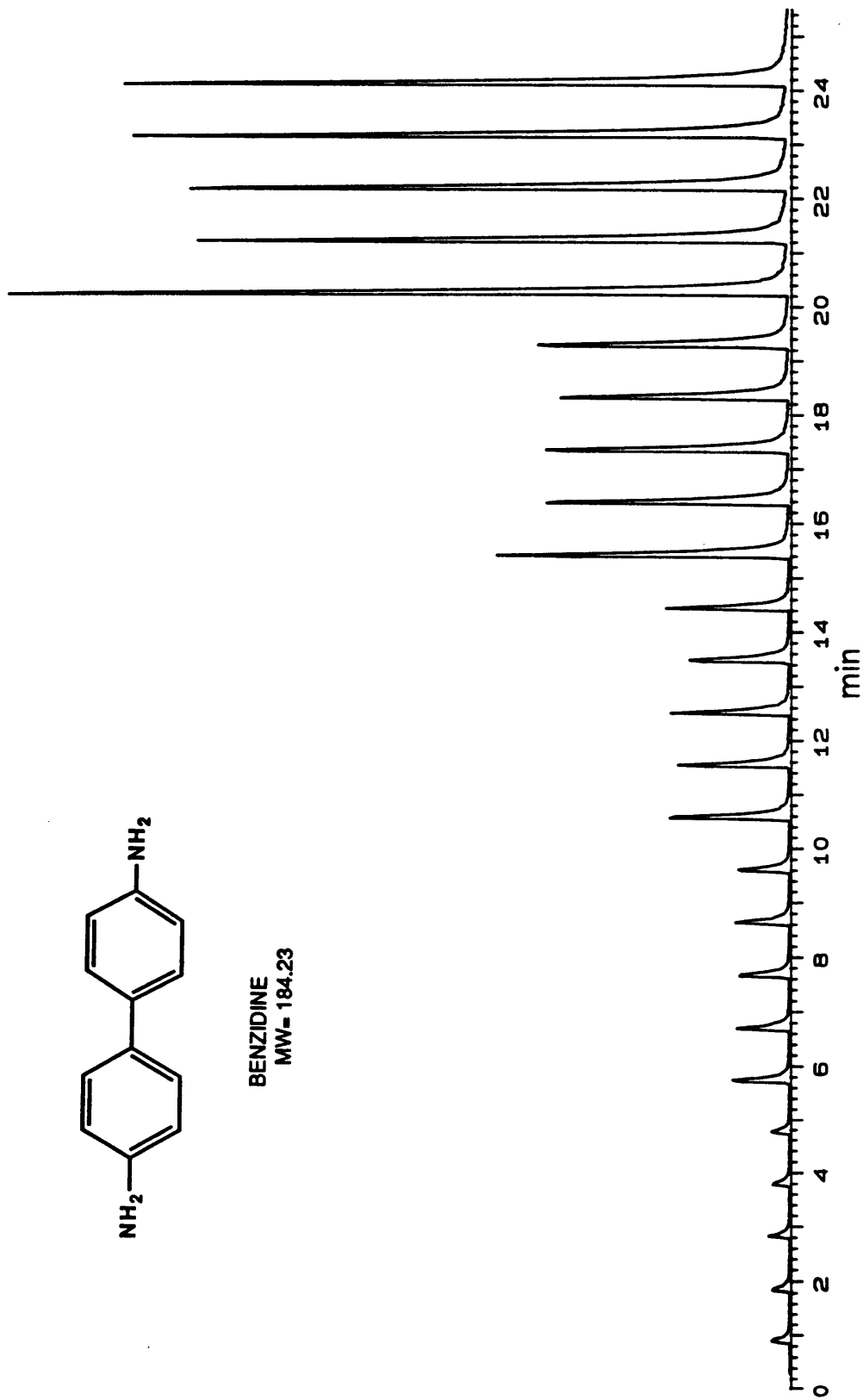


Figure 12: Ion chromatogram at m/z 184 of Benzidine

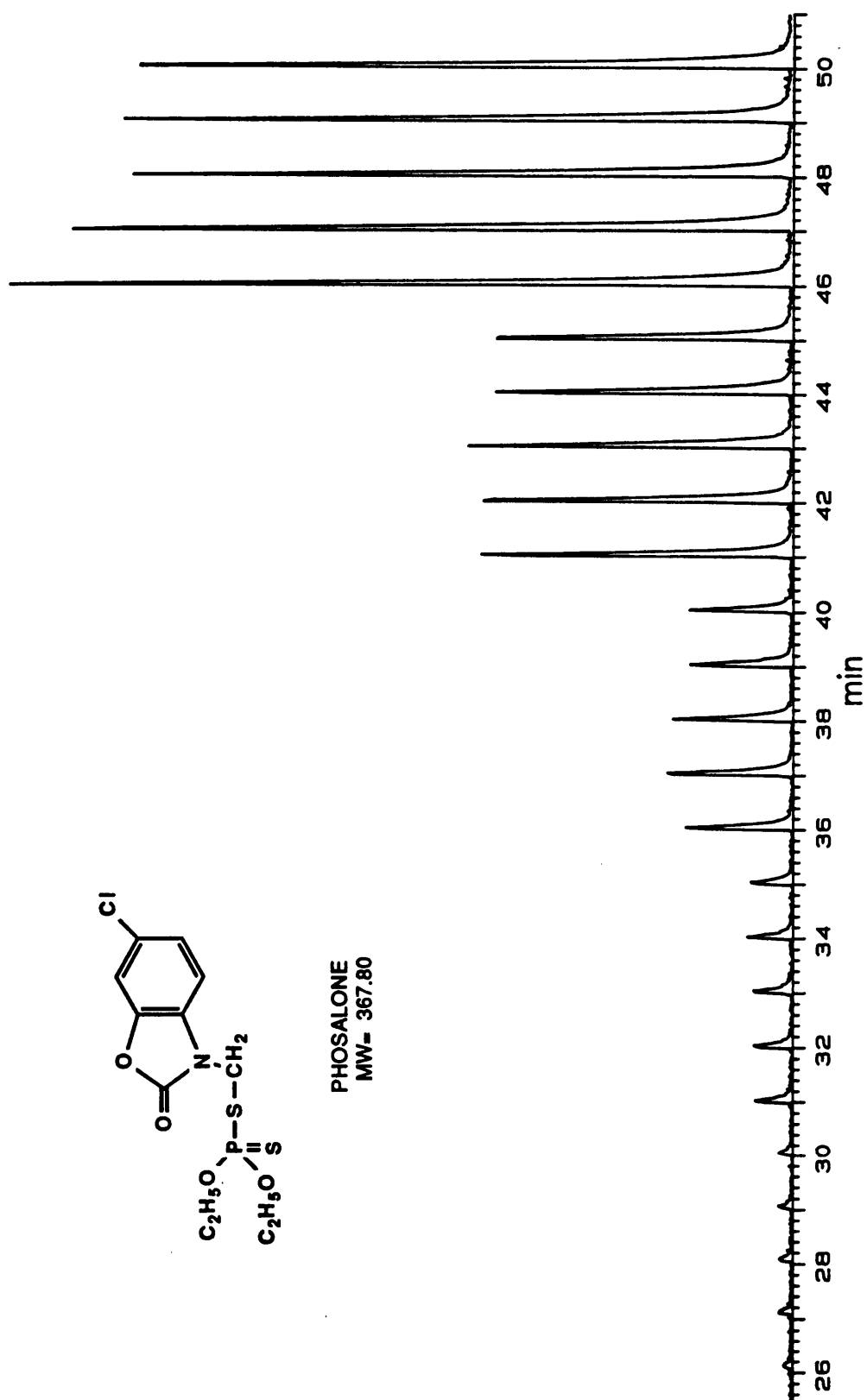


Figure 13: Ion chromatogram at m/z 182 of Phosalone

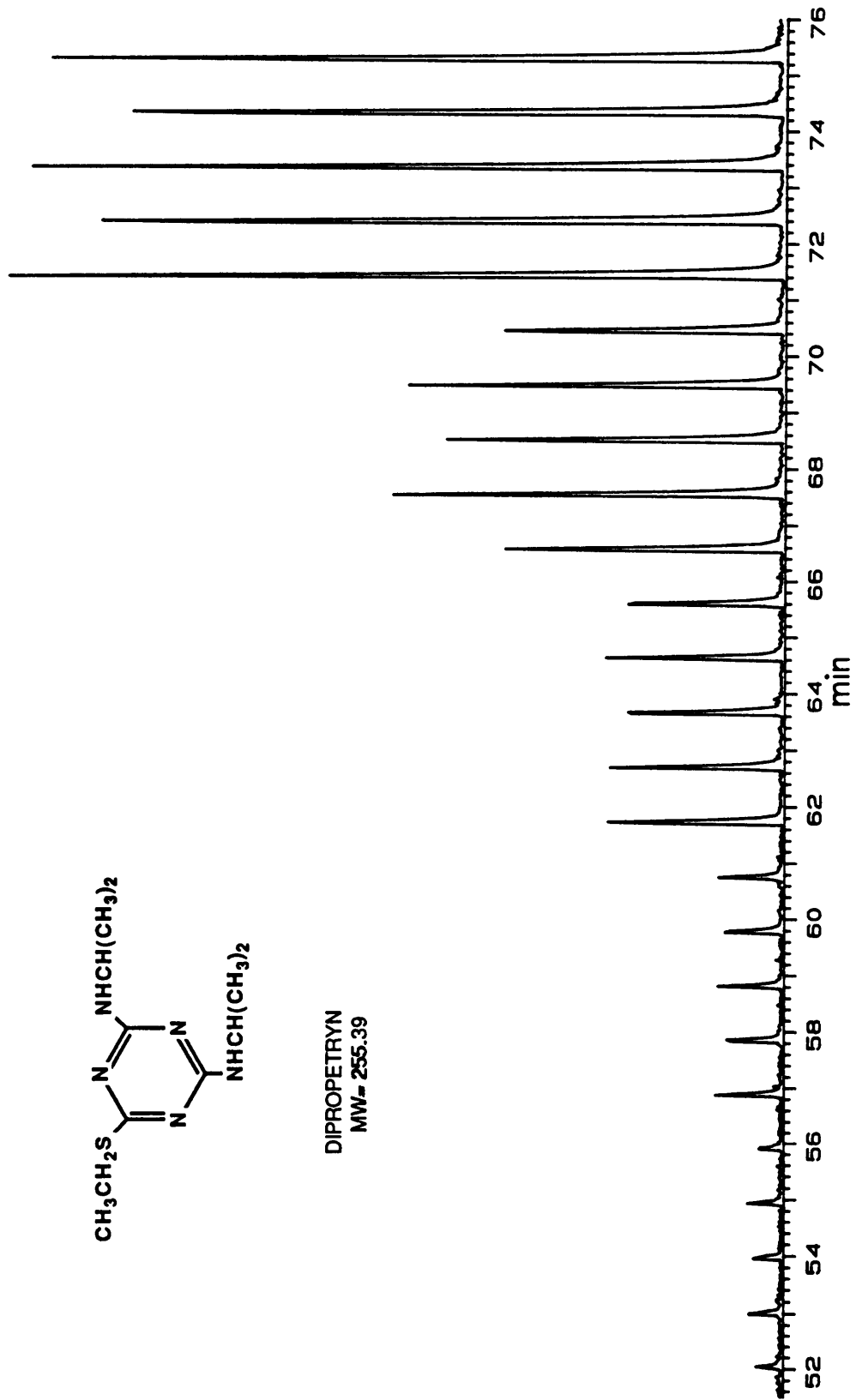


Figure 14: Ion chromatogram at m/z 58 of Dipropetryn

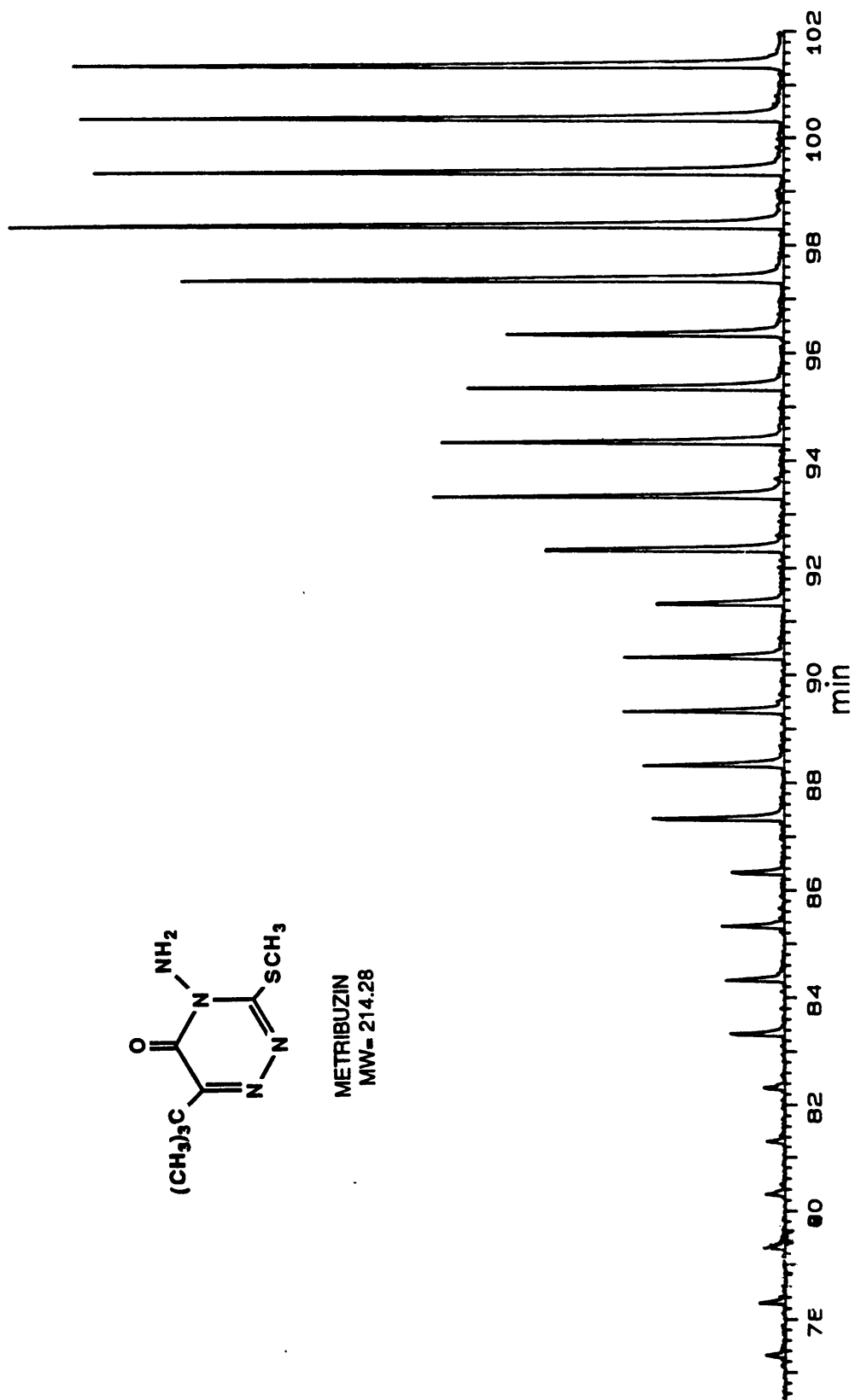
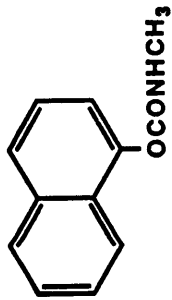
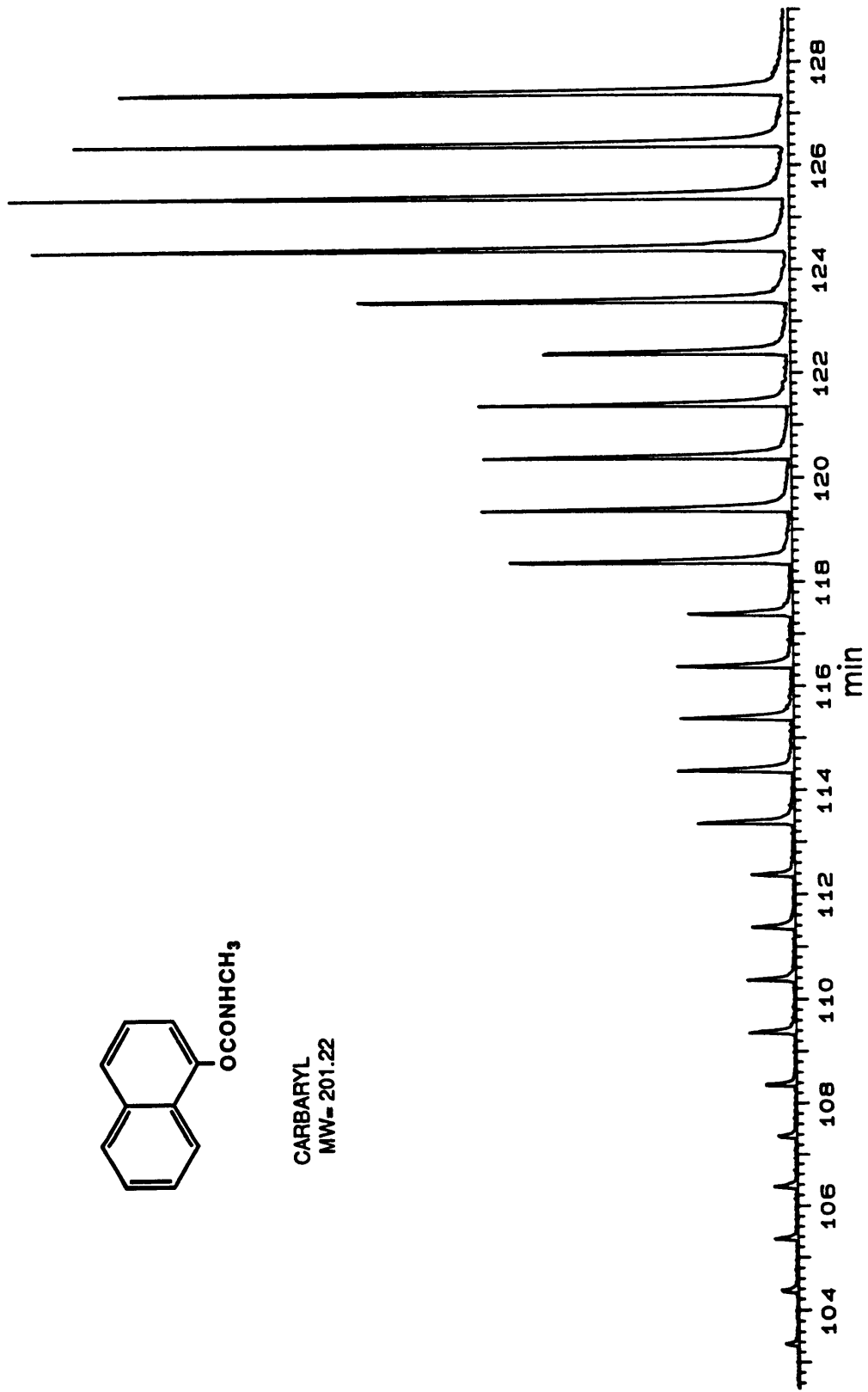


Figure 15: Ion chromatogram at m/z 198 of Metribuzin



CARBARYL
MW = 201.22

Figure 16: Ion chromatogram at m/z 144 of Carbaryl

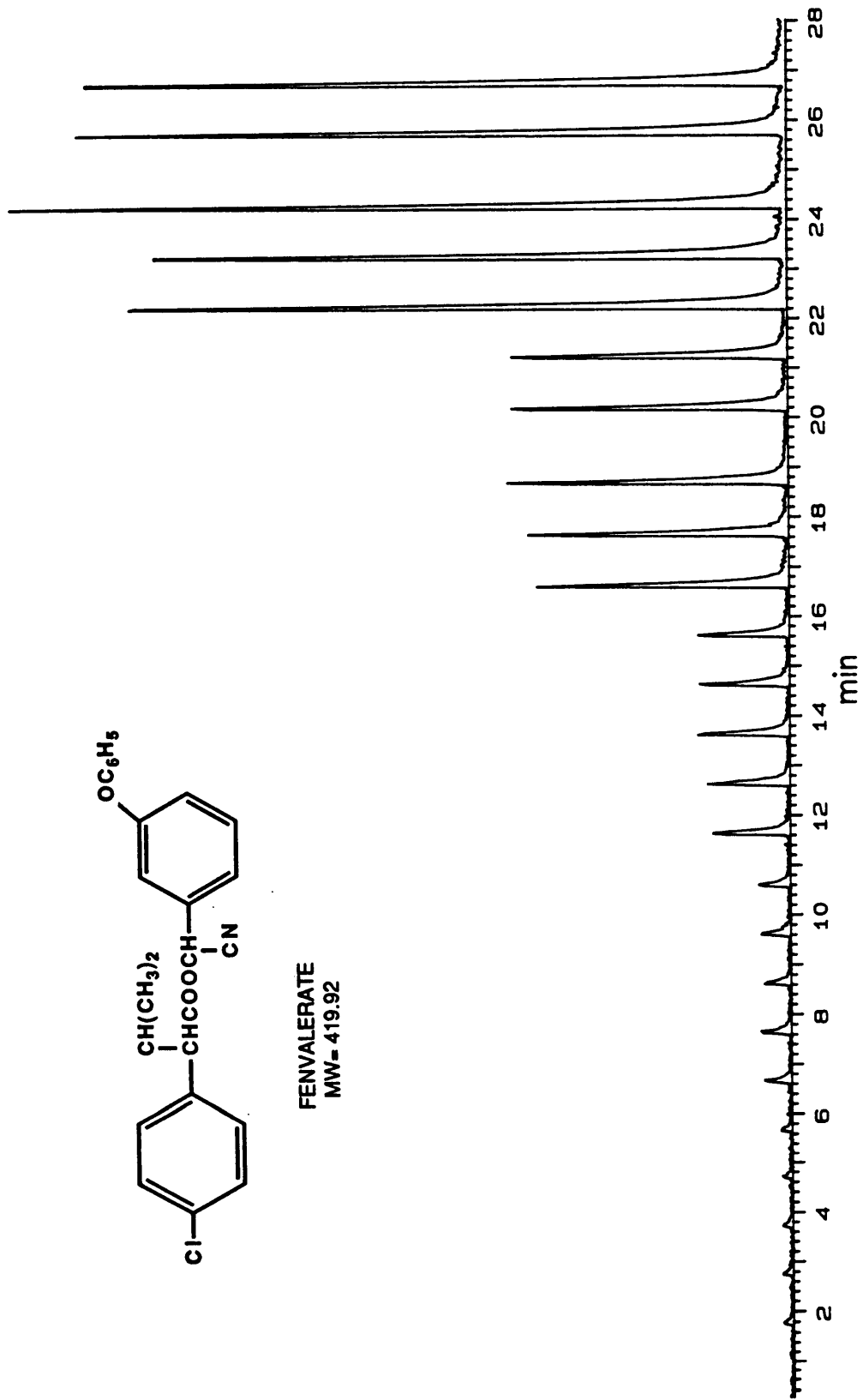


Figure 17: Ion chromatogram at m/z 125 of Fenvalerate

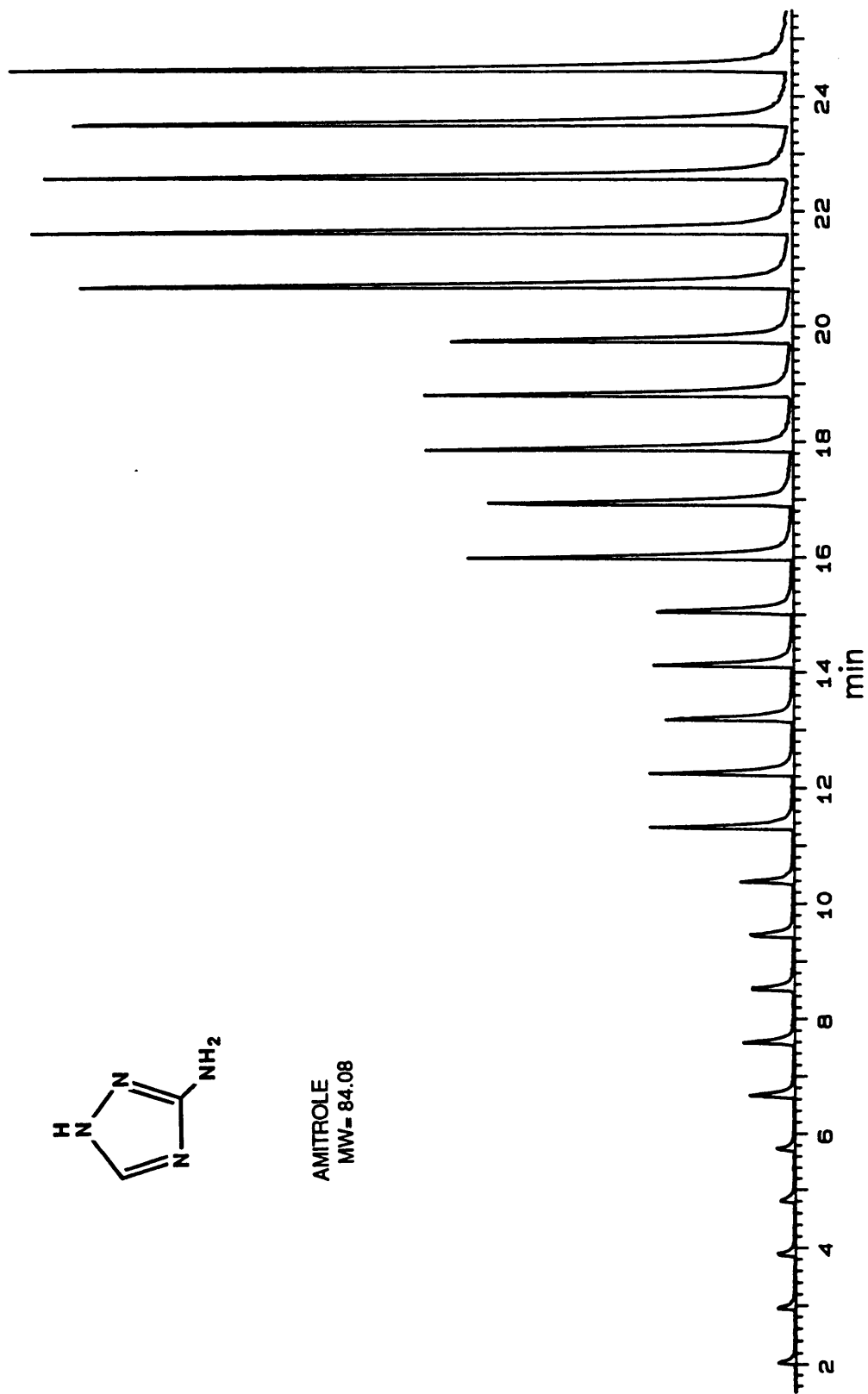


Figure 18: Ion chromatogram at m/z 84 of Amitrole



ALDICARB
MW=190.08

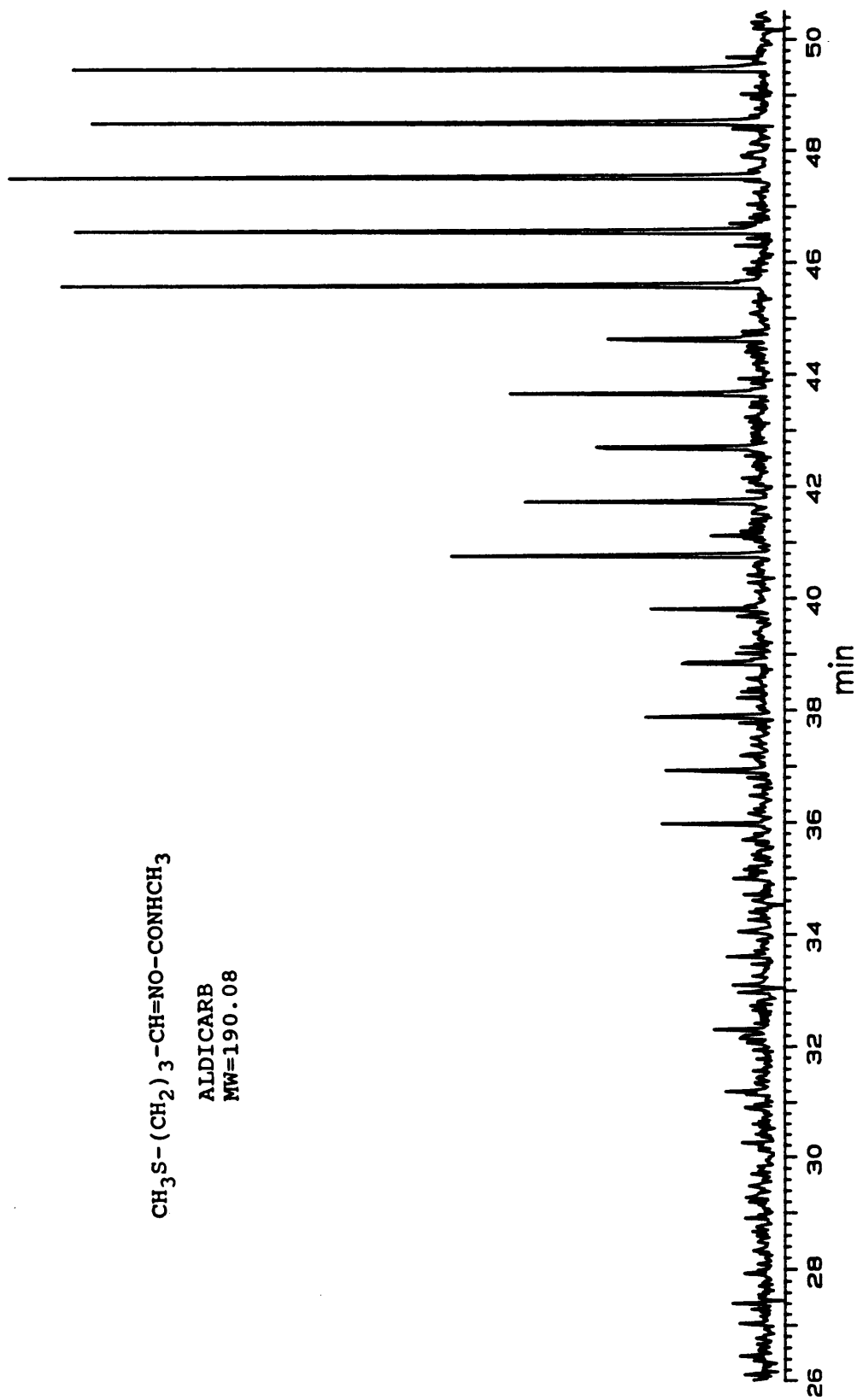


Figure 19: Ion chromatogram at m/z 68 of Aldicarb

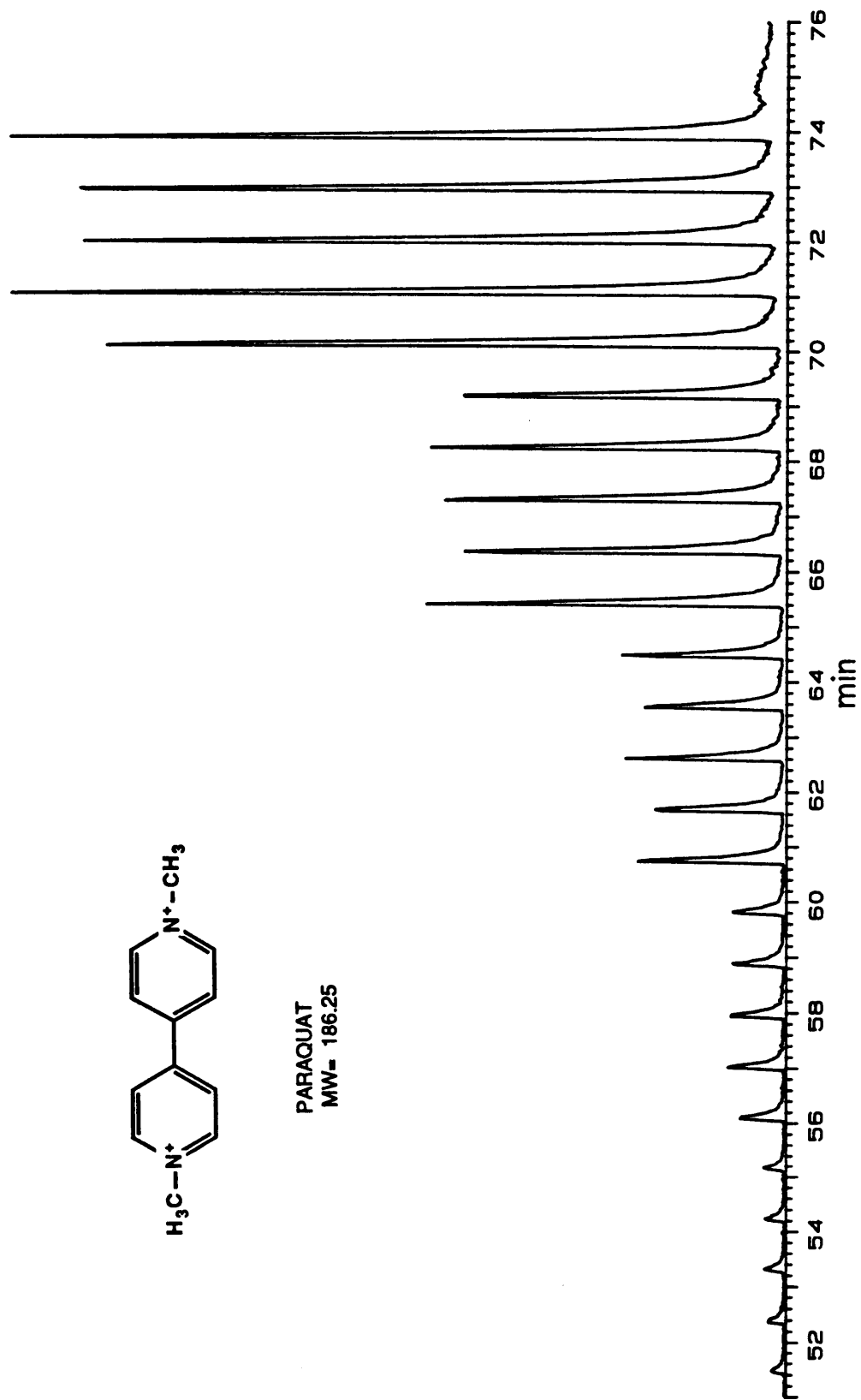


Figure 20: Ion chromatogram at m/z 171 of Paraquat

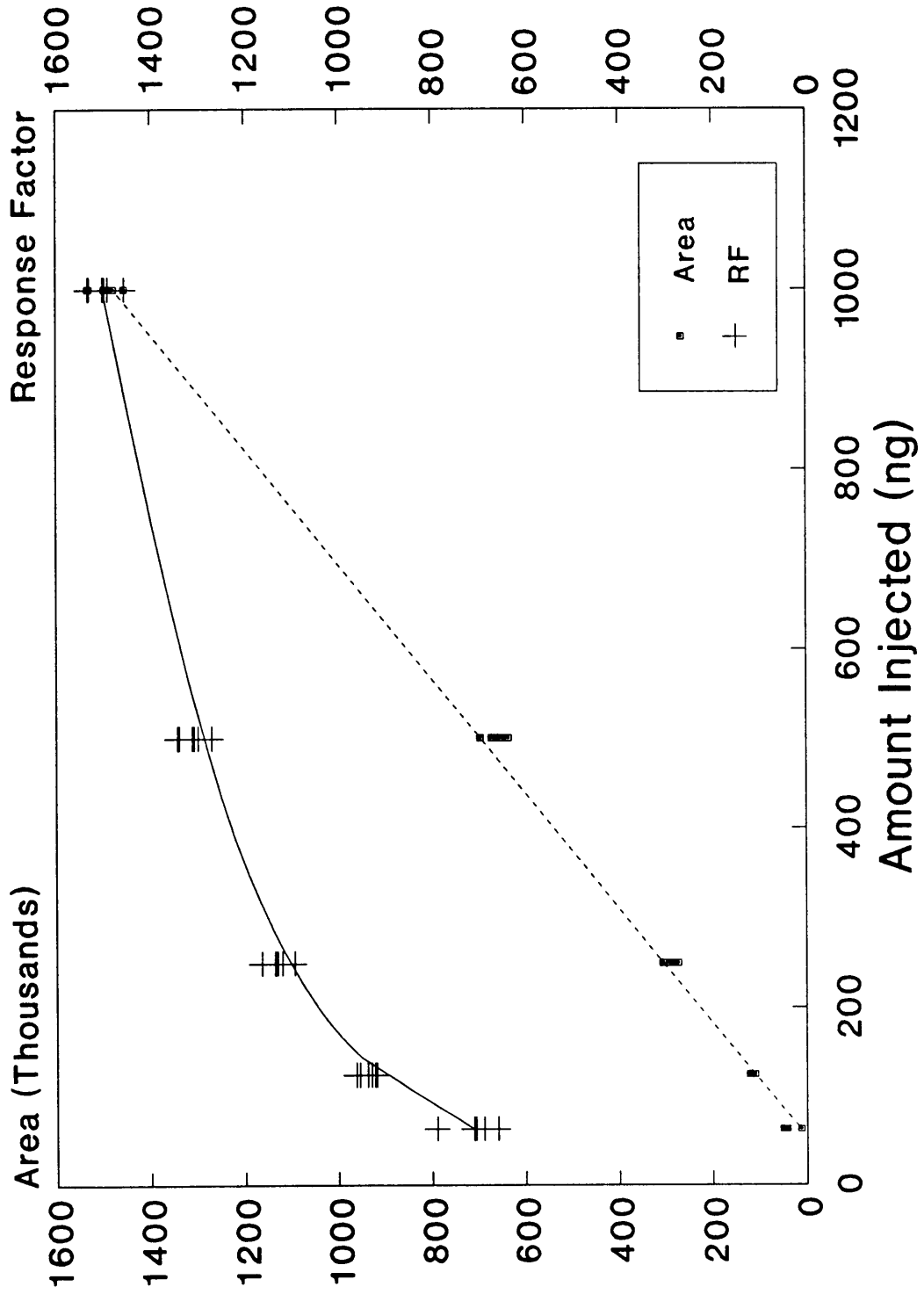


Figure 21: Area and RF vs Amount Injected of Diuron

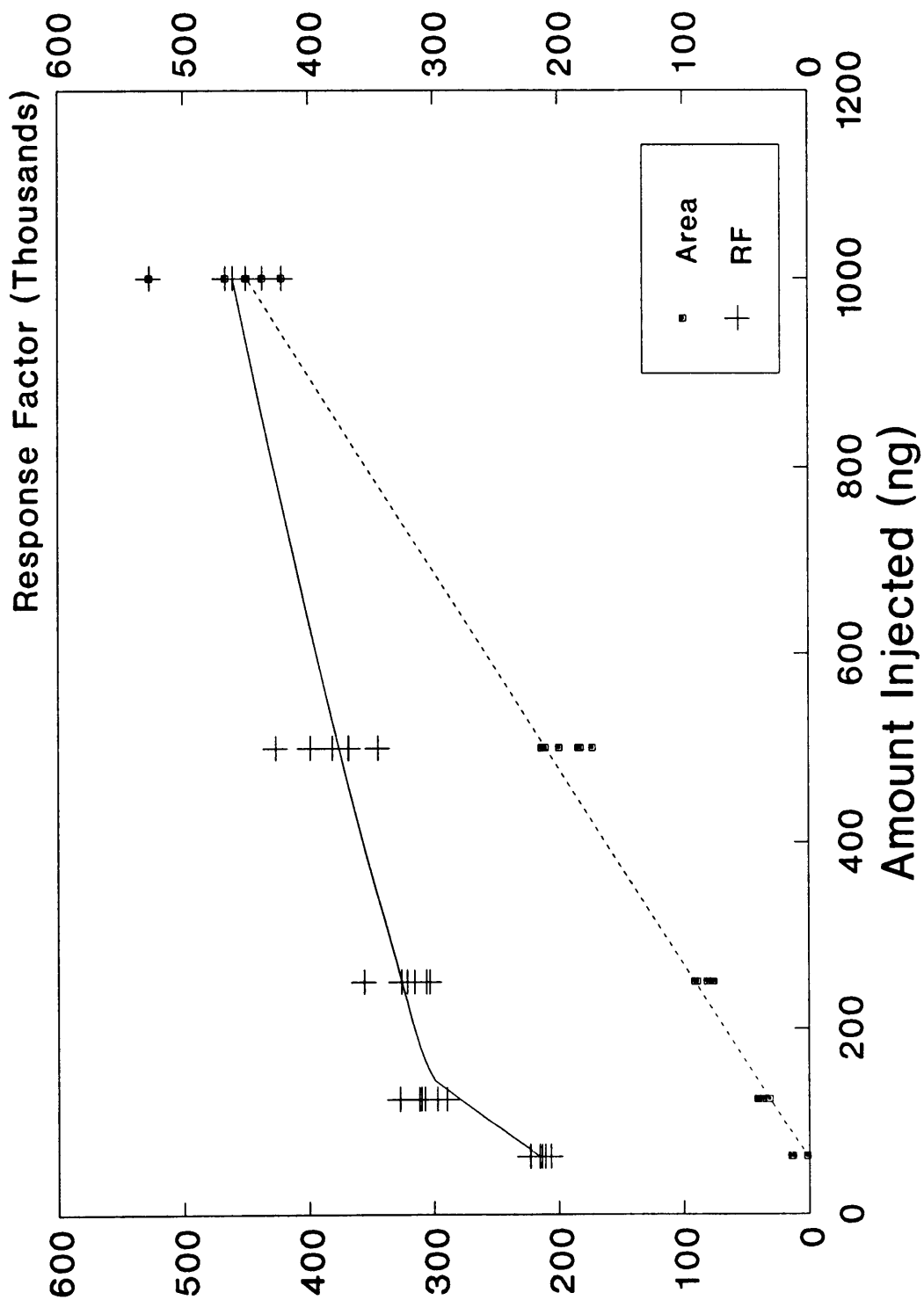


Figure 22:Area and RF vs Amount Injected of Benzidine

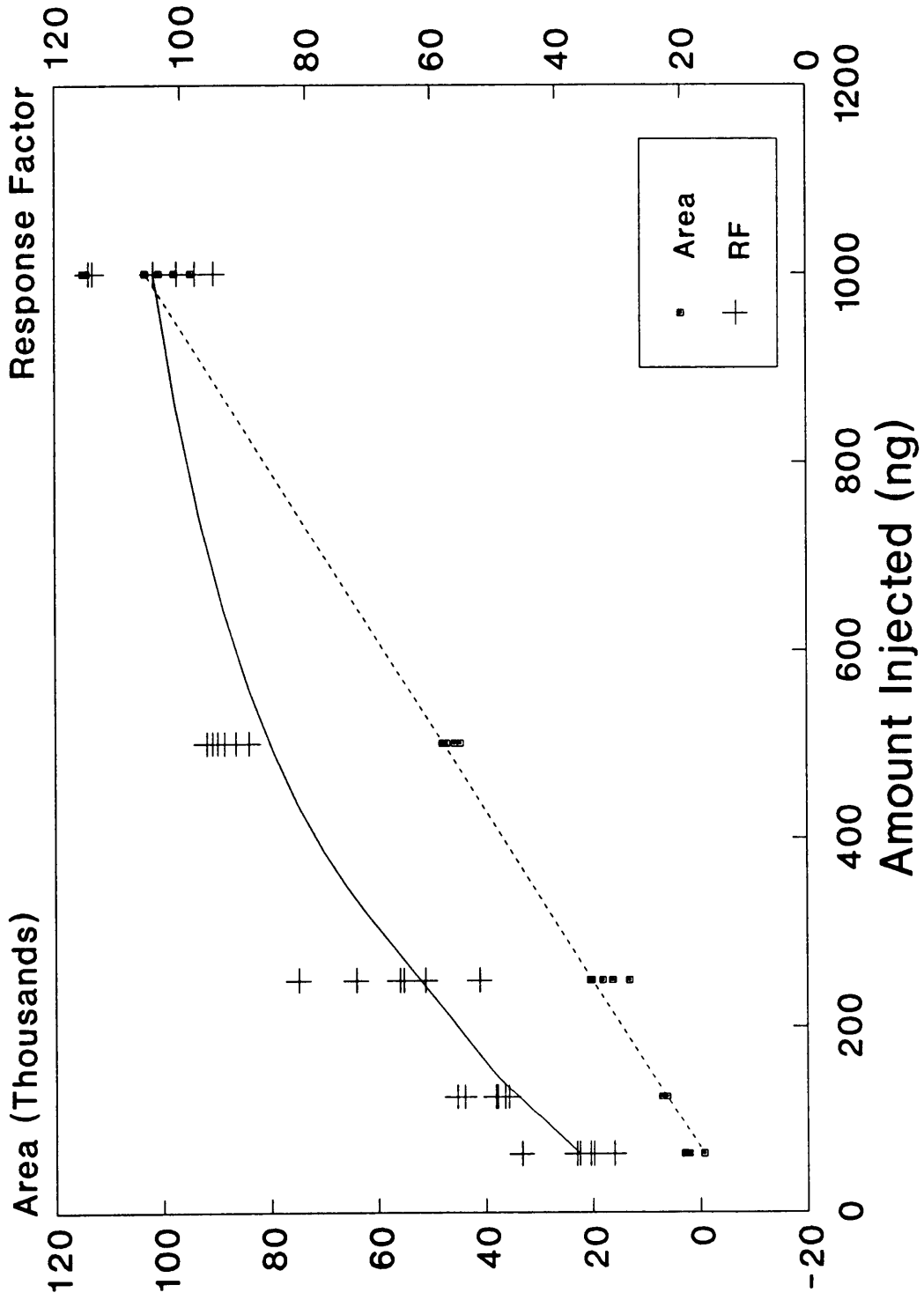


Figure 23 :Area and RF vs Amount Injected of Phosalone

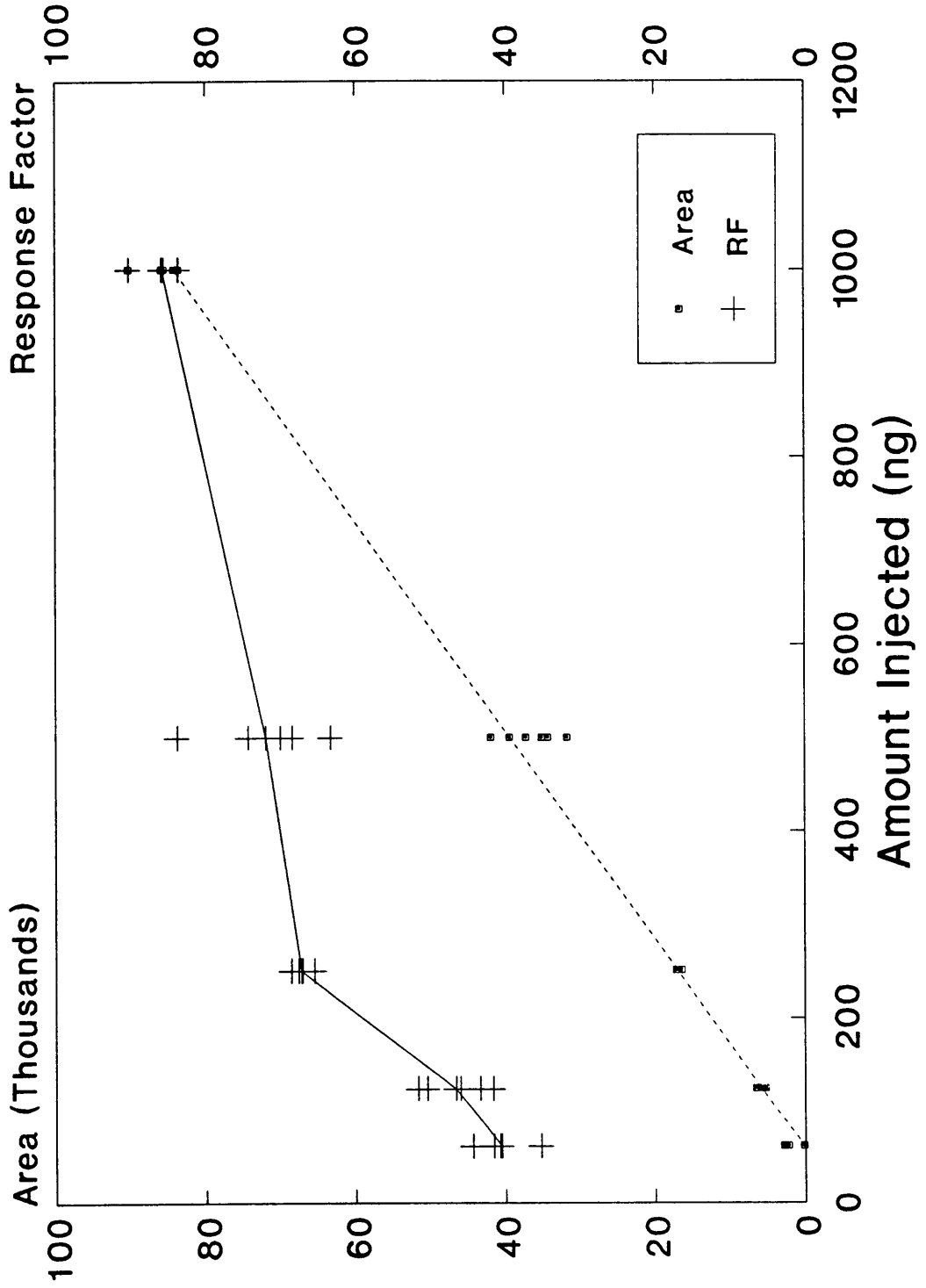


Figure 24:Area and RF vs Amount Injected of Dipropetryn

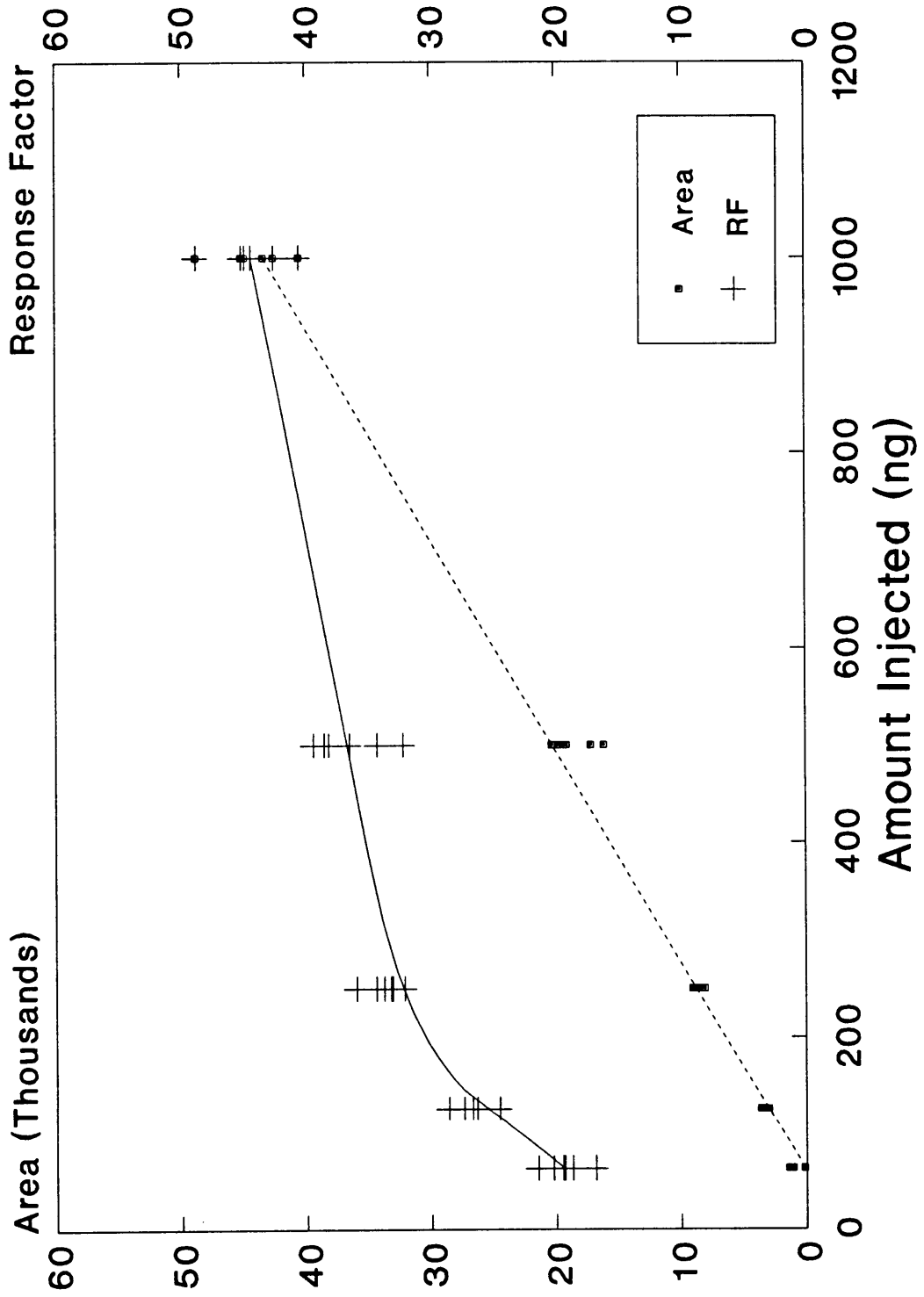


Figure 25 :Area and RF vs Amount Injected of Metribuzin

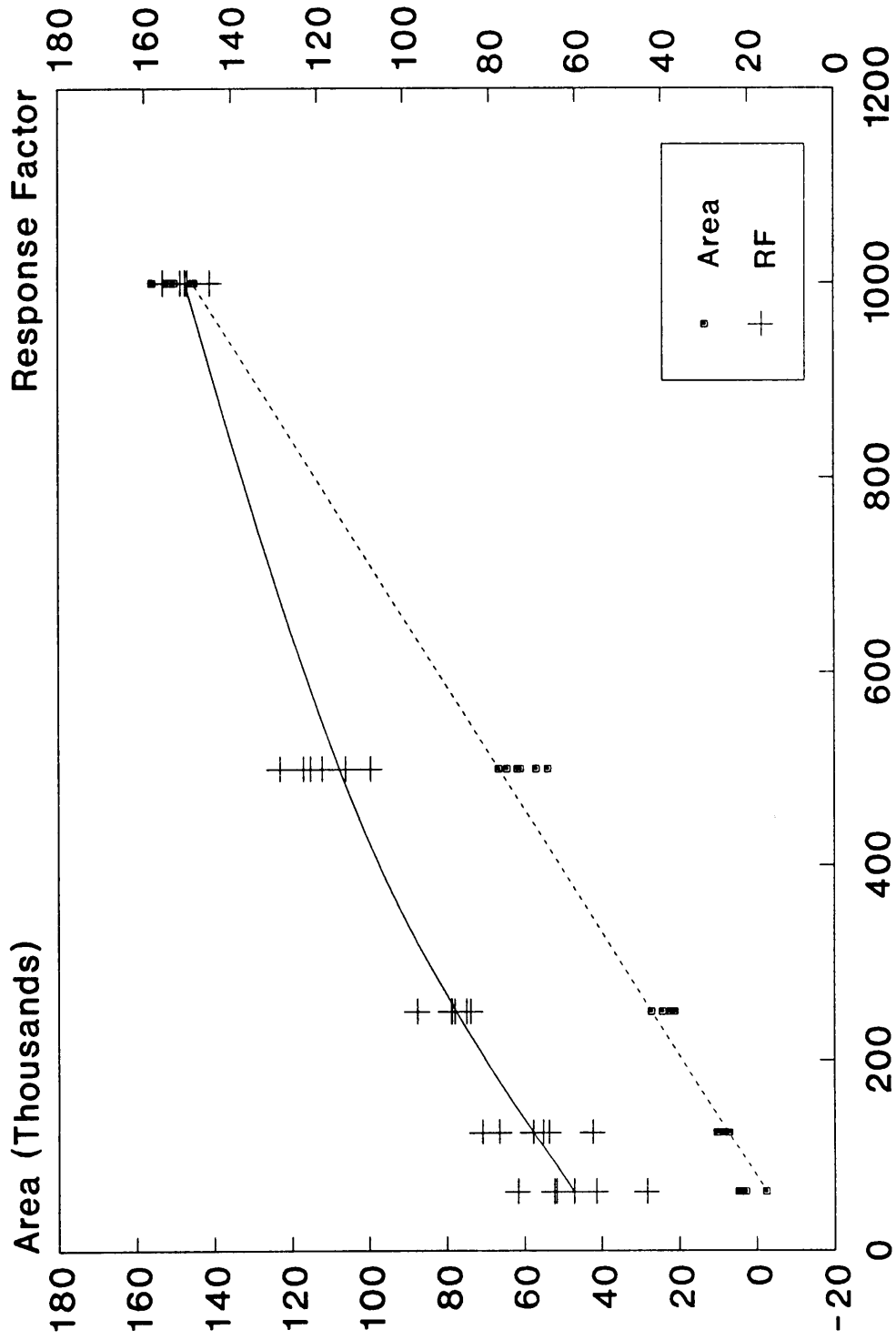


Figure 26: Area and RF vs Amount Injected of Carbaryl

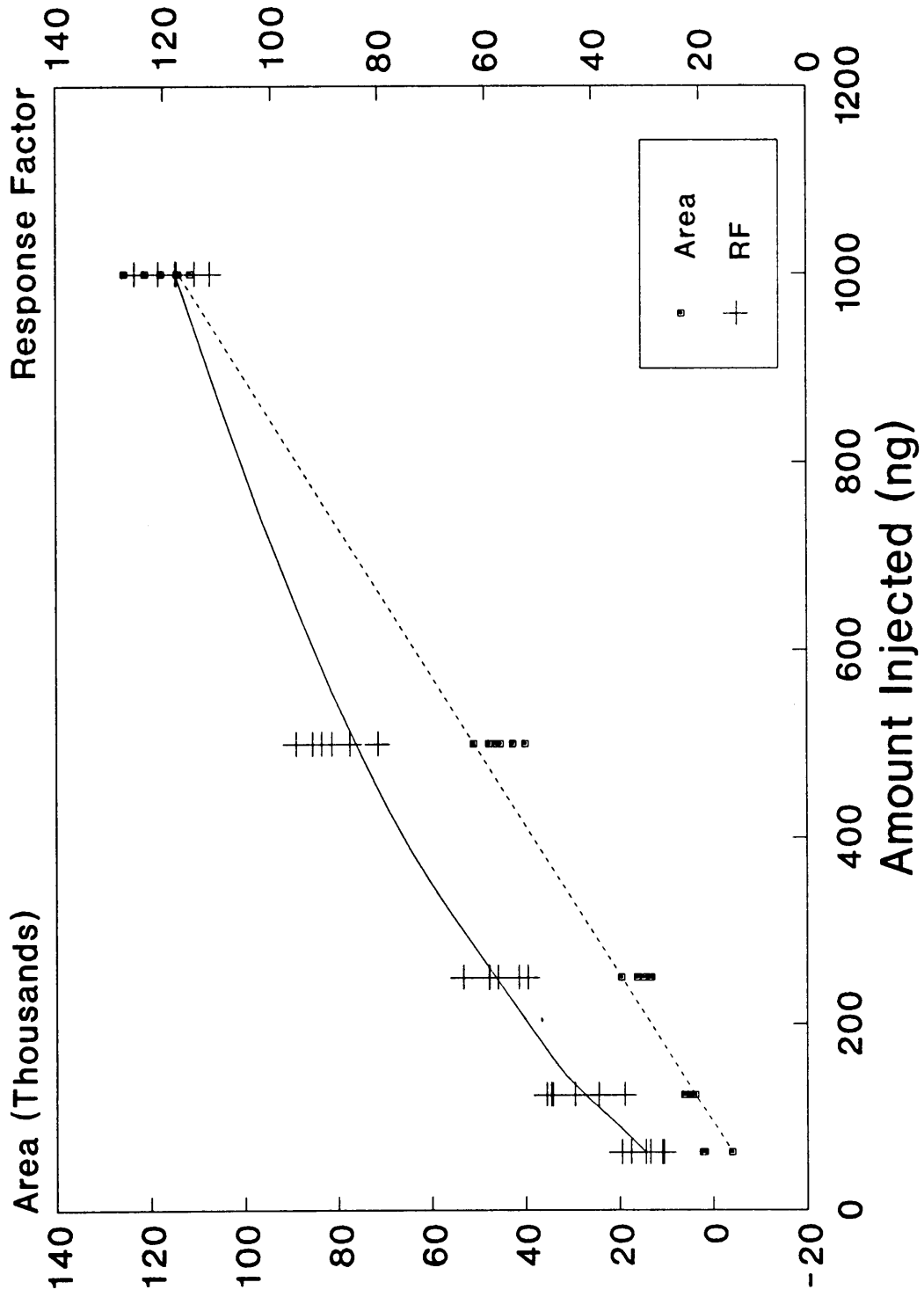


Figure 27 :Area and RF vs Amount Injected of Fenvalerate

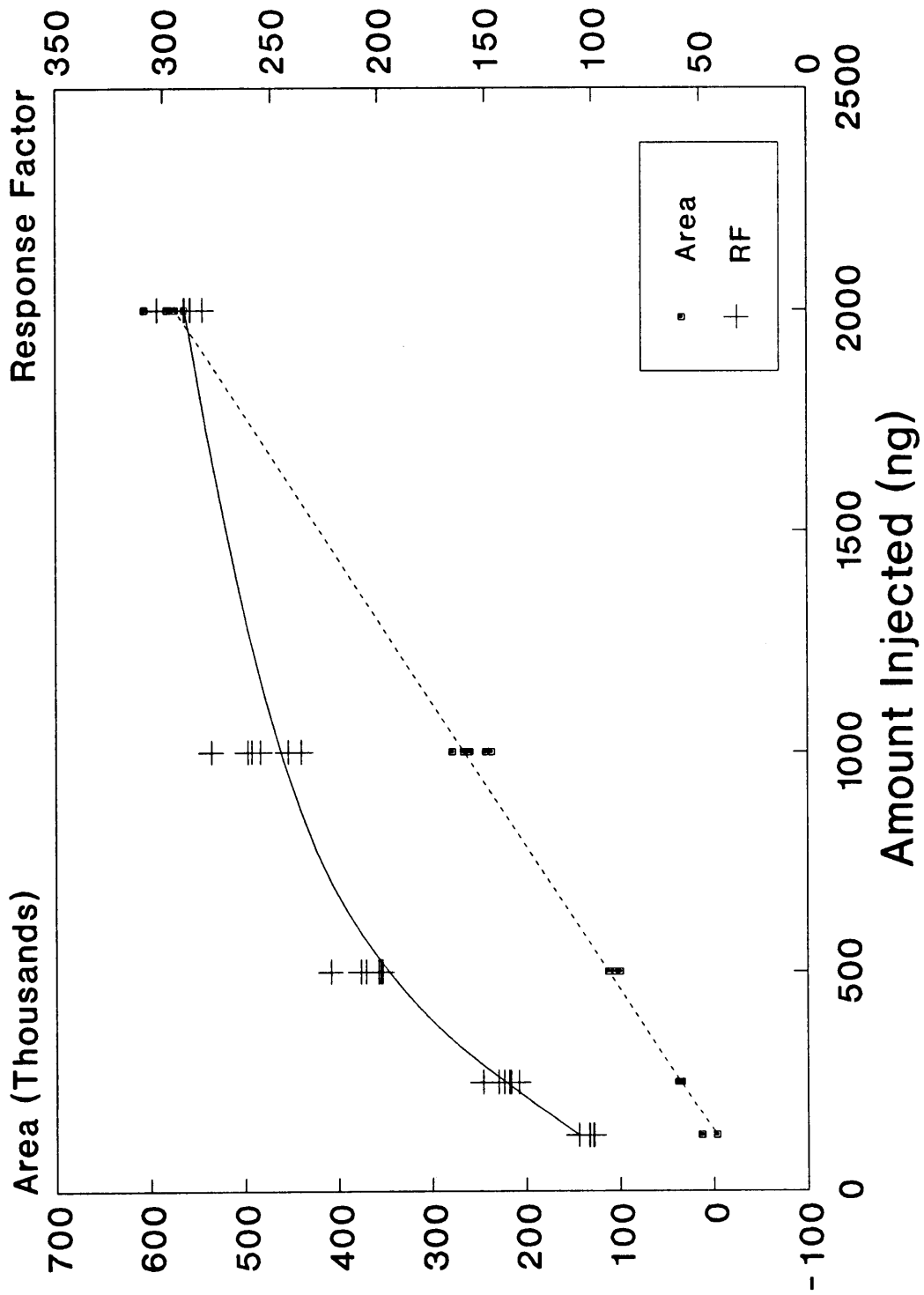


Figure 28:Area and RF vs Amount Injected of Amitrole

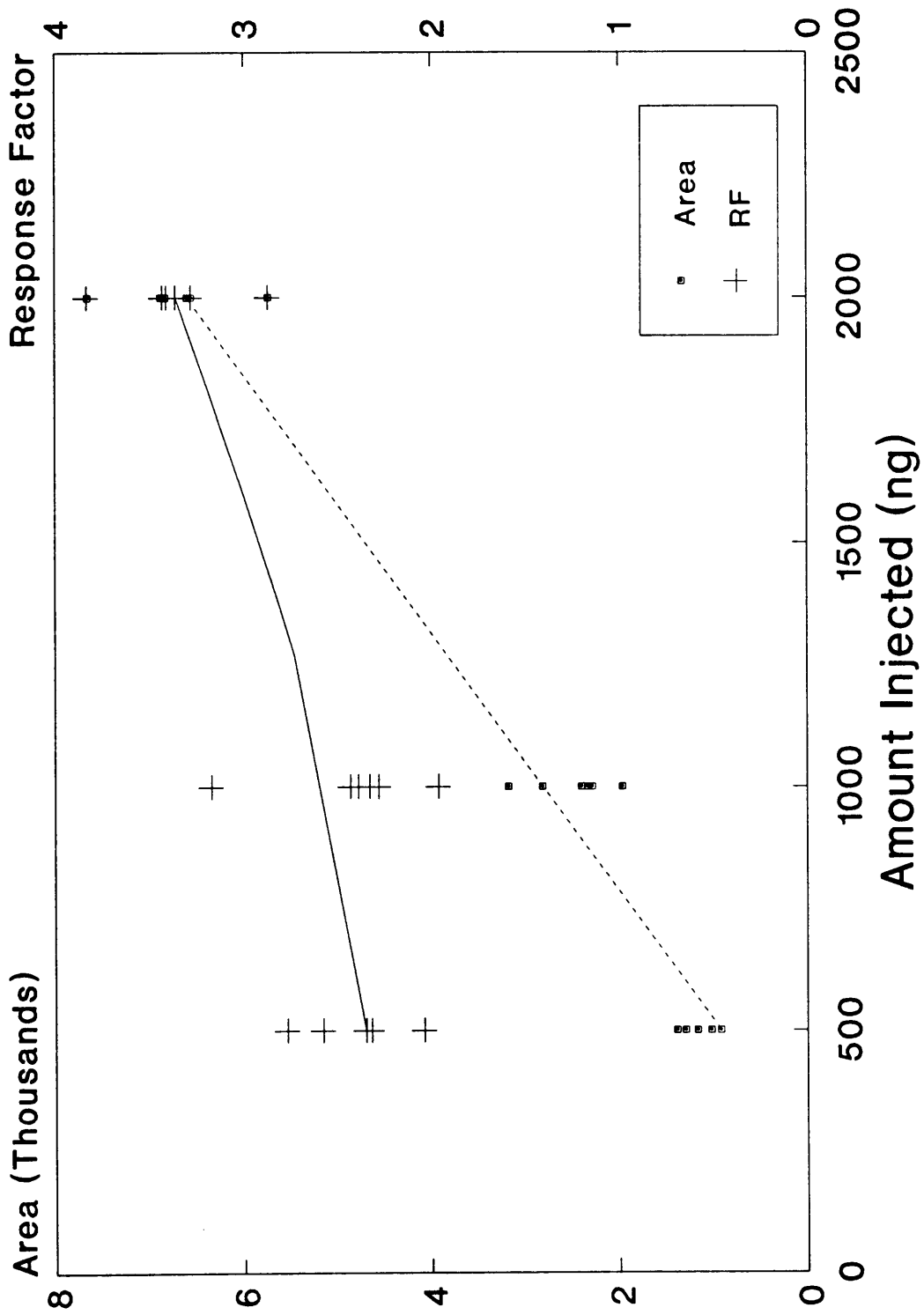


Figure 29: Area and RF vs Amount Injected of Aldicarb

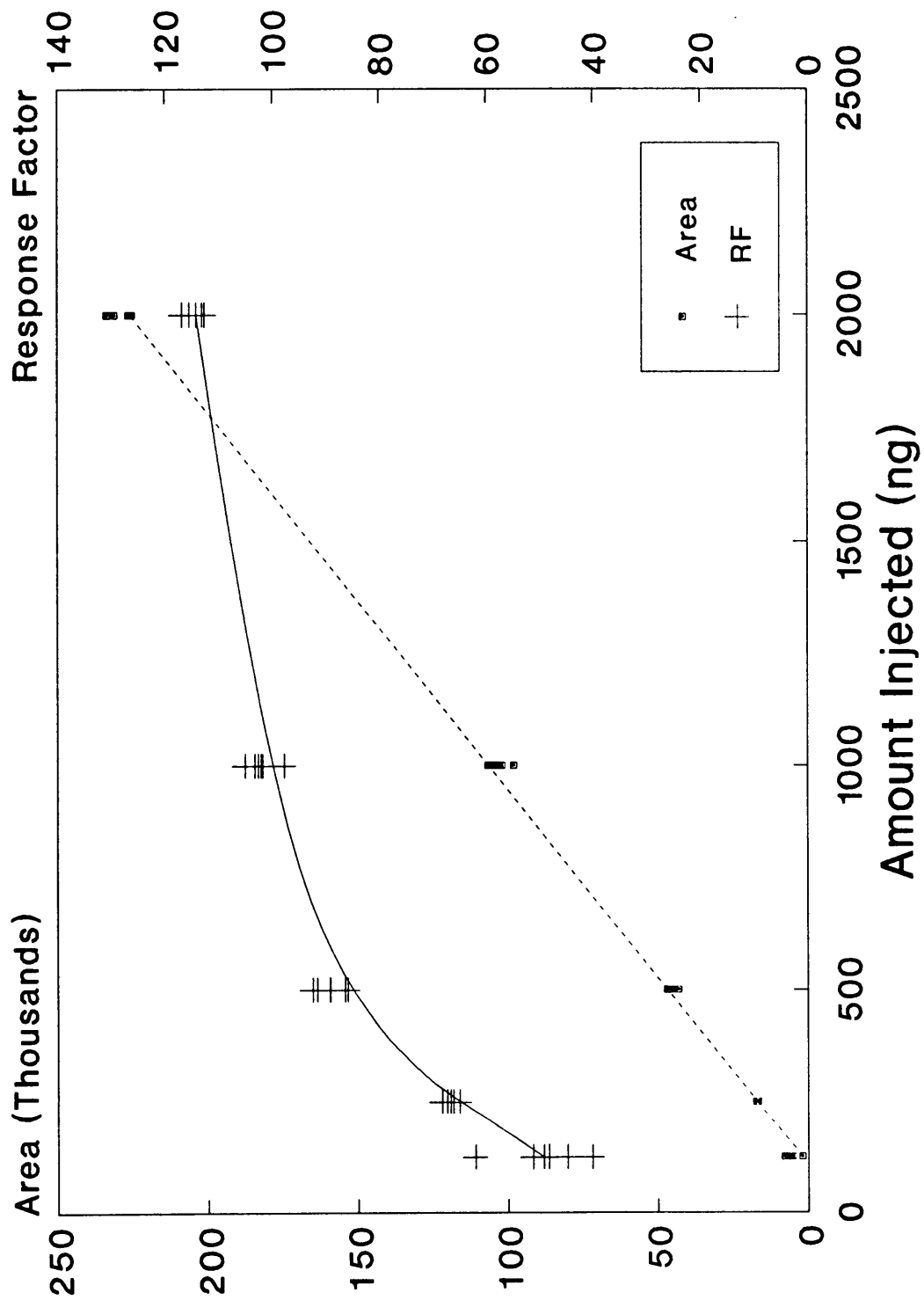


Figure 30:Area and RF vs Amount Injected of Paraquat

the %RSD of the areas and RF's was calculated and found to be less than 20% in each case. The overall average %RSD was found to be 8.64 ± 6.21 . In addition, the %RSD for each compound describing the variation in RF over the range of concentration was found to vary between 27% and 49%. If one compares these values to allowable limits of 25 to 100 %RSD for various compounds set in the official EPA methods 624 and 625, these are reasonable results. Methods 624 and 625 are current methods for the determination of priority pollutants by GC/MS.

Ideally, a plot of RF values versus concentration would generate a straight horizontal line. This would show that an increase in the amount injected gives a corresponding increase in the signal detected. All the compounds tested, except aldicarb, gave acceptable signal levels for the sample amounts tested. However, this interface does not give a linear response over the concentration range tested. All compounds showed a significant decrease in signal at lower levels (see figs. 21 to 30). The straight line shown on each graph represents the best fit line through the experimental areas. It is interesting to note that each line intersects the concentration axis well above the calculated MDQ listed in table 1 (see table 6). Therefore, the MDQ's determined in the previous study

TABLE 6
Extrapolated and Experimental MDQ's

Compound Name	Extrapolated MDQ (ng)	Experimental MDQ (ng)
Diuron	0.6	55
Benzidine	0.6	62
Phosalone	0.7	176
Dipropetryn	2.1	57
Metribuzin	2.7	61
Carbaryl	4.4	71
Fenvalerate	1.3	99
Amitrole	3.7	132
Aldicarb	16.2	269
Paraquat	2.4	109

must be regarded as ideal MDQ's. It would not be reasonable to expect to achieve such sensitivity in the laboratory for most compounds.

The reasons for the signal loss demonstrated in the response factor plots could be two-fold. First, as mentioned above, a finite amount of sample could be lost as it is transported through the interface. This could be caused by adsorption of the analyte onto the walls and orifices of the interface. This small and constant loss in sample does not effect the response at high sample amounts because it is a small proportion of the total sample. This is not the case at the lower sample amounts and therefore, a greater loss in signal is seen. Second, lower sample amounts will result in a lower concentration of analyte in the effluent. This will result in a smaller particle size once the solvent has been evaporated from the droplets. These smaller particles have smaller mass and hence less momentum. Because of this, transport of these particles through the momentum separator will be less efficient.

The results for aldicarb in this experiment were particularly disappointing but not surprising. They can be explained as follows. Aldicarb is a carbamate and is well known as a difficult problem for MS analysis. Normal analysis of aldicarb is by CI or thermospray, both very mild MS ionization methods. Even by these methods,

much of the sample is thermally decomposed in a hot ion source prior to ionization. EI analysis of aldicarb yields a mass spectrum containing a high degree of fragmentation (see mass spectrum in appendix A). This fails to produce any one m/z with a significant S/N. It should also be noted that the EI mass spectrum generated for aldicarb and spectra for the other nine compounds in the experiment (see appendix A) were matched at a high confidence level (i.e. > 90 %) with the corresponding spectra in the National Bureau of Standards (NBS) library.

3.4 BAND BROADENING

In this study, a series of experiments involving helium flow (HE), source temperature (ST), mobile phase composition (MP), and desolvation chamber temperature (DCT) were used to evaluate the individual and additive effects on peak width. The response surfaces are in terms of sigma. A simple calculation to determine the total effect in time experienced by the peak can be made assuming that 4 sigma adequately defines the width at base (19). In order to design an experiment to incorporate these independent variables a program called "EXPERTimental Design"™ (Statistics Programs, Houston, TX) was used. By asking a series of questions, concerning available resources, independent, and dependent variables, time constraints, response

surfaces, etc., the program helps choose an appropriate design model and answers any questions concerning that design. The recommended design for this study was a Box-Behnken model. Figure 31 gives a geometrical representation of this model. It is a full second order polynomial model used in response surface studies involving 3 or more independent variables. A central composite design would also have been adequate, but the Box-Behnken is a highly fractional 3-level factorial design and is more efficient. A factorial experiment is one in which each factor (or independent variable) has multiple levels. A full factorial design would require every combination of factors at each level to be tested. Because the Box-Behnken design is highly fractional, only a subset of the relevant combinations need to be performed. In order to eliminate the unnecessary combinations, all necessary factors and levels for the Box-Behnken design were entered into a program called "Statgraphics (version 2.6) "TM (STSC, Rockville, MD). This program determined the subset of combinations necessary to evaluate the effects of the four variables on sigma. Table 7 lists the 27 combinations used in the experimental design.

Caffeine was the probe used for this study. Five replicate injections of a 10 ng/ul solution of caffeine were made for each of the runs. Sigma was measured in

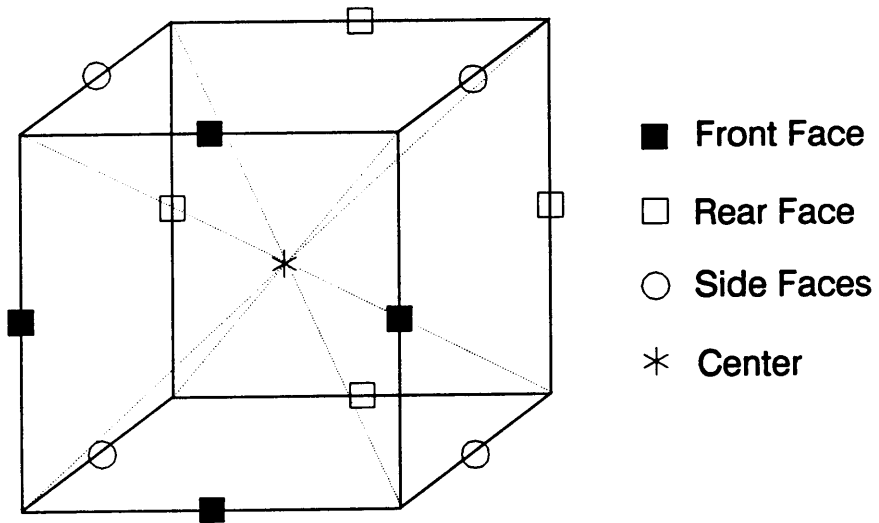


Figure 31: Geometrical Representation of 3-Dimensional Box Behnken Design

TABLE 7

Combinations of Independent Variables

Run #	He Flow (L/min)	DC Temp* (C)	Source Temp(C)	% Methanol
1	1.5	45	250	50
2	2.0	45	350	50
3	1.5	55	150	50
4	1.5	45	150	0
5	1.5	55	350	50
6	1.5	45	350	100
7	1.5	45	150	100
8	1.5	35	350	50
9	1.5	55	250	100
10	2.0	45	250	0
11	1.5	45	350	0
12	1.0	45	250	0
13	1.0	45	350	50
14	1.0	35	250	50
15	1.0	45	250	100
16	2.0	35	250	50
17	2.0	45	250	100
18	2.0	55	250	50
19	1.5	35	250	100
20	1.0	45	150	50
21	1.0	55	250	50
22	1.5	35	150	50
23	1.5	55	250	0
24	1.5	45	250	50
25	2.0	45	150	50
26	1.5	35	250	0
27	1.5	45	250	50

* DC Temp = Desolvation chamber temperature

seconds. Table 8 is a list of the observed and fitted values of sigma and the corresponding residuals. The residuals are defined as $\sigma(\text{obs}) - \sigma(\text{fit})$. An analysis of the residuals provided information concerning the data and serial correlation. Because the experiments were carried out over an extended period of time, the results could demonstrate a trend related to the passage of time. (i.e. source deterioration or sample degradation) A Durbin-Watson statistic can be calculated using the residuals to determine if there is such a time correlation (20). The Durbin-Watson test, in this case is 1.7 which falls in the noncorrelation range. To graphically inspect the data for nonnormality, a normal probability plot of the residuals was constructed (see fig. 32). If the residuals are normally distributed, as in this study, the plot will approximate a straight line when graphed with a y axis corresponding to the cumulative distribution function of a normal distribution (22).

After the data was tested for nonnormality, a multiple regression model was generated. The computer program, "STATGRAPHICS (version 2.6)"TM (STSC, Rockville, MD) was used to develop and test the model. A multiple regression analysis of the data was necessary to prove that each term included in the model equation was unique. Model fitting, in this case, was done by testing

TABLE 8

Experimental and Fitted Sigmas and Residuals

Observation Number	Observed Sigma*	Fitted Sigma*	Residuals
1	1.9	2.3	-0.4
2	1.9	2.0	-0.1
3	2.5	2.7	-0.2
4	4.2	3.8	0.4
5	1.6	1.2	0.4
6	1.9	2.2	-0.3
7	3.3	3.2	0.1
8	2.6	2.6	0.0
9	1.7	1.7	0.0
10	2.6	2.6	0.0
11	2.3	2.4	-0.1
12	2.2	2.5	-0.3
13	2.2	2.0	0.2
14	2.6	2.2	0.4
15	2.3	2.1	0.2
16	2.6	2.7	-0.1
17	2.0	2.1	-0.1
18	1.7	1.2	0.5
19	2.4	2.3	0.1
20	3.1	3.2	-0.1
21	1.7	1.6	0.1
22	3.7	3.5	0.2
23	1.5	1.7	-0.2
24	1.9	2.3	-0.4
25	3.3	3.3	0.0
26	3.5	3.2	0.3
27	1.9	2.3	-0.4

*Sigma and Residual values are in seconds.

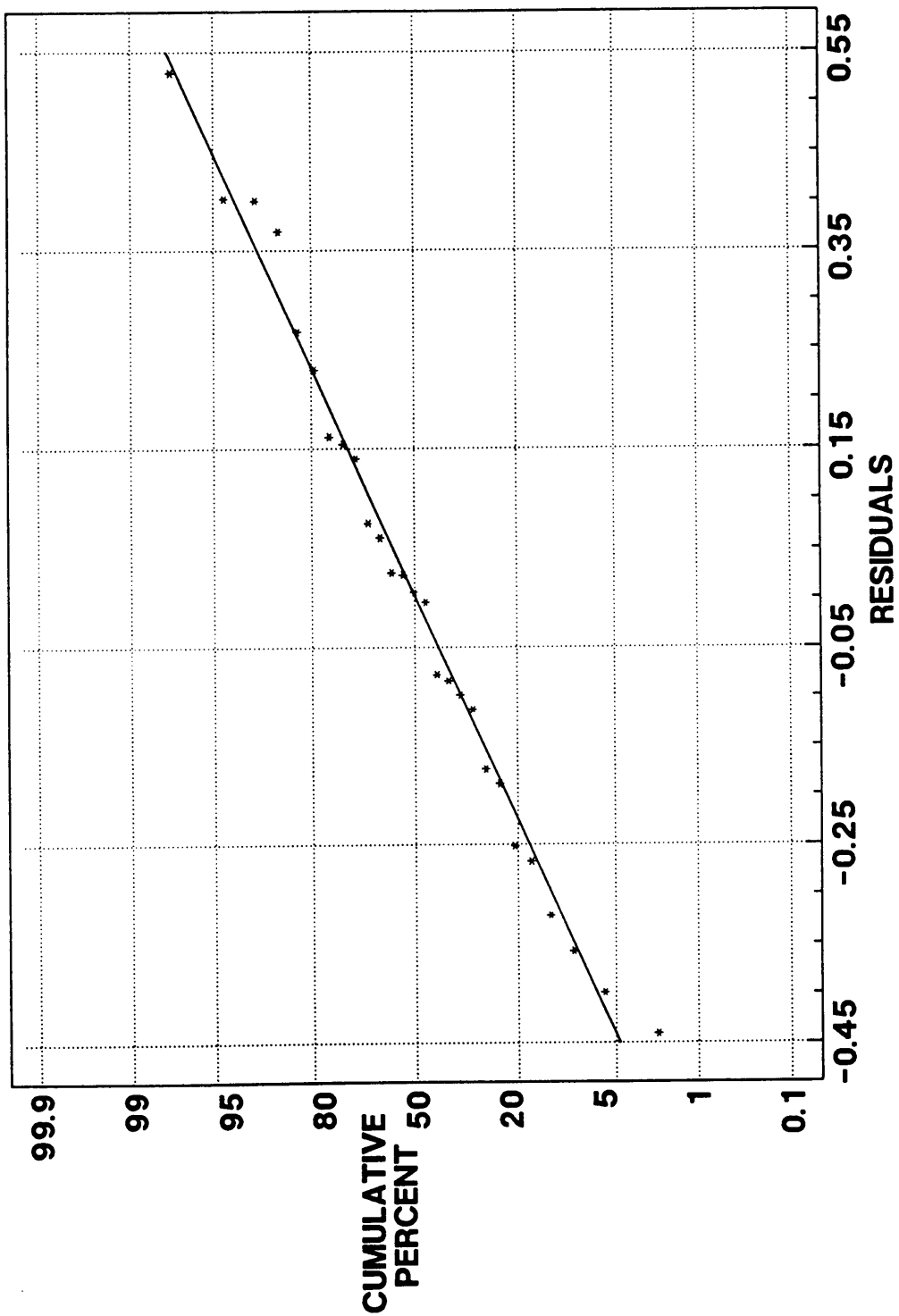


Figure 32: Normal Probability Plot of Residuals

combinations of linear and secondary terms of the variables until all terms with no significance were eliminated. A simple guideline for evaluating each term's significance is by observing its contribution to the coefficient of determination (R^2). R^2 is defined as the proportion of variability in the dependent variable that is accounted for by the independent variable (21). Therefore a maximum coefficient is desired ($R^2=1$). For the model developed, R^2 was 0.9821. The best fit equation for the data included the following terms:

$$C_1(HE) + C_2(DCT) + C_3(ST) + C_4(MP) + C_5(HE)^2 + \\ C_6(DCT)^2 + C_7(ST)^2 + C_8(MP)^2 + C_9(MP)(ST) + \\ C_{10}(ST)(DCT) + C_{11}(HE)(DCT)$$

This equation was used to generate response surfaces illustrating the effect of the independent variables in sigma. Figures 33 to 38 show surfaces for each combination of independent variables. It is demonstrated by figures 33, 35, and 38 that sigma is inversely proportional to source temperature. As source temperature increases, sigma decreases. The magnitude of this effect for caffeine is between 1.0 - 1.6 sec. which approximates a 4.0 - 6.4 sec. change in total peak width. It is likely that this effect is independent of the

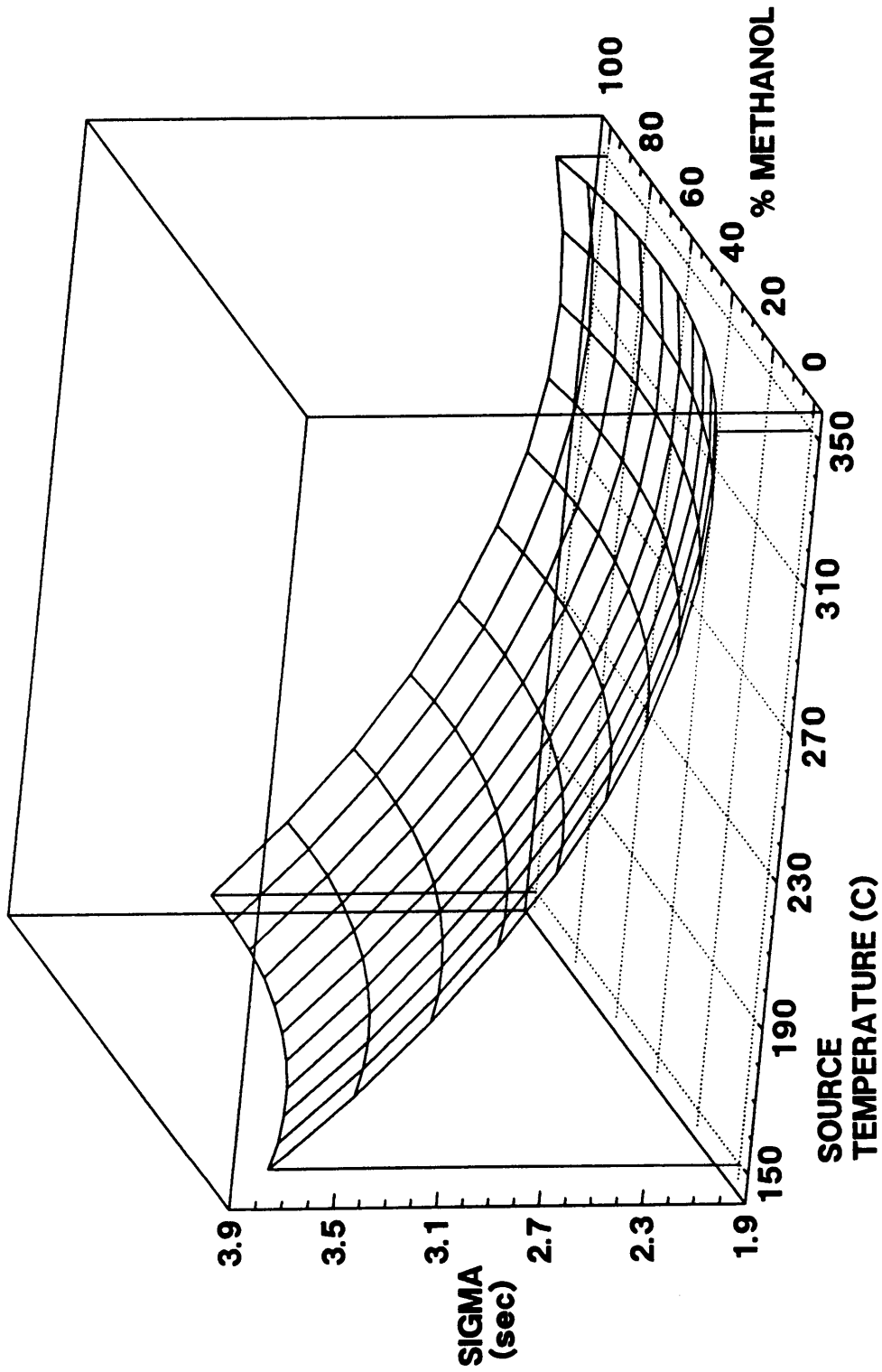


Figure 33: Effect of Source Temperature and % Methanol on Sigma

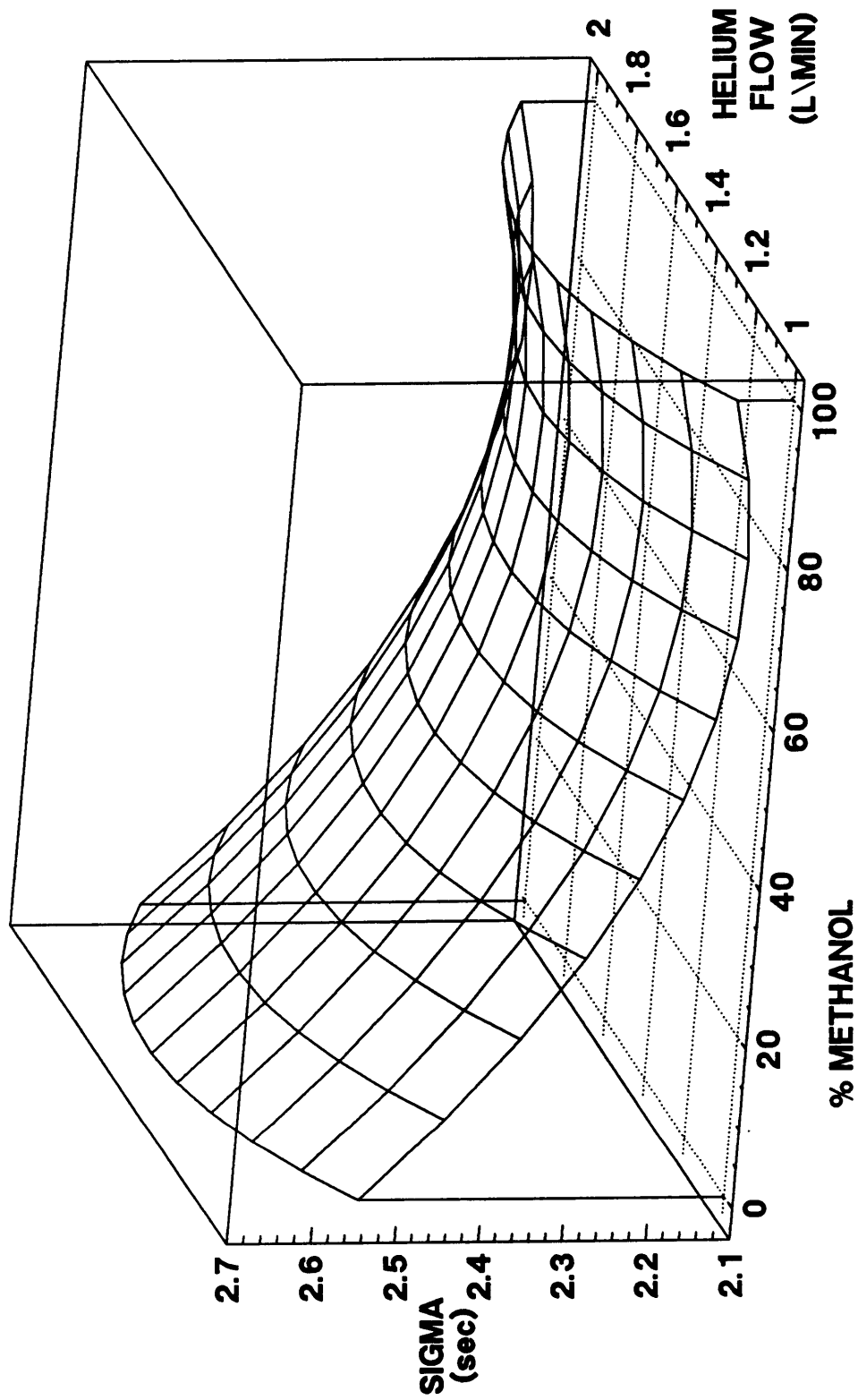


Figure 34: Effect of % Methanol and Helium Flow on Sigma

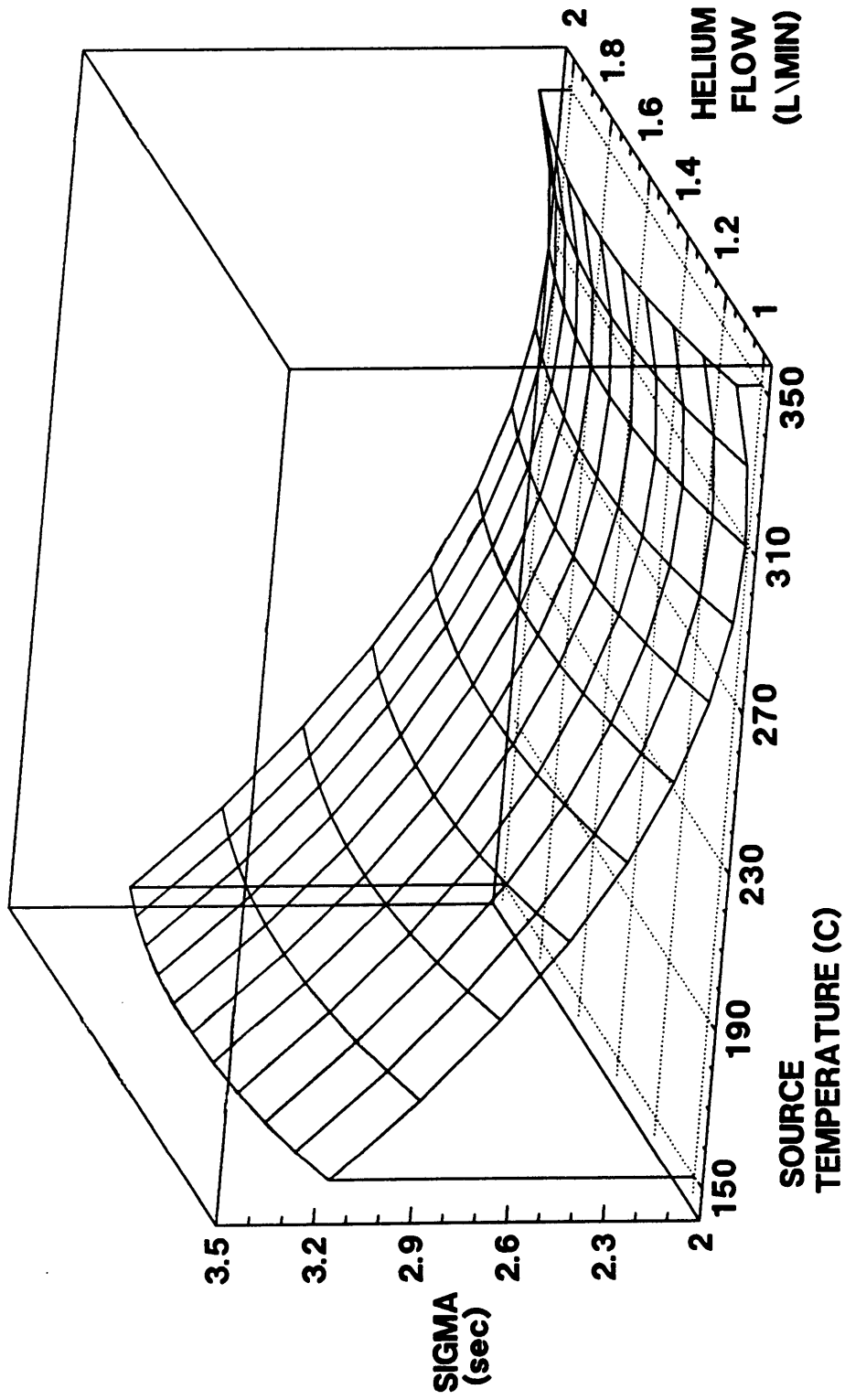


Figure 3.5: Effect of Source Temperature and Helium Flow on Sigma

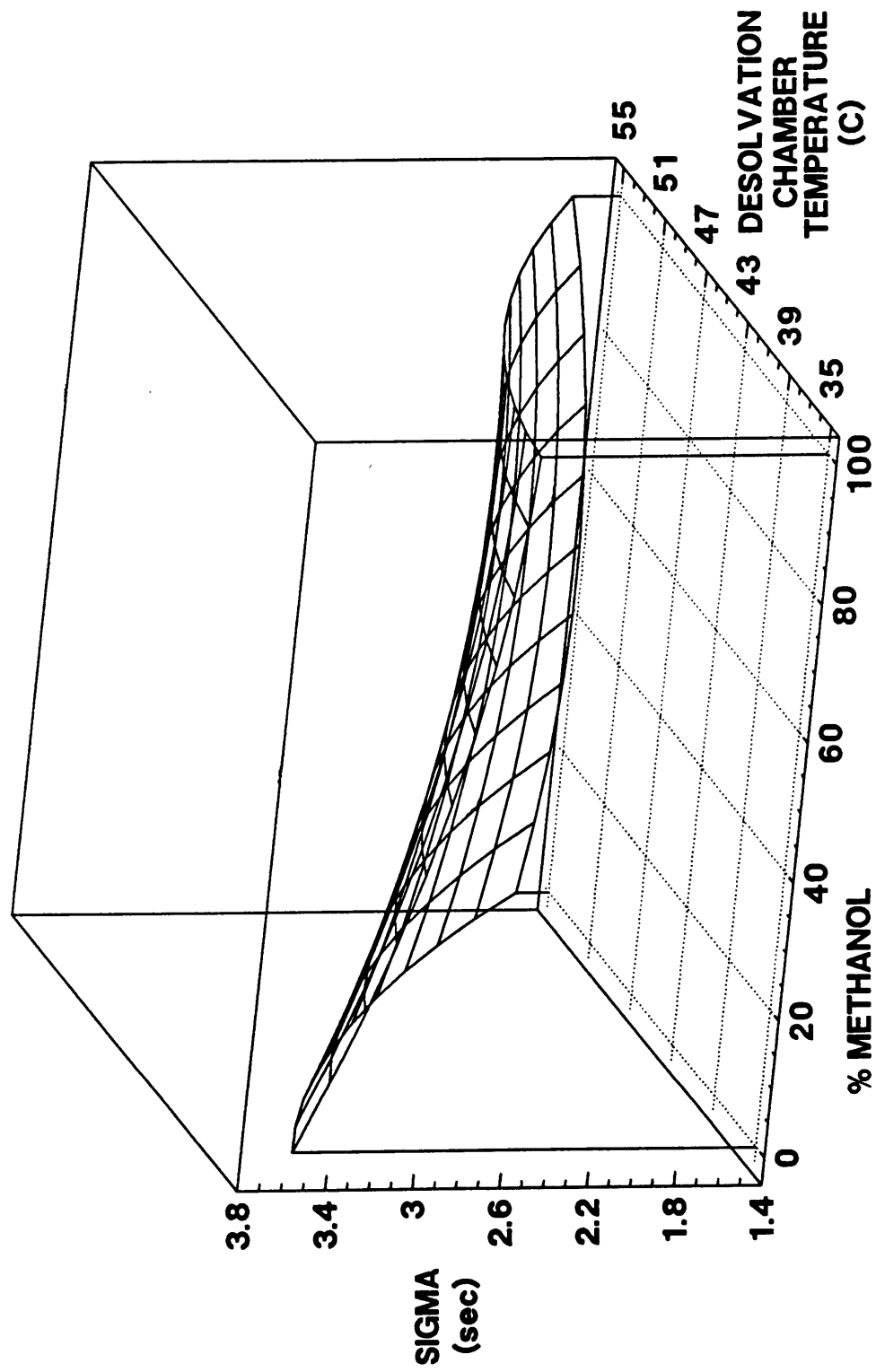


Figure 3.6: Effect of % Methanol and Desolvation Chamber Temperature on Sigma

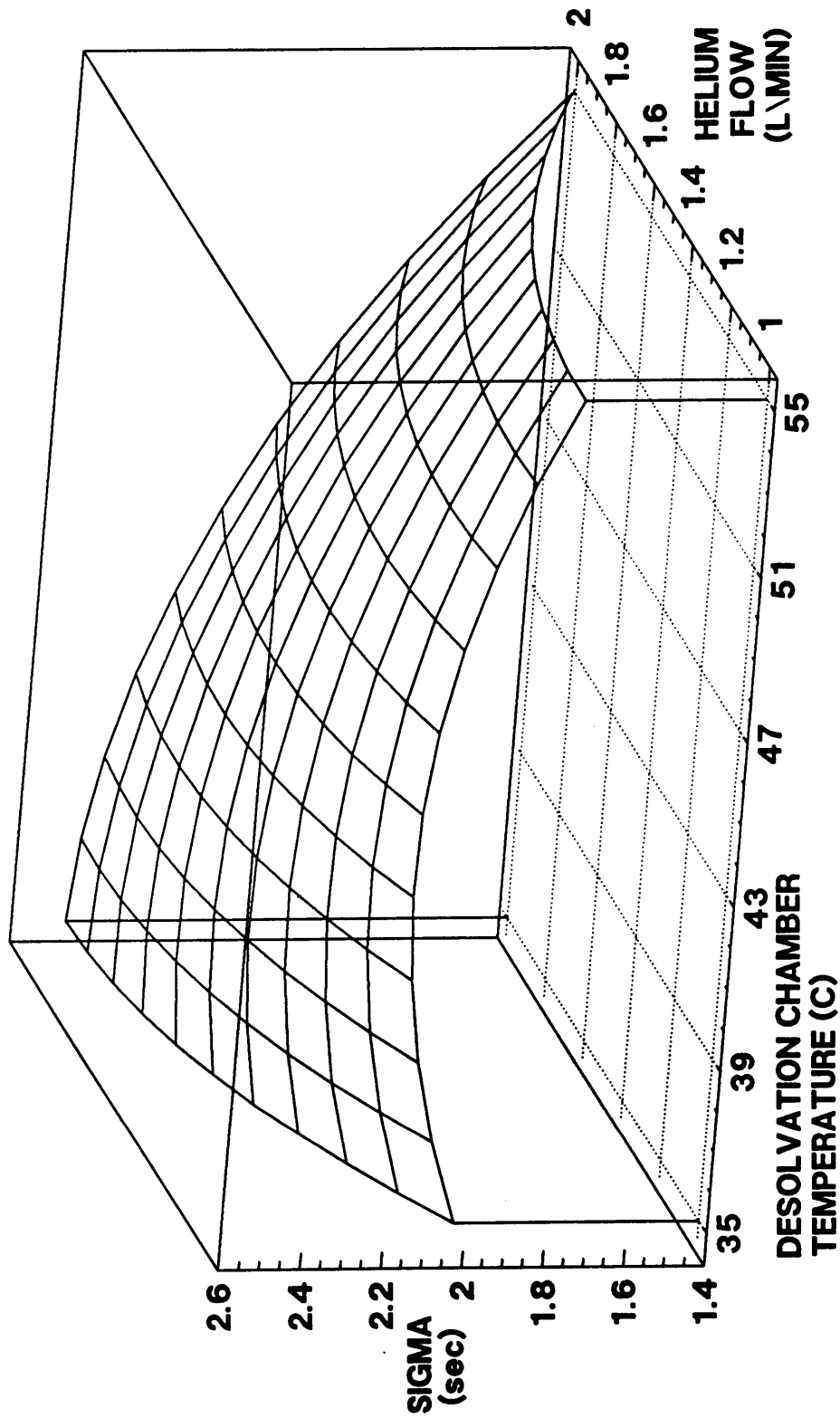


Figure 37: Effect of Desolvation Chamber Temperature and Helium Flow on Sigma

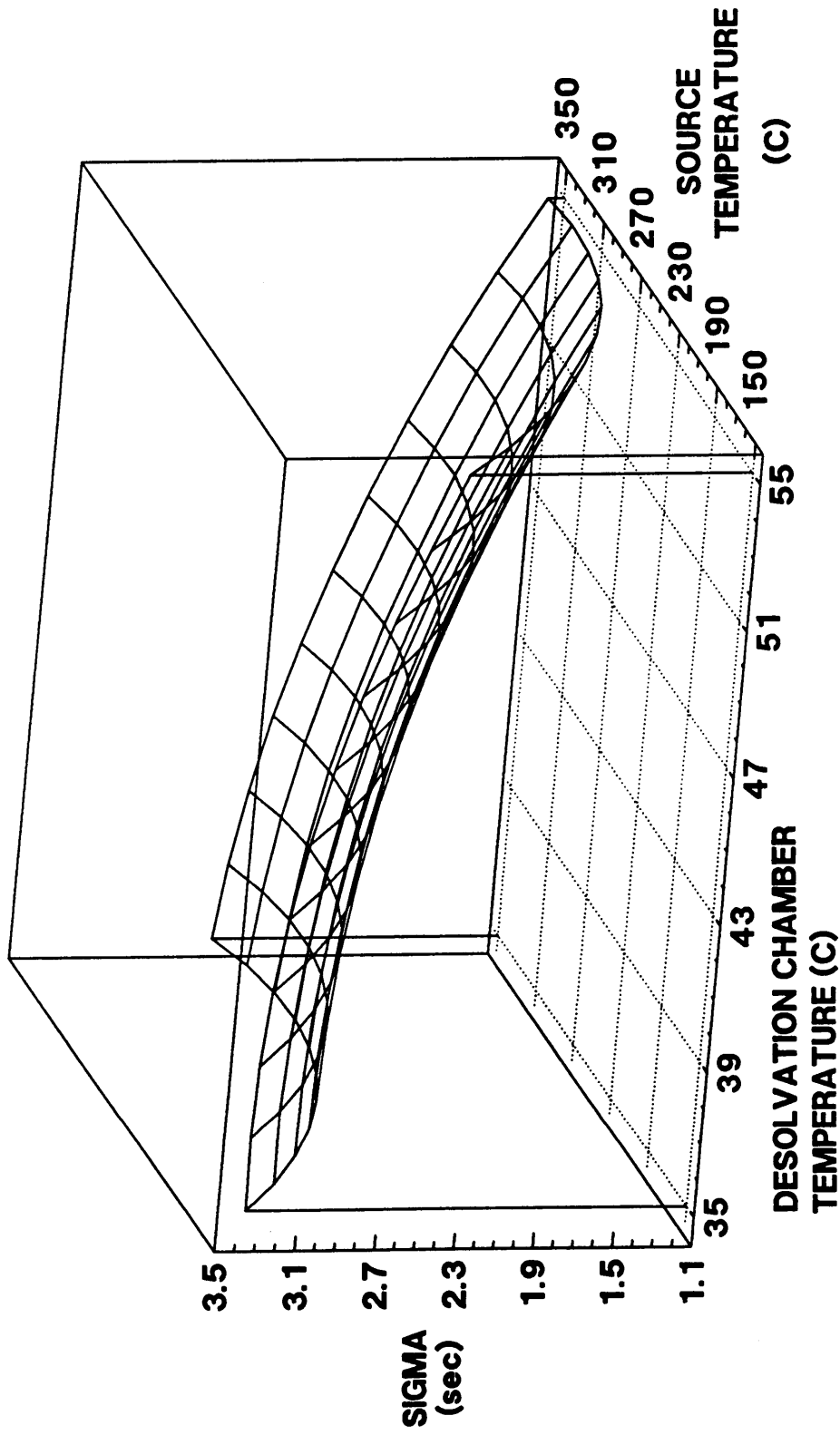


Figure 38: Effect of Desolvation Chamber Temperature and Source Temperature on Sigma

analyte due to greater vaporization efficiency at higher source temperatures. The mass spectral quality, however, is greatly affected by source temperature and is therefore considered an analyte dependent variable. In figures 34, 35, and 37, the helium flow shows an increase in sigma of 0.2 - 0.4 sec. when operated between 1.3 - 1.6 liters/min. The nebulizer normally gives a maximum response at a helium flow of approximately 1.5 liters/min. It is fortunate that the increase in band width attributed to the helium flow is small in comparison to other variables. Mobile phase composition affects sigma by decreasing band width with an increasing proportion of methanol (see figs. 33, 34, and 36). This change in sigma is in the range of 0.2 - 0.8 sec. and so the effect on total band width is between 0.8 and 3.2 sec. The signal response mimicks this trend in sigma by showing an increase in intensity with increasing percent organic in the mobile phase. The desolvation chamber temperature (DCT), like the source temperature has a great affect on the sigma. As DCT is increased, sigma is decreased by 1.0 - 2.0 sec. This affect is pronounced when the mobile phase contains a high proportion of water (see fig. 36). When the DCT is increased at a helium flow of 2 liters/min. a change in sigma of 1.2 sec. is observed. This seems intuitively obvious, since at the higher proportions of water the solvent is less volatile and

more polar. This makes the solvent more difficult to evaporate in the aerosol leading to a more solvated analyte in the system resulting in a larger sigma and ghosting. By increasing the helium flow and the DCT the aerosol droplets become smaller increasing their surface area. More surface is exposed to the heated atmosphere allowing for rapid water evaporation. Unfortunately the smaller droplets may also yield smaller particles which do not perform as well in the momentum separator. This study was duplicated at a later time. The results of the second study give the same results as the one described above. The response surfaces for this study can be found in Appendix B.

CHAPTER IV

CONCLUSIONS

Particle Beam has been shown to perform adequately in all three studies undertaken. The MDQ study tested the general application of particle beam to many different types of compounds. The linearity study investigated particle beam's potential for quantitative analyses. The band broadening study summarized the operating variables and their effects on the chromatographic peak width.

The MDQ study showed that the particle beam effectively transports a wide variety of compounds into the MS ion source. These compounds contained many different types of functional groups. Particle beam LC/MS allowed one to detect and obtain mass spectra for all compounds in this thesis. Despite this general applicability, there were differences in analyte response between the three ionization modes (EI, PCI, and NCI). In some cases, these differences in sensitivity may be a function of the compounds structure. However, it is likely the overall sensitivity increase achieved in NCI was due, at least in part, to instrumental design. Dynode conversion in the detector during NCI can lead to such an increase. Since the completion of these studies, Hewlett-Packard has introduced a high energy

detector which offers the same sensitivity enhancements for the positive ion modes (EI and PCI).

The linearity study showed good response and reproducibility for all compounds tested except aldicarb. The %RSD's obtained for the five replicate injections at each concentration were very good ($8\% \pm 6\%$). The %RSD's for the response factors in the calibration curves, while not excellent, are acceptable by GC/MS standards for priority pollutant analyses. A drop in response at lower concentrations was evident for each compound. This could be attributed to the formation of smaller particles with less momentum. Improved transport of these smaller particles should be a topic of further research. It is important to note that the linearity study demonstrated that response factors are not constant at low concentrations. This indicates that the extrapolated MDQ's in section 3.2 must be considered ideal cases because they are based on the assumption that the response factors remain constant regardless of sample concentration.

The response surfaces generated for the band broadening study showed source temperature to have the most significant effect on peak width. Conversely, helium flow and desolvation chamber temperature were shown to have little effect. In general, this demonstrates that the particle beam interface has a negligible contribution to band broadening when compared to the contribution of the mass spectrometer ion source.

REFERENCES

1. Arpino, P.J. and Guiochon, G. ,Anal. Chem. ,1979 ,
51 ,682A.
2. Covey, T.R. , Lee, E.D. , Bruins, A.P. ,and Henion,
J. ,Anal. Chem. ,1986 ,58 , 1451A.
3. Lau, J.M. , McNeil, M. ,Darvill, A. ,and Albershcim,
P. ,Carbohyd. Res. ,1985 ,137 , 111.
4. Kenyon, C. ,Ellis ,R. ,Dixon ,D. ,HP Technical Paper
MS-13 ,1981 ,23-5952-5873.
5. Barcelo, D. ,LC-GC ,1988 ,6-4 ,324.
6. Funch, F. and Lisbjerg,S. ,Z. Lebensm Unter Forsch ,
1988 ,186 ,29.
7. Rushneck, D.R. ,editor ,Spectra ,1986 ,10-4 ,1.
8. Goodely, P.C. and Thorp,J. ,HP Technical Paper AN
176-41 ,1986 ,23-5952-5851.
9. Unger, S.E. ,Warrack ,B.M. ,Spectroscopy ,1986 ,1-3 ,
33.
10. Hewlett Packard Publication No. 43-3954-9178.
11. Snyder, L.R. and Kirkland, K.K. , "Introduction to
Modern Liquid Chromatography" , John Wiley and
Sons, Inc. ,New York,1979.
12. Kenyon, C. ,Biomedical Mass Spec. ,1983 ,10 ,535.
13. Kenyon, C. ,Goodely ,P. ,Dixon ,D. ,Whitney ,J.
 ,Faull ,K. ,Barches ,J. ,American Laboratory ,1983
 ,Jan ,38.
14. Garteiz, D. ,Vestal ,M. ,LC Mag. ,1985 ,3 ,334.
15. Lau, P. ,McNeil ,M. ,Davill ,A. ,Alberscheim ,P.
 ,Carbohyd. Res. ,1987 ,137 , .
16. Arpino, P. ,J. Chromatography ,1985 ,323 ,3.
17. Willoughby, R. ,Browner ,R. ,Anal. Chem. ,1984 ,56
 ,2626.

18. Apffel, A. ,HP Particle Beam LC/MS Book of Spectra
,HP Technical Publication No. 23-5959-7105 ,1988 .
19. Ott, L. , "An Introduction to Statistical Methods and
Data Analysis" ,3rd ed. ,PWS-Kent Publishing Co.,
Boston ,1988 ,125.
20. IBID. ,593.
21. IBID. ,542.
22. IBID. ,587.
23. Winkler, P. ,C. ,Ph.D. Dissertation ,Department of
Chemistry ,Georgia Tech. ,1986 ,54-57.

APPENDIX A

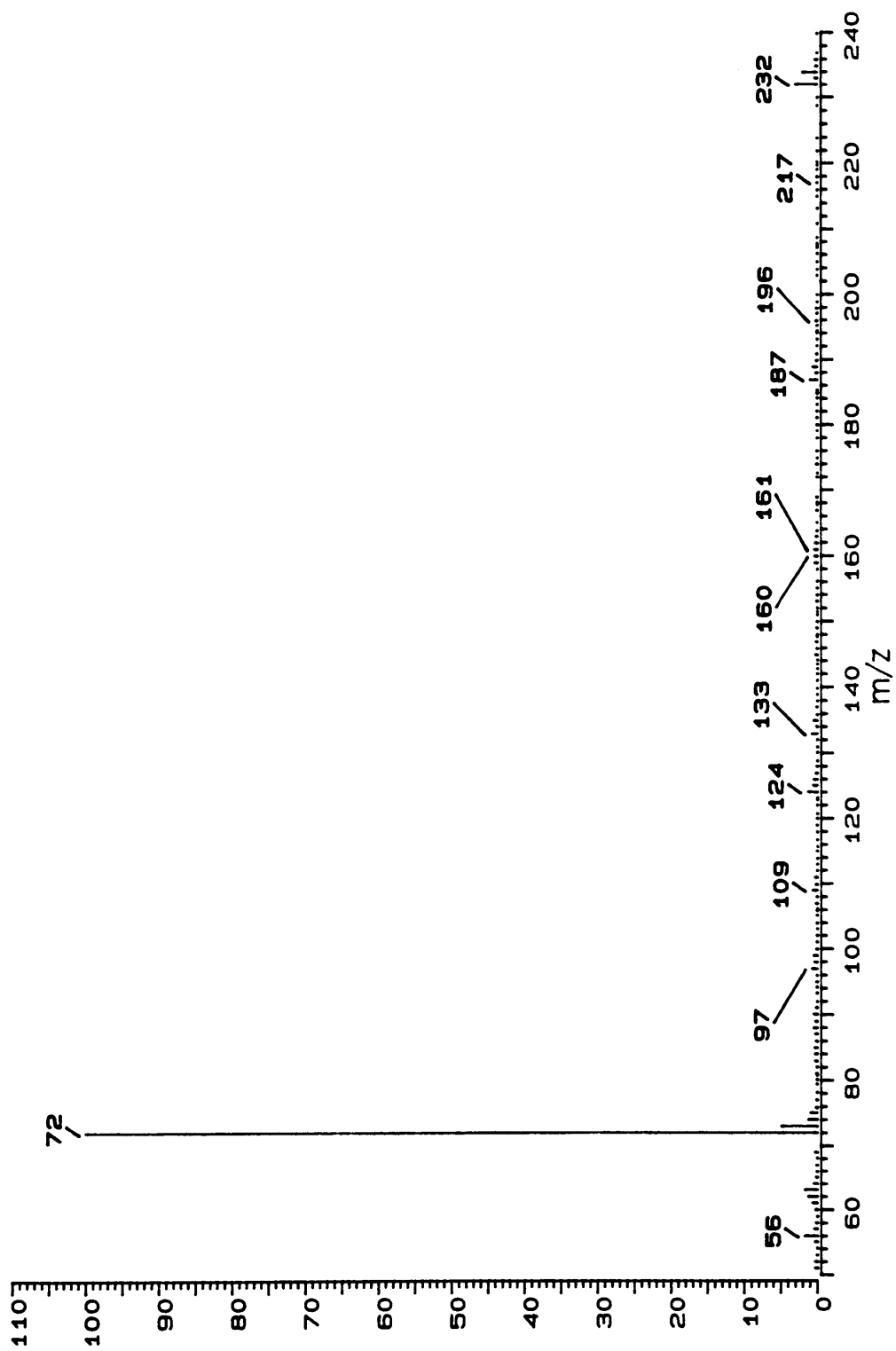


Figure A1: EI mass spectrum of Diuron

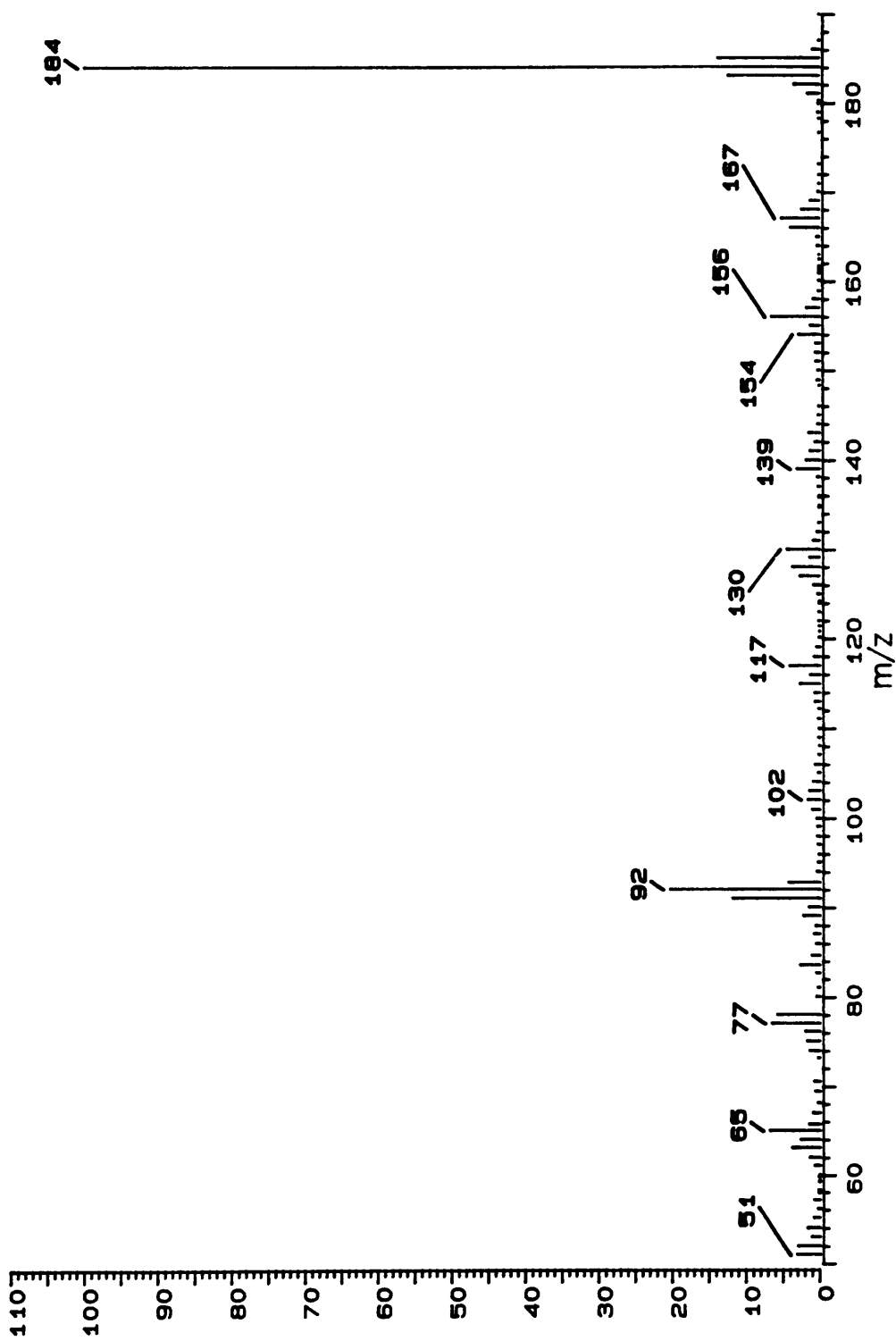


Figure A2: EI mass spectrum of Benzidine

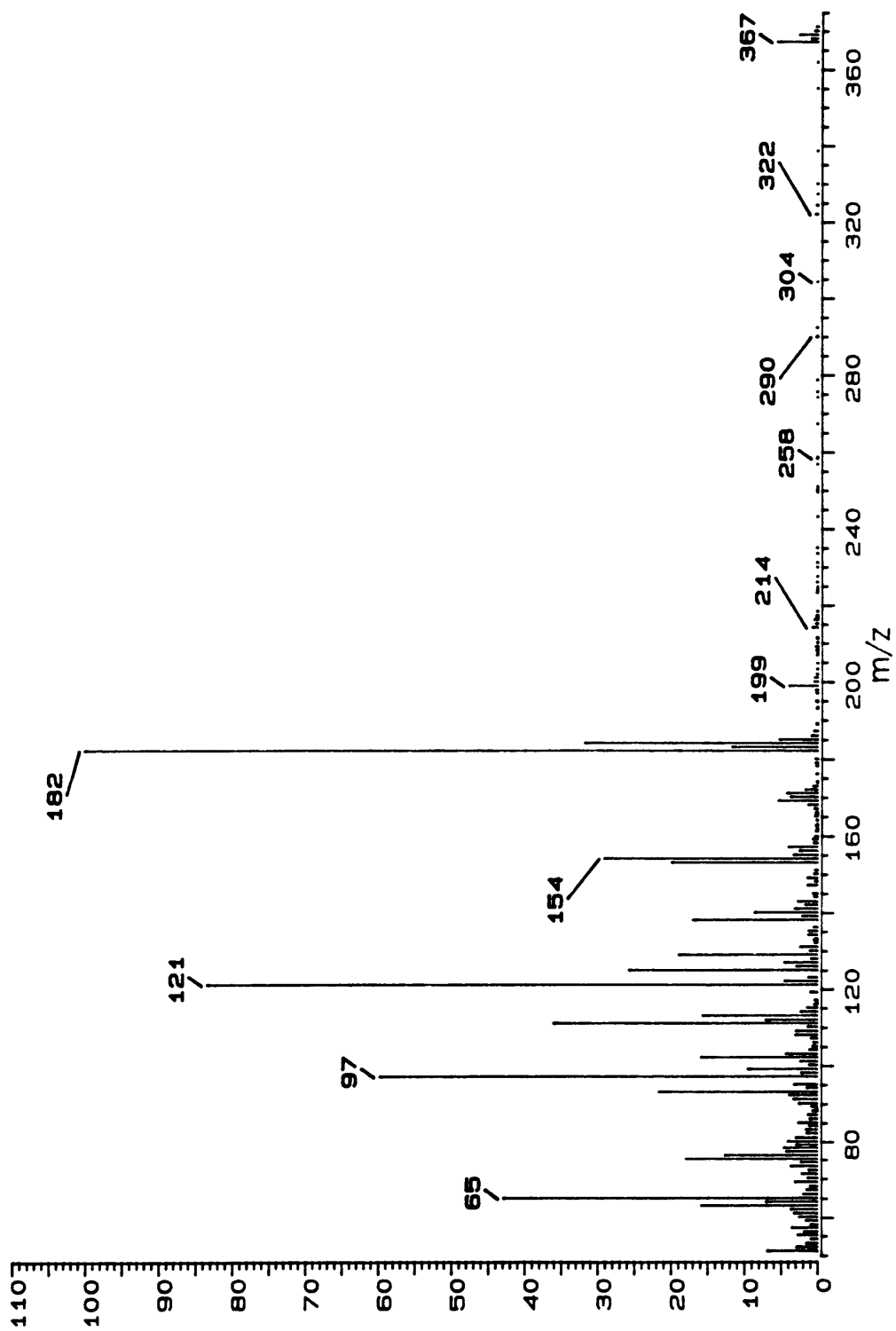


Figure A3: EI mass spectrum of Phosalone

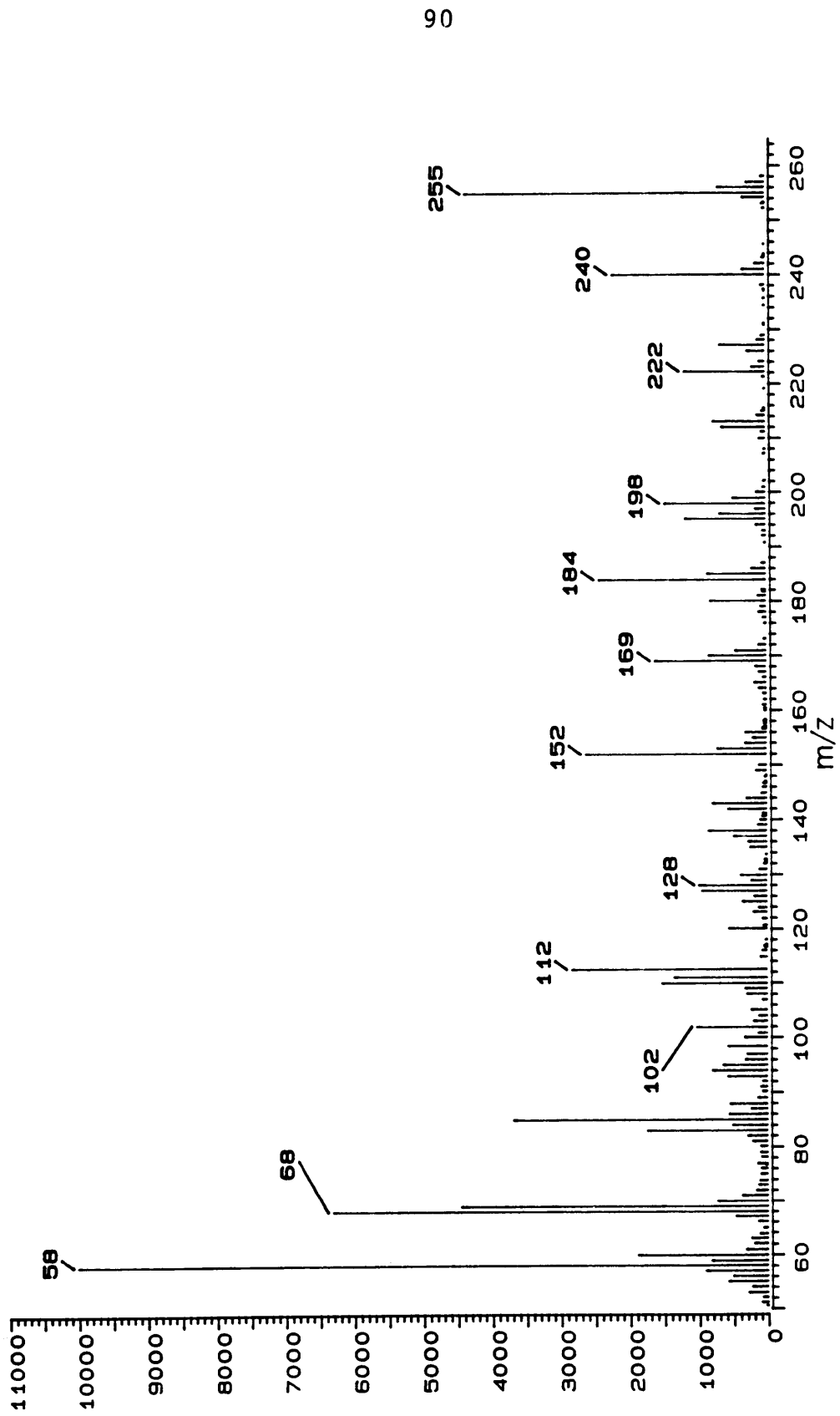


Figure A4: EI mass spectrum of Dipropetryn

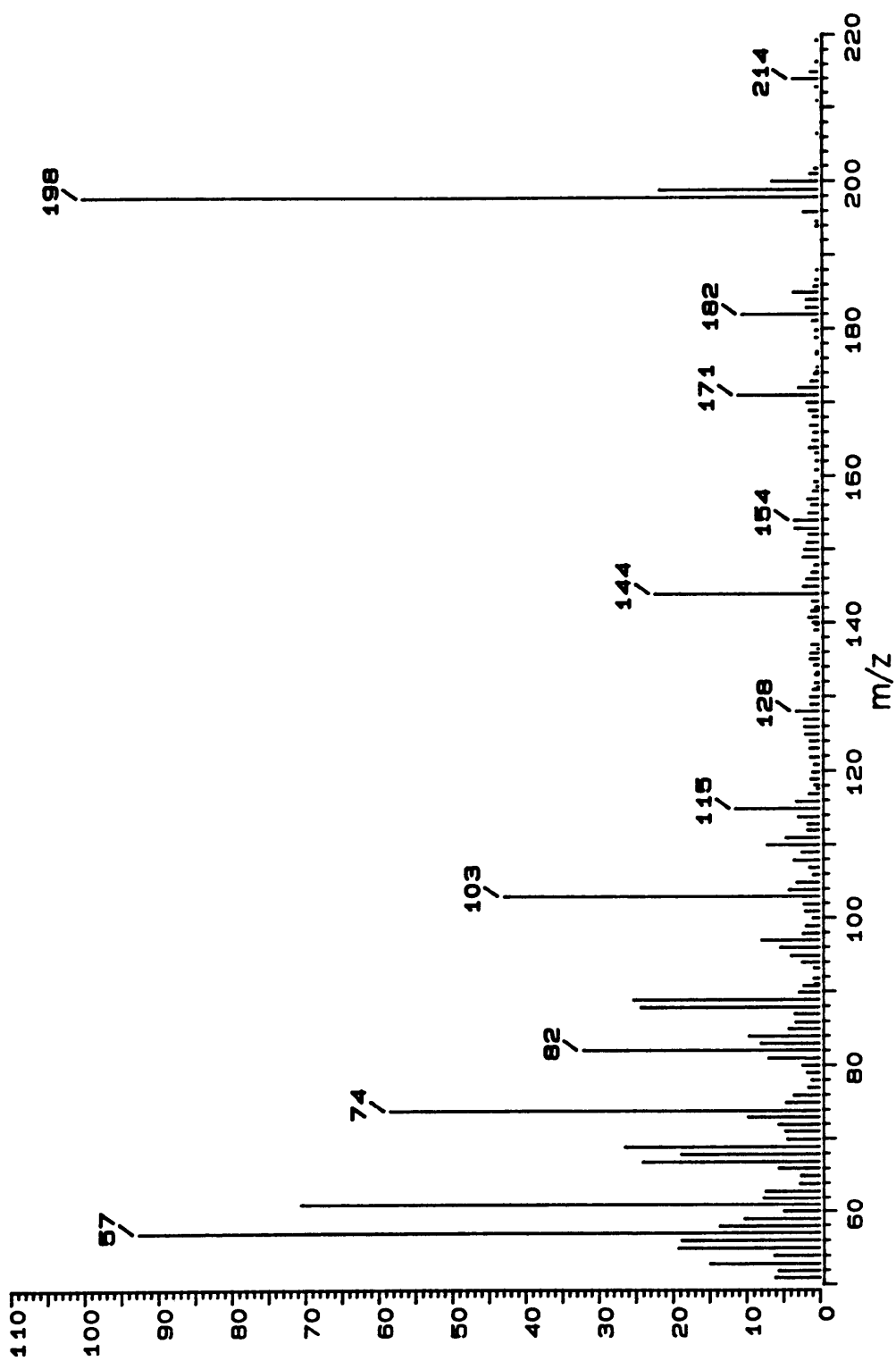


Figure A5: EI mass spectrum of Metribuzin

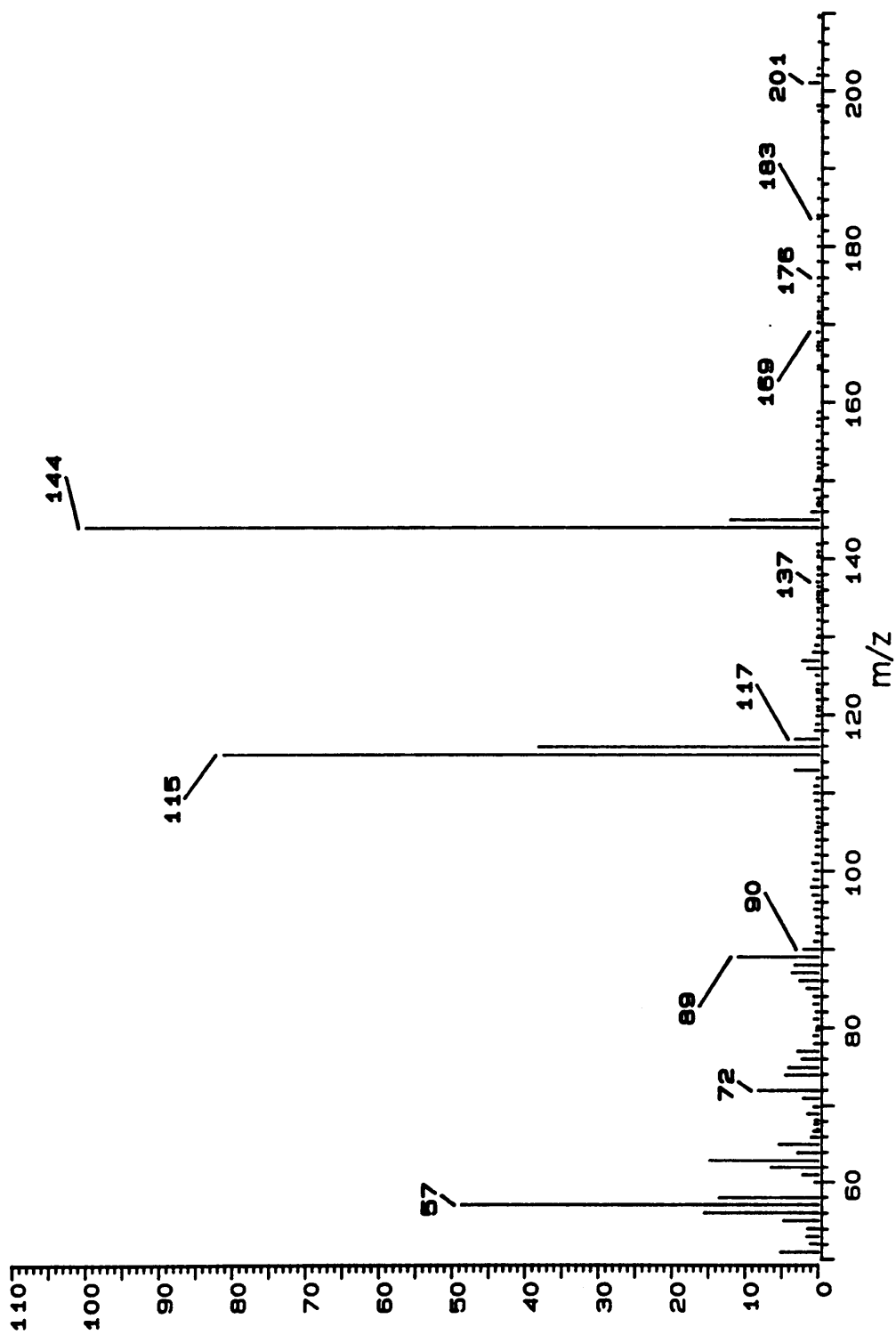


Figure A6: EI mass spectrum of Carbaryl

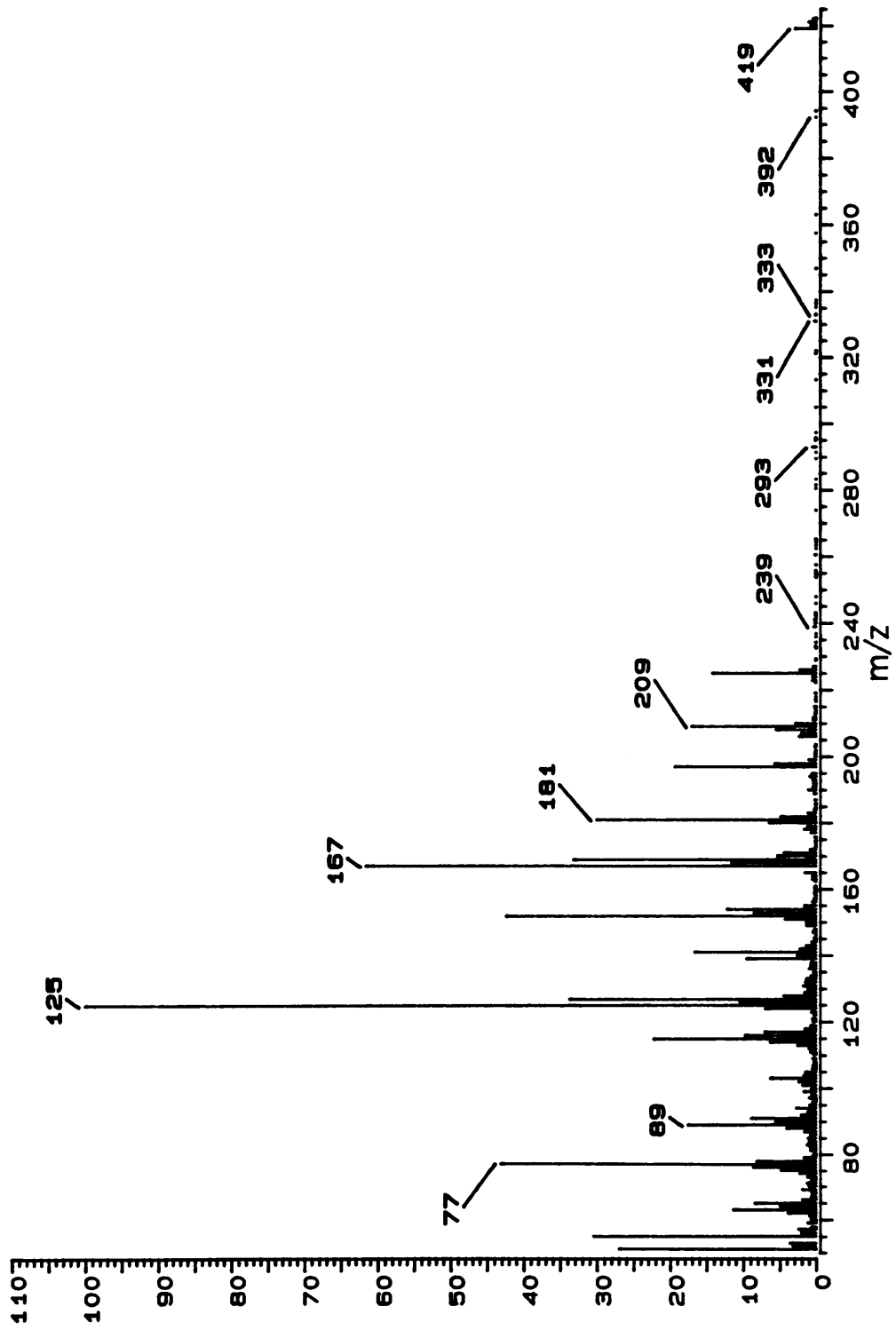


Figure A7: EI mass spectrum of Fenvalerate

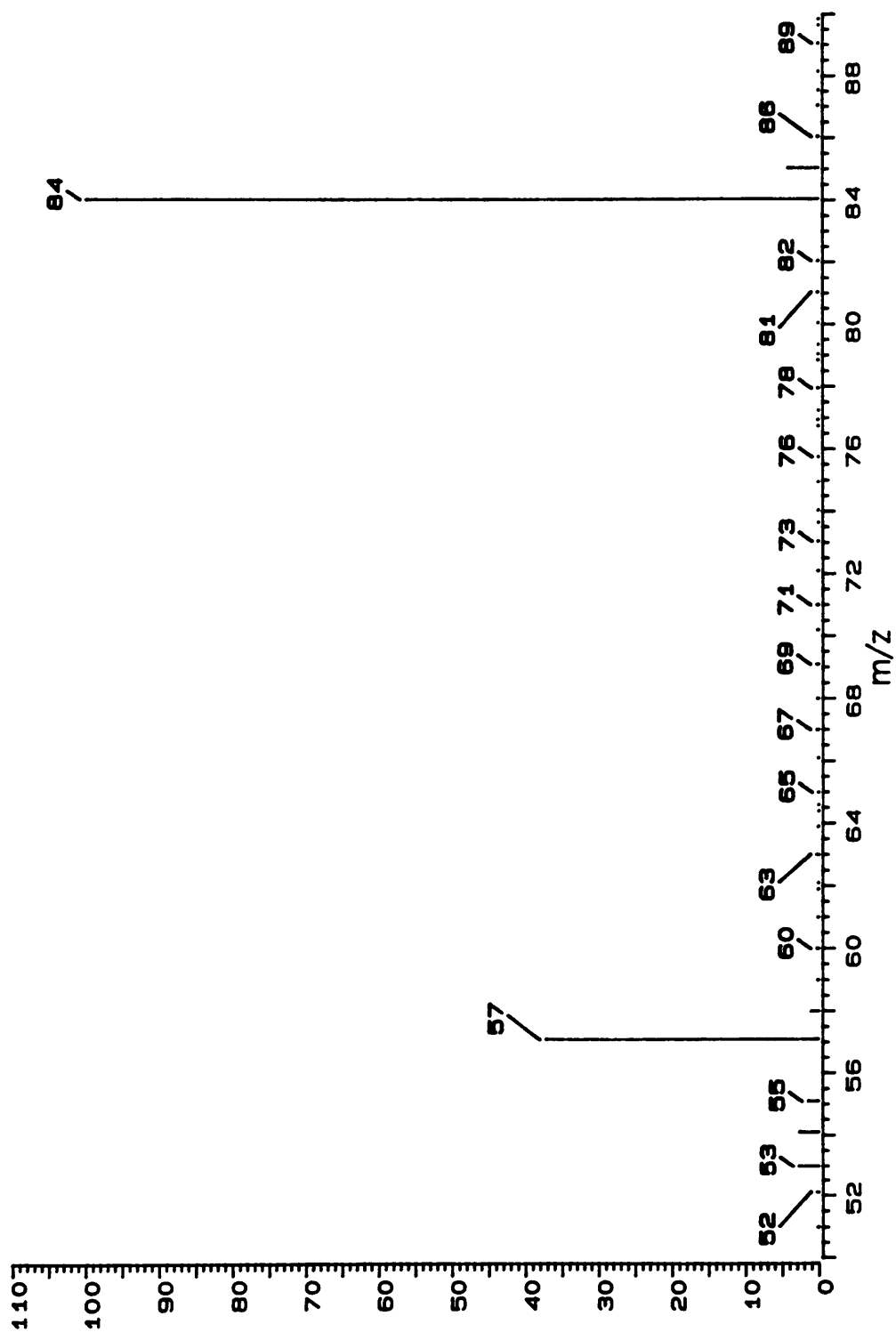


Figure A8: EI mass spectrum of Amitrole

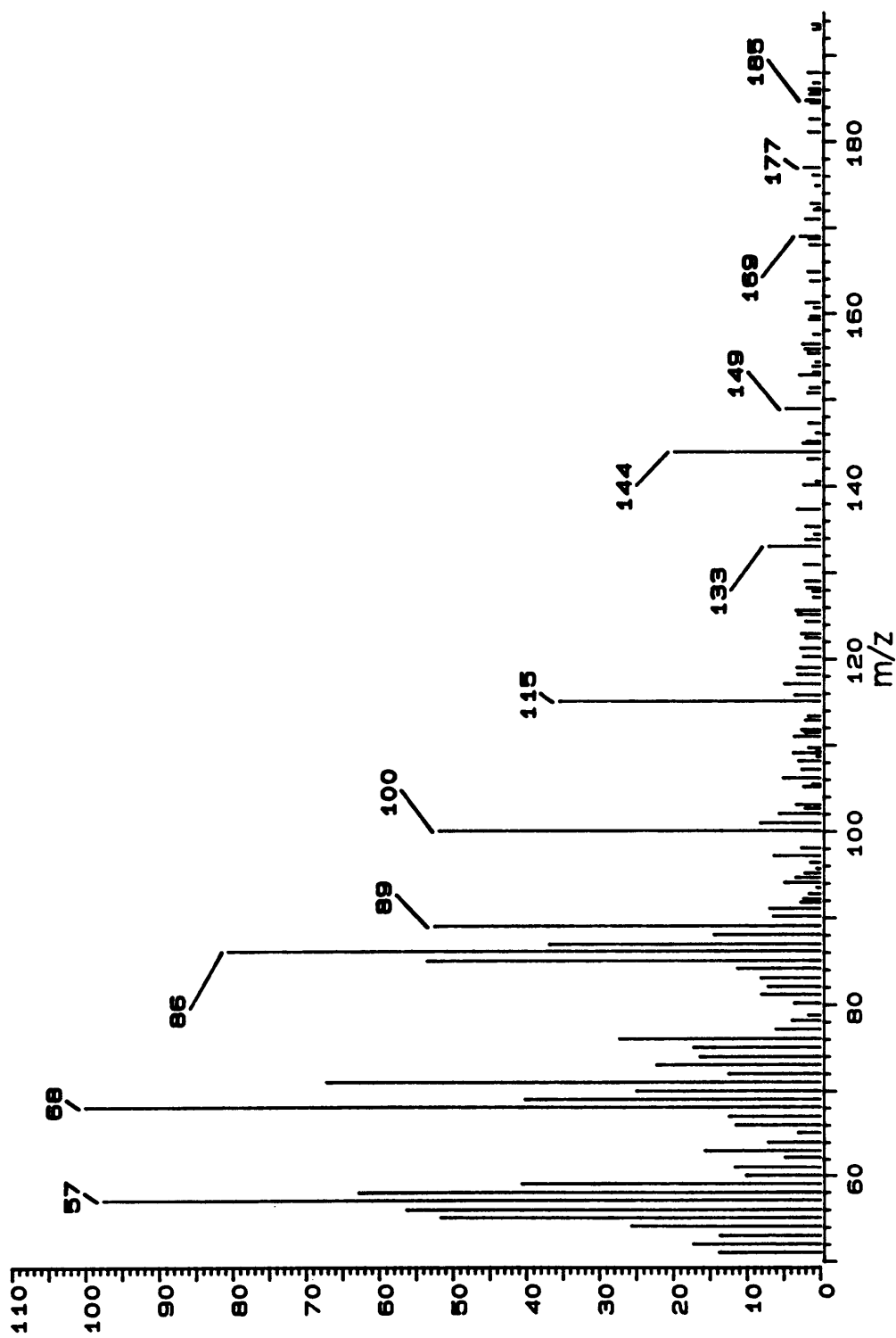


Figure A9: EI mass spectrum of Aldicarb

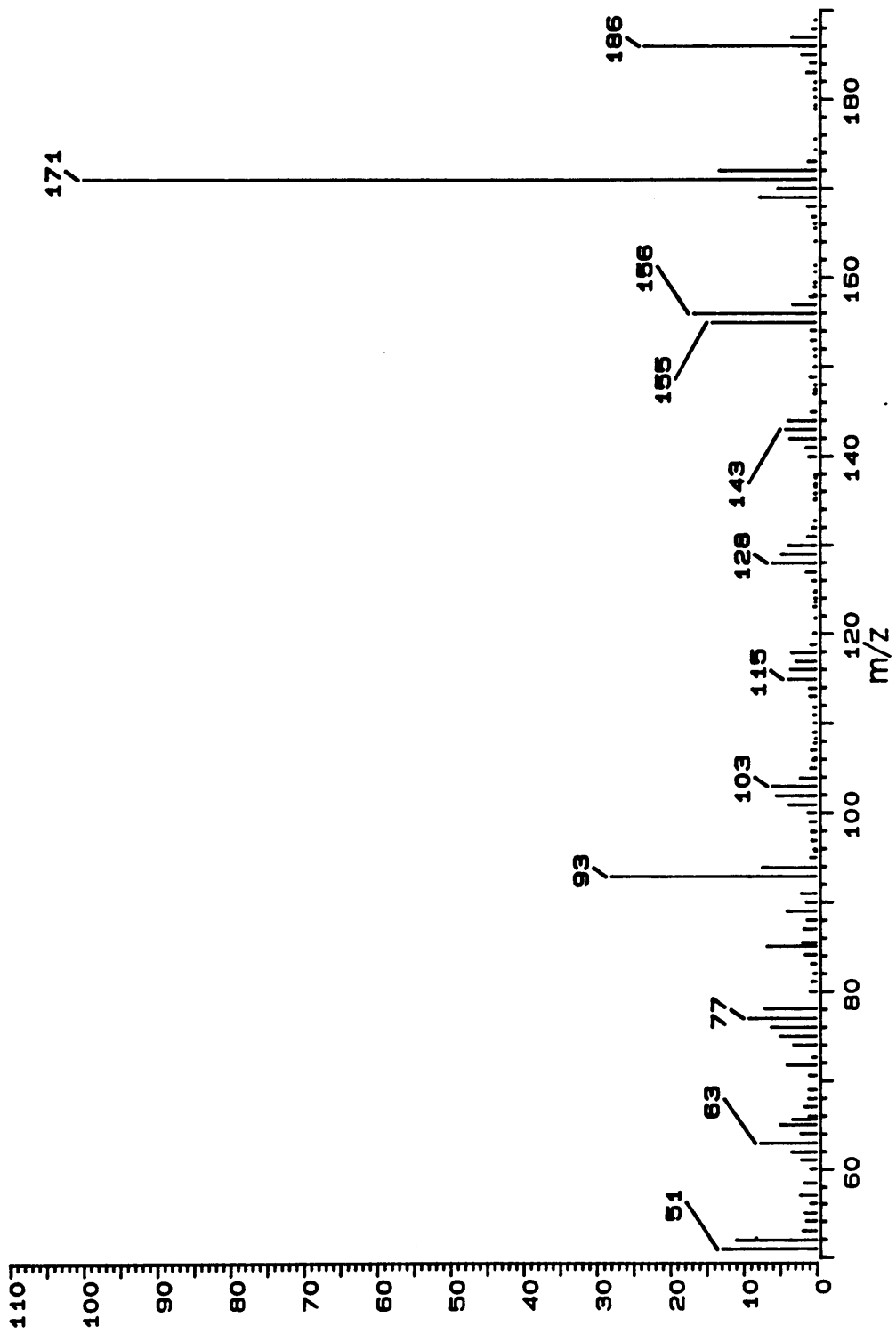


Figure A10:EI mass spectrum of Paraquat

APPENDIX B

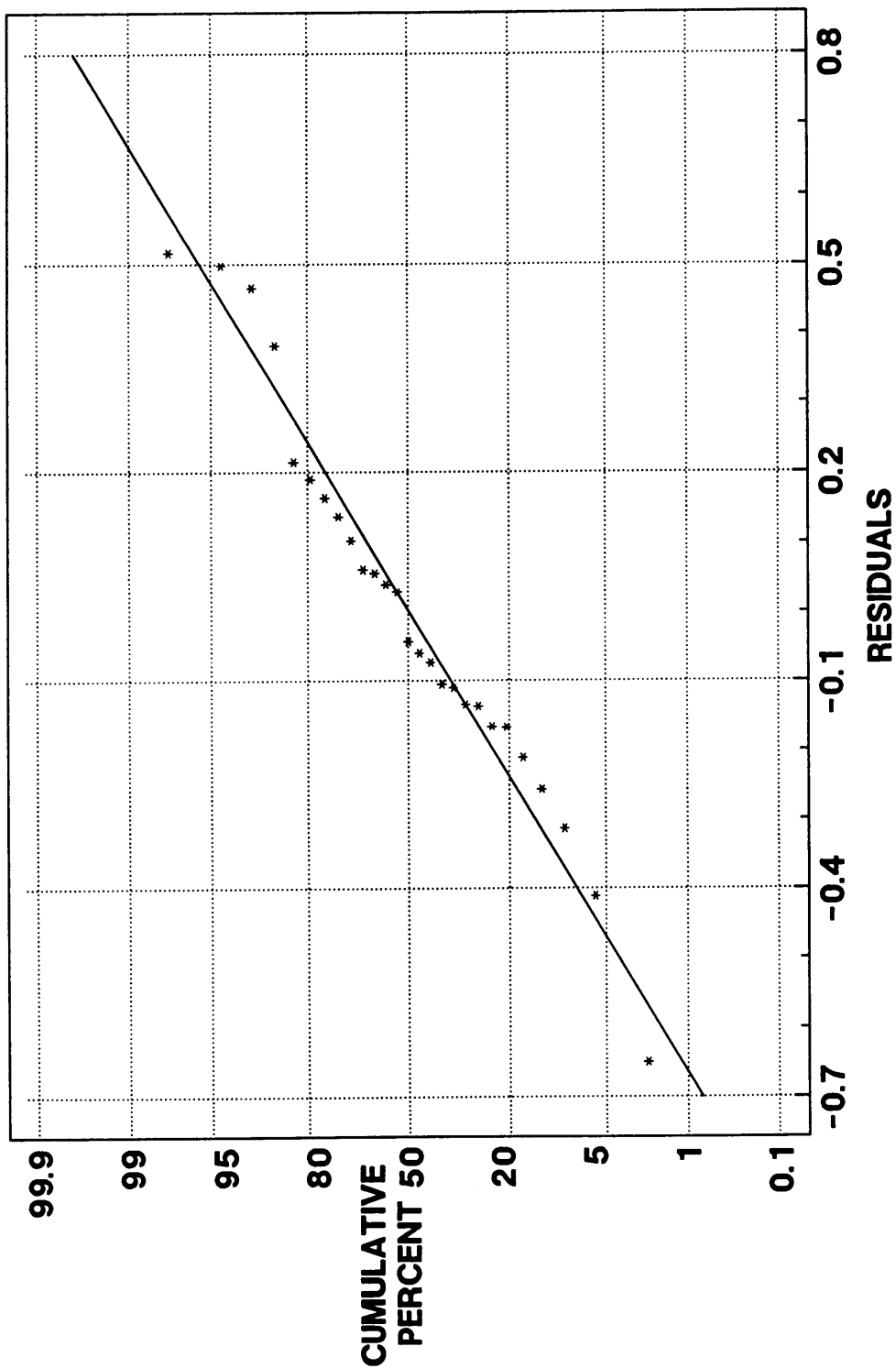


Figure B1: Normal Probability Plot of Residuals

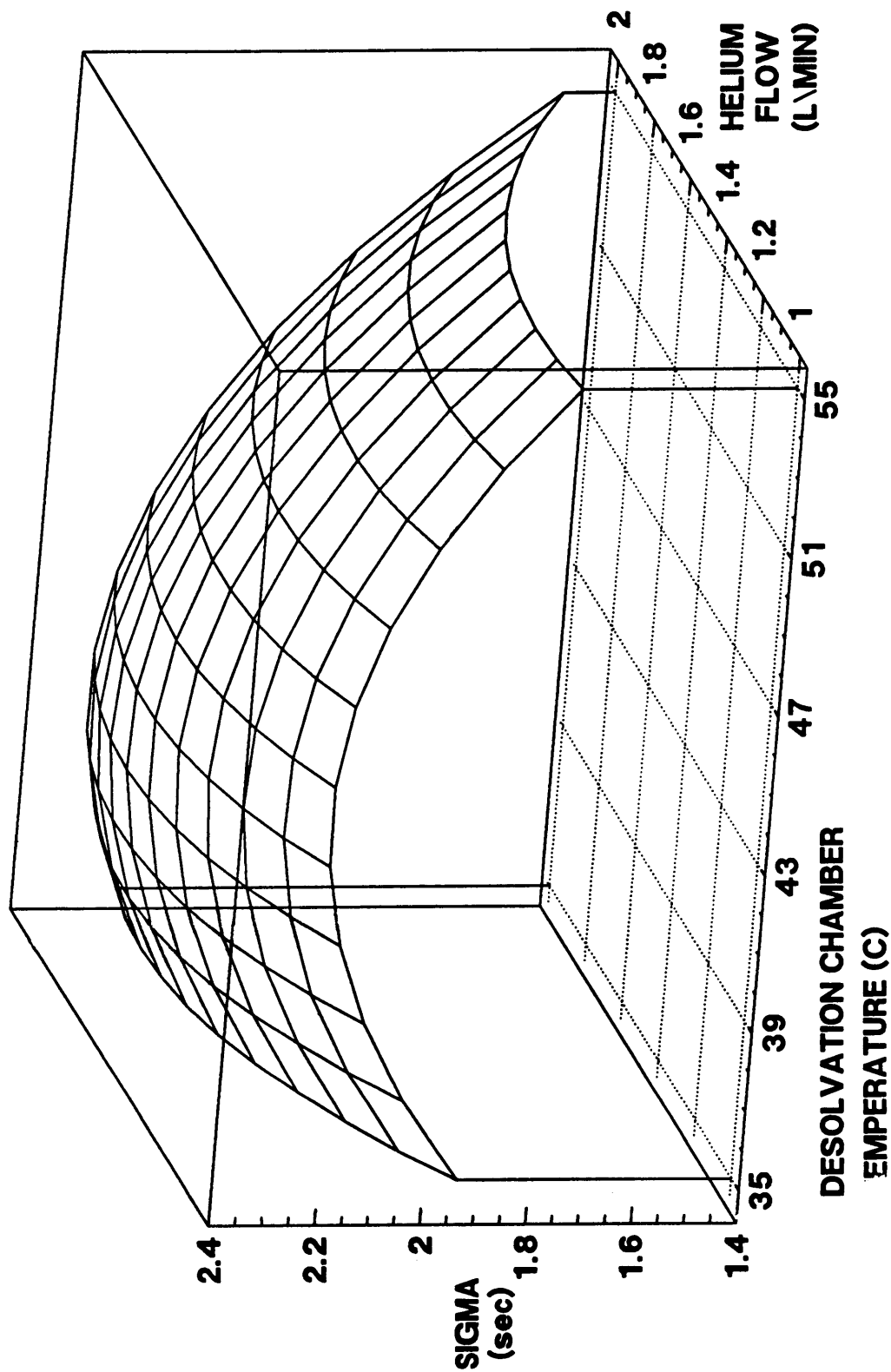


Figure B2: Effect of Desolvation Chamber Temperature and Helium Flow on Sigma

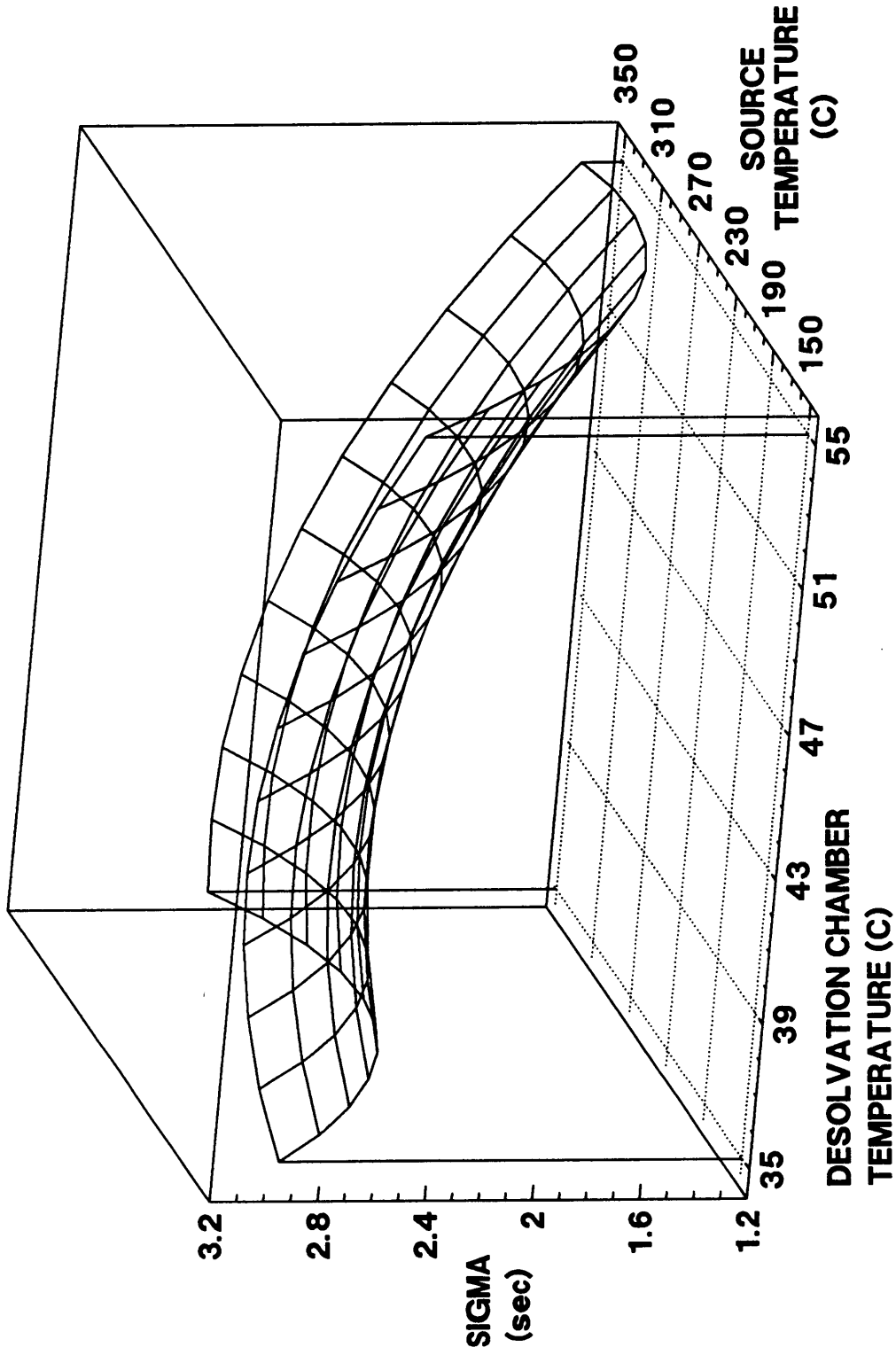


Figure B3: Effect of Desolvation Chamber Temperature and Source Temperature on Sigma

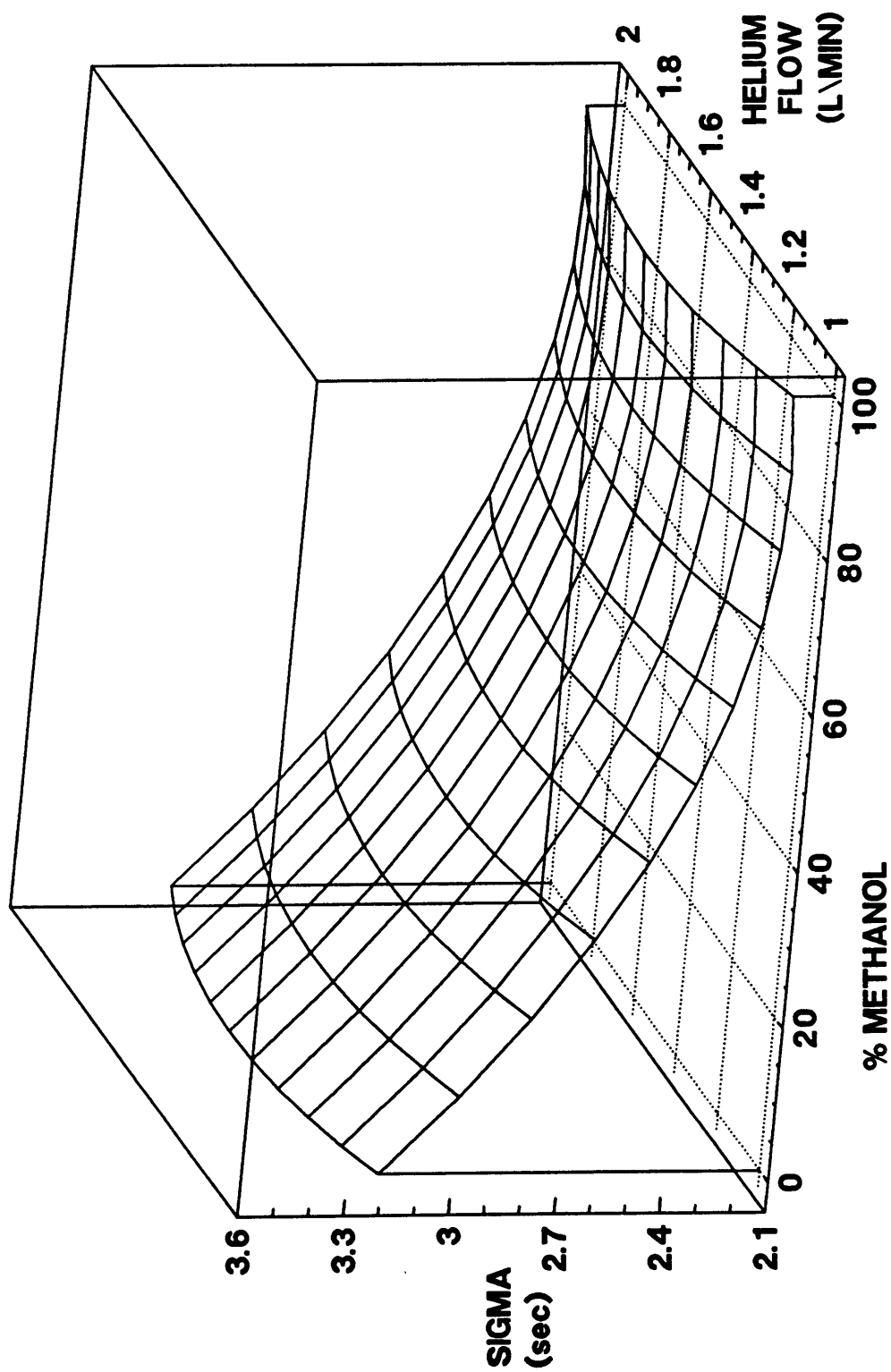


Figure B4: Effect of % Methanol and Helium Flow on Sigma

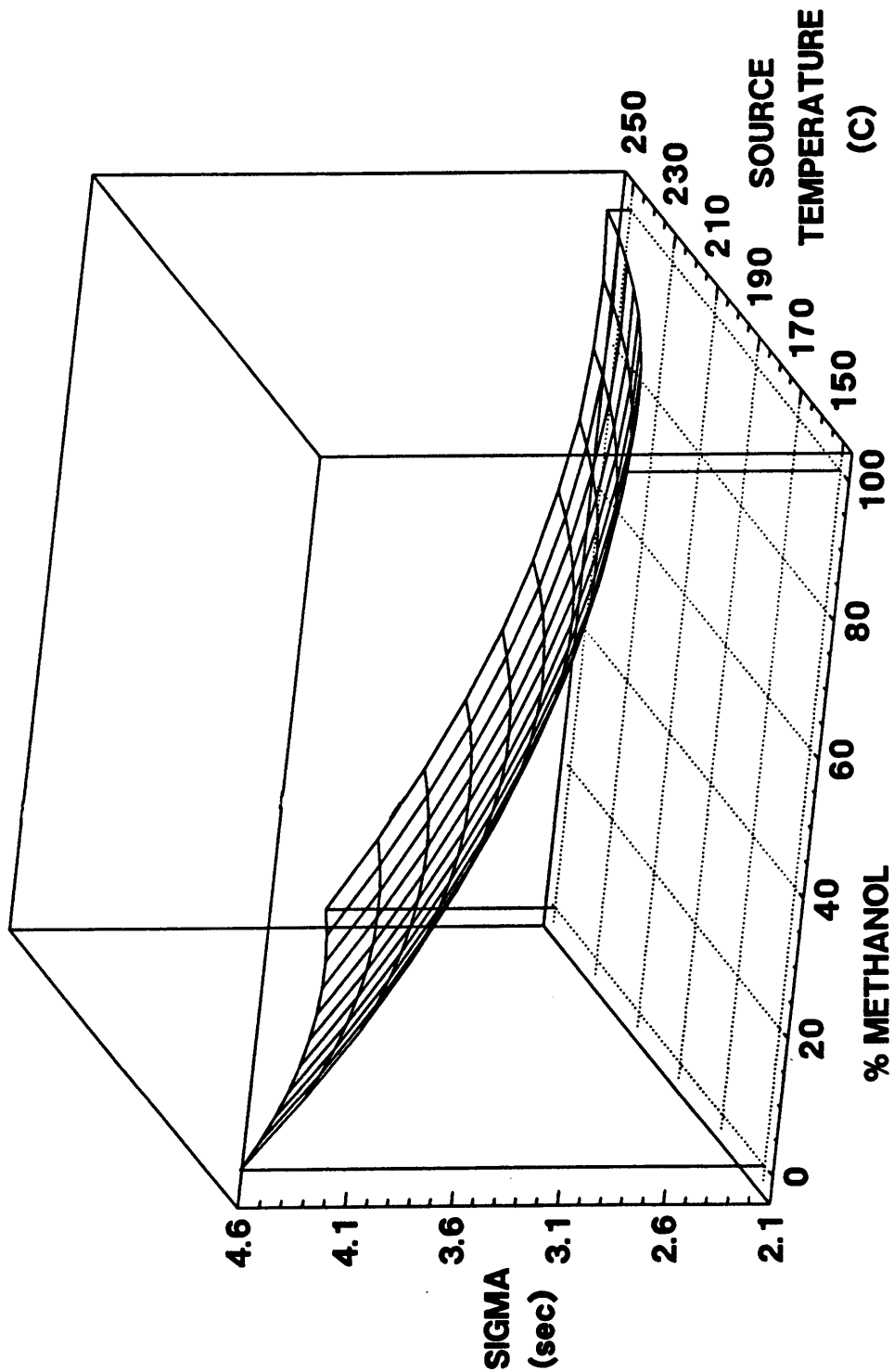


Figure B5: Effect of % Methanol and Source Temperature on Sigma

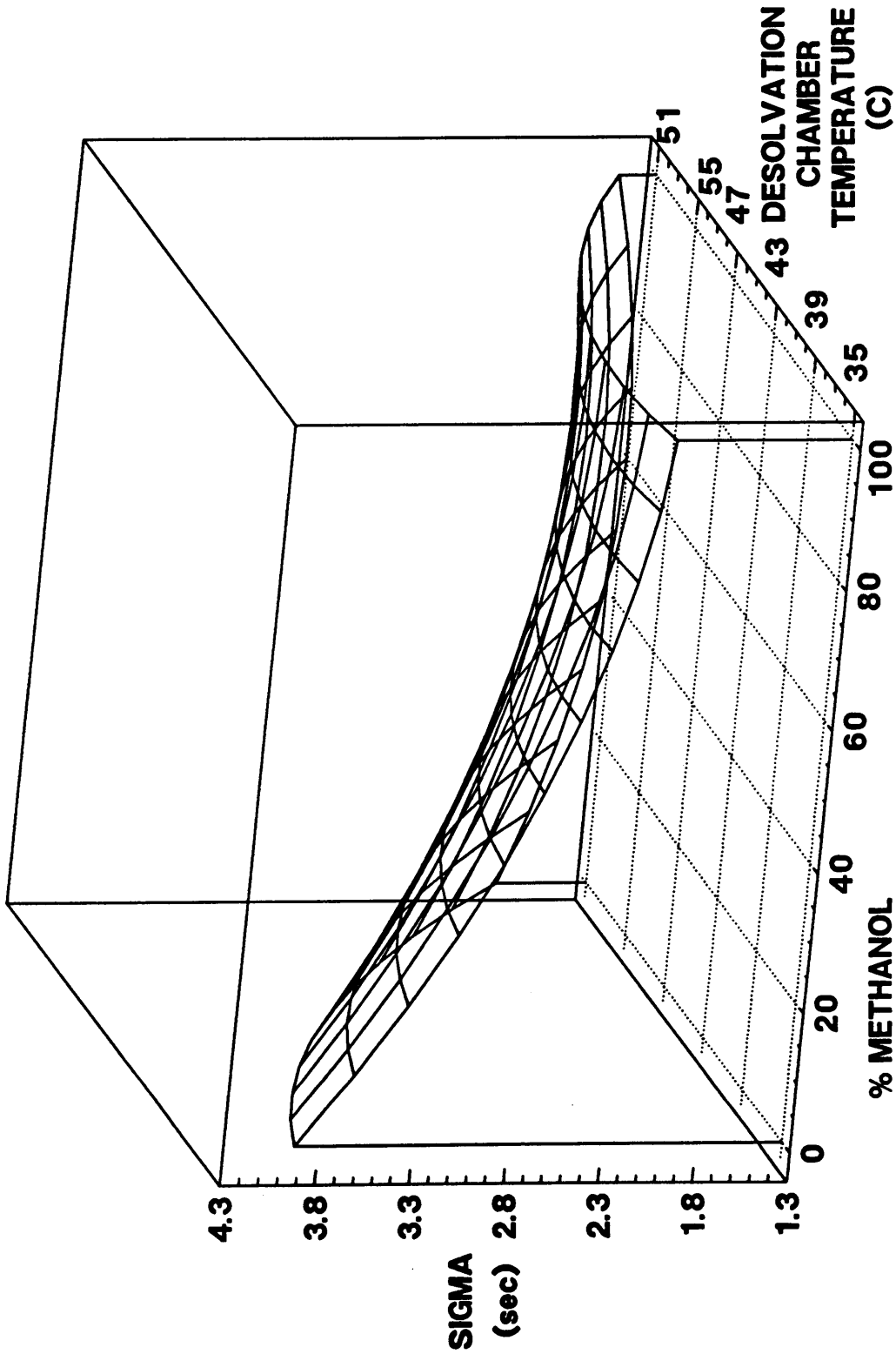


Figure B6: Effect of % Methanol and Desolvation Chamber Temperature on Sigma

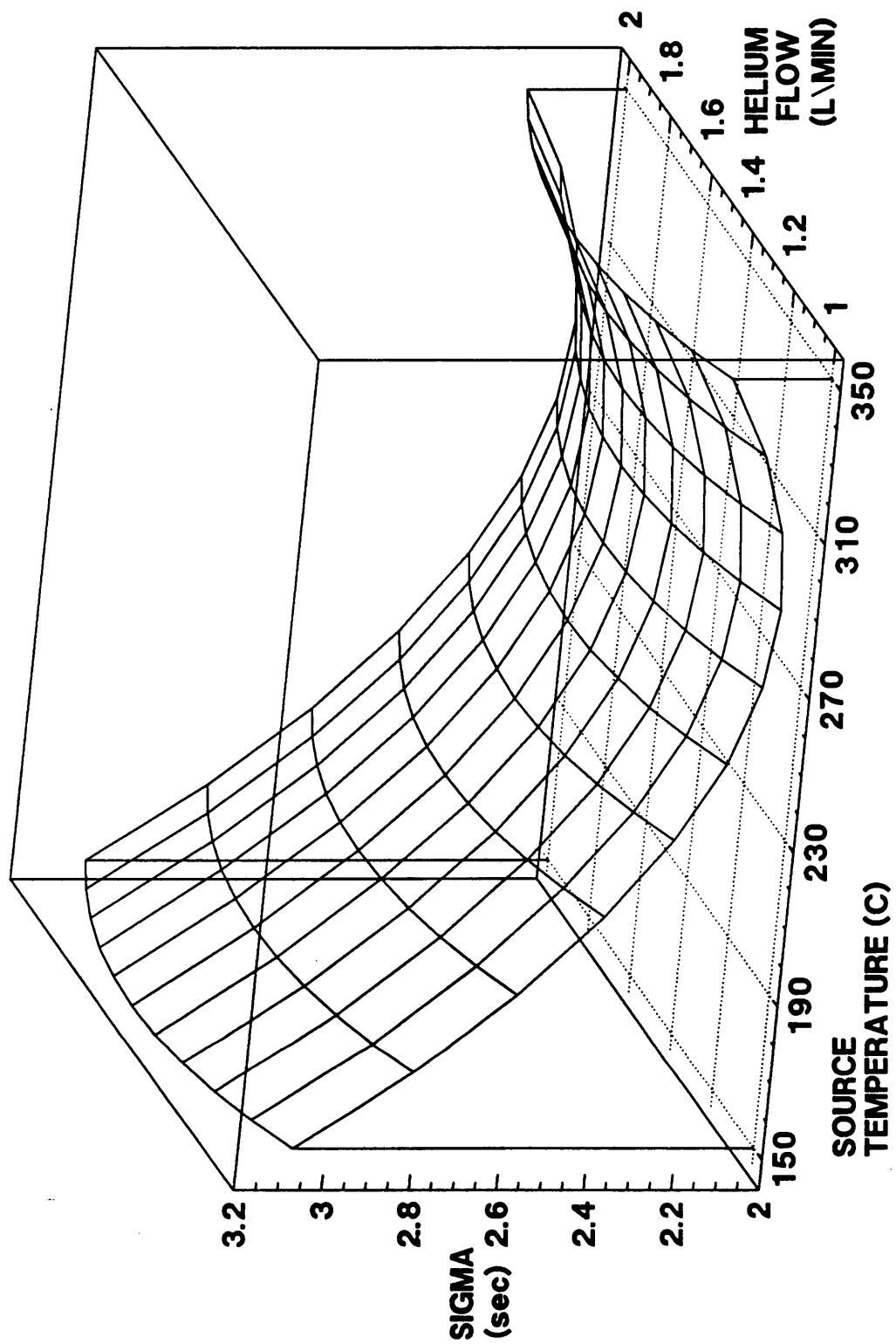


Figure B7: Effect of Source Temperature and Helium Flow on Sigma

**The vita has been removed from
the scanned document**

Evaluation of a Particle Beam Interface for LC/MS

by

Laura F. Cerruti

(ABSTRACT)

The performance of a Hewlett Packard Particle Beam LC/MS interface is evaluated using EPA appendix VIII and IX compounds. The behavior of these priority pollutants in the interface could determine its feasibility as a future EPA certified technique.

The evaluation process consists of studies to determine minimum detectable quantities (MDQ), linear response, and band broadening contributions. The MDQ's of the analytes in electron impact and chemical ionization modes are extrapolated from experimental signal to noise data. The linearity study involves ten compounds analyzed at five different concentrations. The response factors (RF) are calculated and discussed. The study concerning the band broadening contributions of the interface involves four independent variables (helium flow, desolvation chamber temperature, source temperature, and % methanol) and their effects on peak width. A Box-Behnken experimental design is used and described. Response surfaces are generated from the best fit equation describing the data.